AD A124 861 BASIC EW TECHNOLOGY ADVANCEMENT FOR C(3)I SYSTEMS VOLUME IVA COUPLING OF ... (U) SOUTHEASTERN CENTER FOR ELECTRICAL ENGINEERING EDUCATION INC S..

UNCLASSIFIED R T ABRAHAM ET AL. NOV 82 F/G 17/2 NL

1/2

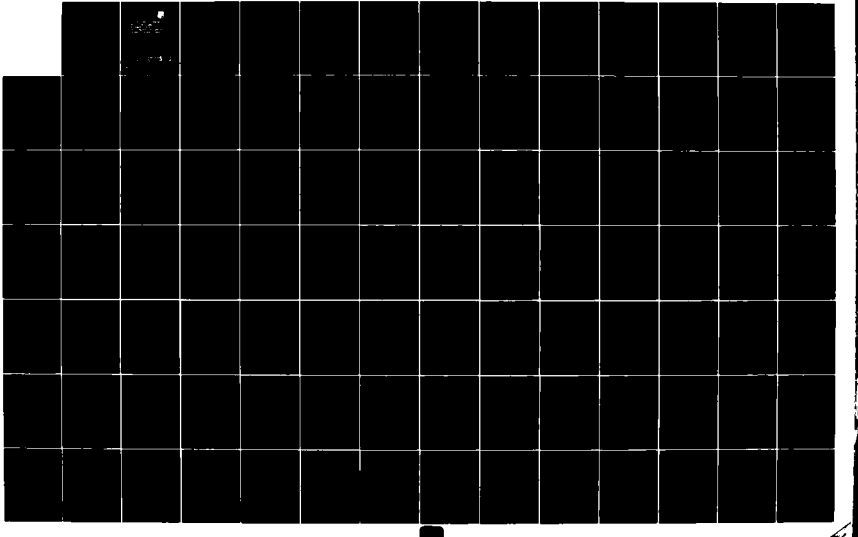

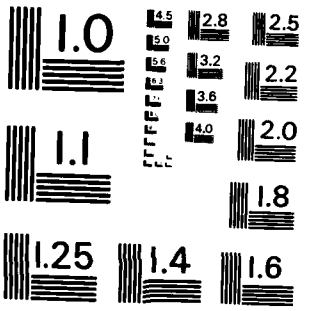

MICROCOPY RESOLUTION TEST CHART
NATIONAL BUREAU OF STANDARDS - 1963 - A

RADC-TR-82-286, Vol IV A (of six)
Phase Report
November 1982

BASIC EMC TECHNOLOGY ADVANCEMENT FOR C³ SYSTEMS - Coupling of Electromagnetic Fields onto Transmission Lines: A Comparision of the Transmission Line Model and the Method of Moments

Southeastern Center for Electrical Engineering Education

Robert T. Abraham
Clayton R. Paul

APPROVED FOR PUBLIC RELEASE; DISTRIBUTION UNLIMITED

This report has been reviewed by the RADC Public Affairs Office (PA) and is releasable to the National Technical Information Service (NTIS). At NTIS it will be releasable to the general public, including foreign nations.

RADC-TR-82-284, Volume IV A (of six) has been reviewed and is approved for publication.

APPROVED: [signature]

GERARD T. CAPRANO
Project Engineer

APPROVED: [signature]

EDMUND J. WESTCOTT
Technical Director
Reliability & Compatibility Division

FOR THE COMMANDER: [signature]

JOHN P. HUSS
Acting Chief, Plans Office

[redacted]

UNCLASSIFIED

SECURITY CLASSIFICATION OF THIS PAGE (When Data Entered)

REPORT DOCUMENTATION PAGE		READ INSTRUCTIONS BEFORE COMPLETING FORM
1. REPORT NUMBER RADC-TR-82-286, Vol IV A (of six)	2. GOVT ACCESSION NO. AD-A124861	3. RECIPIENT'S CATALOG NUMBER
4. TITLE (and Subtitle) BASIC EMC TECHNOLOGY ADVANCEMENT FOR C^3 SYSTEMS, Coupling of Electromagnetic Fields onto Transmission Lines: A Comparison of the Transmission Line Model and the Method of Moments		5. TYPE OF REPORT & PERIOD COVERED Phase Report Jun 81 - Dec 81
		6. PERFORMING ORG. REPORT NUMBER N/A
7. AUTHOR(s) Robert T. Abraham Clayton R. Paul		8. CONTRACT OR GRANT NUMBER(s) F30602-81-C-0062
9. PERFORMING ORGANIZATION NAME AND ADDRESS Southeastern Center for Electrical Engineering Education 1101 Massachusetts Avenue, St Cloud FL 32796		10. PROGRAM ELEMENT, PROJECT, TASK AREA & WORK UNIT NUMBERS 62702F 23380335
11. CONTROLLING OFFICE NAME AND ADDRESS Rome Air Development Center (RBCT) Griffiss AFB NY 13441		12. REPORT DATE November 1982
		13. NUMBER OF PAGES 163
14. MONITORING AGENCY NAME & ADDRESS(if different from Controlling Office) Same		15. SECURITY CLASS. (of this report) UNCLASSIFIED
		15a. DECLASSIFICATION/DOWNGRADING SCHEDULE N/A

16. DISTRIBUTION STATEMENT (of this Report)

Approved for public release; distribution unlimited.

17. DISTRIBUTION STATEMENT (of the abstract entered in Block 20, if different from Report)

Same

18. SUPPLEMENTARY NOTES

RADC Project Engineers: Gerard T. Capraro (RBCT) (See reverse)
Roy F. Stratton (RBCT)

Work was performed at the University of Kentucky, Dept of Electrical Engineering, Lexington KY 40506

19. KEY WORDS (Continue on reverse side if necessary and identify by block number)

Electromagnetic Compatibility
Cable Coupling
Transmission Lines
Multiconductor Transmission Lines
Field-to-Wire Coupling
Method of Moments

20. ABSTRACT (Continue on reverse side if necessary and identify by block number)

The coupling of electromagnetic fields onto transmission lines is investigated. The transmission line model with distributed sources is employed as a computationally efficient method of predicting currents induced on transmission wires by an incident field. Results obtained from the transmission line model solution are compared with predictions made by the more rigorous, but much less efficient, method of moments technique. Two user-oriented computer codes, using different expansion

DD FORM 1 JAN 73 1473 EDITION OF 1 NOV 65 IS OBSOLETE

UNCLASSIFIED

SECURITY CLASSIFICATION OF THIS PAGE (When Data Entered)

and testing functions, have been selected to provide the method of moments solution. Both the prediction accuracy and limitations of the transmission line model are explored in depth using a carefully selected transmission line structure. The structure is modified slightly to illustrate several important characteristics of the transmission line model solution. Low frequency limitations of the method of moments solution are investigated. In addition, the differences between the two method of moments formulations are found to have a significant effect on the integrity of their individual solutions. These differences are illustrated. Finally, the practical use of the transmission line model as an effective method for predicting the coupling of an electromagnetic field into terminal devices is discussed.

Block 18 (Cont'd)

Volumes I - III, V and VI will be published at a later date.

ACKNOWLEDGEMENTS

The authors gratefully acknowledge helpful discussions with Mr. D. E. Warren of the Rome Air Development Center and Professor J. H. Richmond of Ohio State University. The authors would also like to express their appreciation for the typing assistance of Ms. Debbie Shirley.

TABLE OF CONTENTS

LIST OF FIGURES

LIST OF TABLES

LIST OF PLOTS

All plots show differential mode terminal current magnitude (magnitude and phase for plots with two parts: (a) and (b)) versus frequency, unless otherwise indicated. The units are magnitude - amperes, phase-degrees, and frequency-hertz.

CHAPTER 1

INTRODUCTION

Transmission lines are usually thought of as being the wire network connecting a system of electronic devices. These wires are intended to carry signals (often digital signals at bit rates in the low megahertz frequency range) from one electronic device to another. Ideally the signal received at the second device should be the same as the signal launched by the first device. However, very often the connecting transmission lines are immersed in an electromagnetic field (FIGURE 1-1). This field can be generated by nearby radiating antennas (such as onboard aircraft), by other transmission lines carrying high frequency signals (this is referred to as wire-to-wire coupling or crosstalk), or just the high frequency energy that constantly bombards our environment (radio, television, microwave communications, radar). Both electromagnetic theory and experience tell us that this field can add signals to those already being carried by the transmission lines.

It is important to know the level of the unwanted signals (noise) on the transmission lines from the standpoint of device design and from the system analysis standpoint. That is, the designer of an individual electronic device must know what part of the incoming signal is informational and what part is noise in order to set noise level tolerances. The system designer must know what happens to a signal

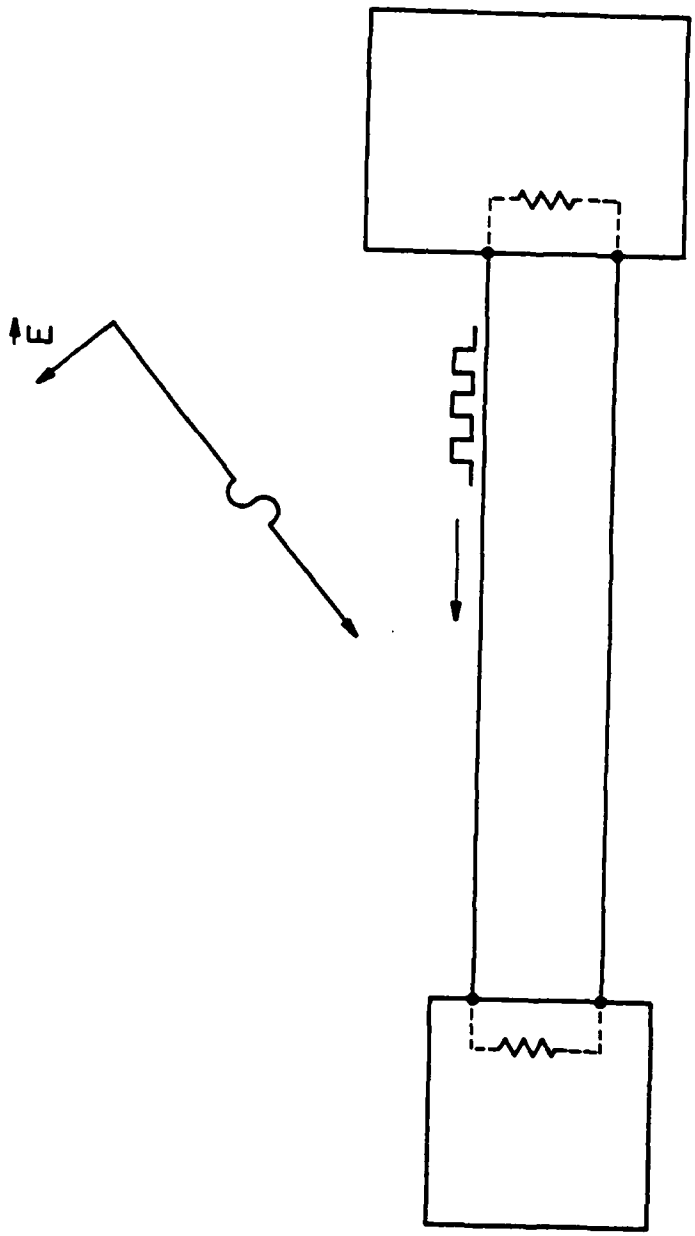

FIGURE 1-1

between the time it leaves one device as an output and is received at another device as an input. Even though a device may work well in an isolated test environment, it must also function properly in close proximity to other devices in the system. In short, given a transmission line network and given an incident electromagnetic field, it is important to be able to predict when and by how much the field will affect the signals being carried on the transmission lines.

From an electromagnetic point of view, the problem here is that the transmission lines are acting like receiving antennas. The surrounding electromagnetic field induces currents on the wires of the transmission network. Unfortunately, the accurate prediction of these induced currents can be a somewhat difficult and expensive task. The problem is real and a computationally efficient model would have practical applications. One such model is the "transmission line model with distributed sources", described in Chapter 2. This model is economical and probably the most efficient method of prediction known but has not been fully validated.

The transmission line model is based on several key assumptions. The model is devised with a particular physical structure in mind. In general, the structure is composed of parallel, thin wires with wire length, separation between wires, and wire radius related in the following way. The wire radius is assumed to be much smaller than the

separation between the wires, and the separation is assumed to be much less than the overall length of the line. The use of the term "thin wire" implies that, at relevant frequencies, the radius is small enough such that currents flow only in a longitudinal path (along the length of the wire) and none flow circumferentially (around the wire). (See FIGURE 1-2.) The separation between wires is assumed to be small enough so that, at relevant frequencies, it is not a significant portion of a wavelength. This assures that the TEM mode will be the primary mode of propagation and that higher order modes will be cutoff.

The transmission line is terminated with some type of load or source. While the source can be an alternating current source and the load can be a complex impedance, either is considered to be a lumped parameter. That is, the termination is considered to be "electrically" small, and the source or load occupies no physical space but is only a mathematical parameter. Take for example one end of a pair of transmission lines that are connected to each other by a resistor. (See FIGURE 1-3.) The current leaving the top wire is exactly the same as the current entering the bottom wire. The resistor, value R, serves only to relate the voltage at the termination to the current entering the termination. The resistor is "electromagnetically invisible" and the termination is not a part of the structure. What this means is that currents induced by some incident electromagnetic

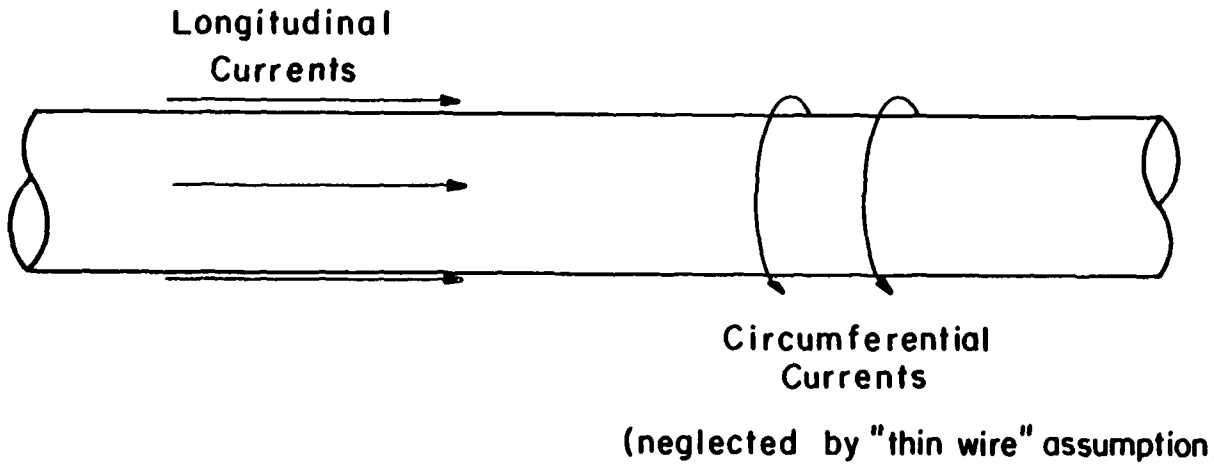
Longitudinal
Currents
Circumferential
Currents
(neglected by "thin wire" assumption)

FIGURE 1-2

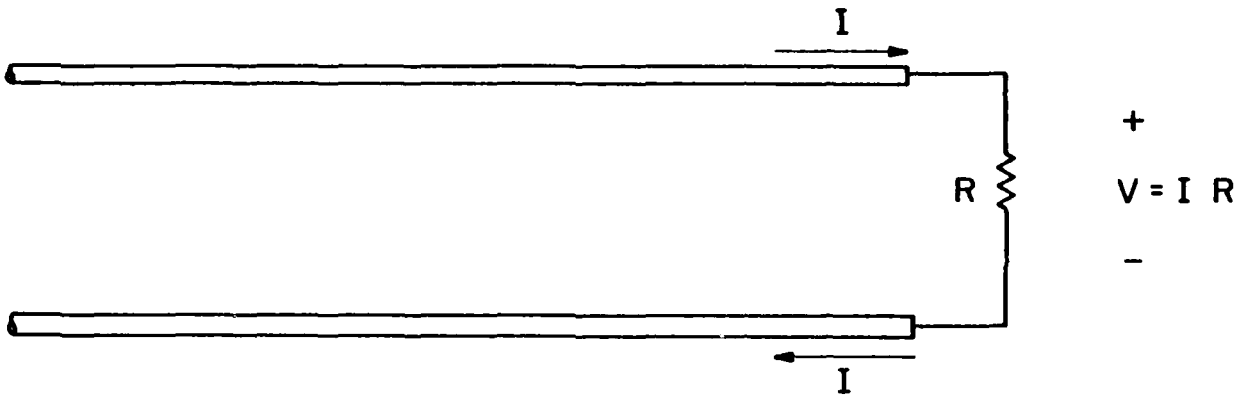

FIGURE 1-3

field will only be induced on the transmission wires themselves, none will be induced in the load. Most of these assumptions are closely related to one another and together give transmission line theory its economy and computational efficiency, but they also place restrictions on the application of the model.

Another technique used in solving for induced currents is referred to as the "method of moments", which is discussed in Chapter 3. This method is drastically different from the transmission line model and was designed specifically for use on a digital computer. The method of moments makes very few assumptions and is a much more rigorous but expensive prediction method than that of transmission line theory. With the method of moments, the entire structure is modeled, including the termination load. This method solves for currents on the entire structure, rather than just at the terminations, by enforcing electromagnetic boundary conditions throughout the entire structure. The only limit to the accuracy of this method is computer core and computer time. In lieu of experimental data, two method of moments computer codes have been selected to generate baseline data with which the transmission line model predictions can be compared. These codes will be discussed further in Chapter 3.

The transmission line method solves for the terminal currents and voltages. This makes it very well suited for a practical application

to the "real world" problems discussed at the beginning of this chapter. The main objective here is to predict how currents induced on transmission lines by an incident electromagnetic field are coupled into an electronic device through its inputs. So while knowledge of the actual currents at various positions on the wires may be important in some cases, such as antenna design, here we are more concerned with prediction of currents in the terminations produced by fields incident on the transmission lines. The method of moments, while very accurate, is very costly. Terminal current predictions at 200 frequencies were calculated using the transmission line model formulation on an IBM 370/165 digital computer in approximately 2 seconds of CPU time. Solution by the method of moments using the same computer for only 10 frequencies took an average of 80 seconds of CPU time. This means that the transmission line model can produce solutions for 800 frequencies in the same amount of computer time required for solution at one frequency by the method of moments.

It is obvious that the method of moments is not a practical solution technique for a large number of frequencies. However, its accuracy makes it an excellent source for baseline data to validate the transmission line results. In general the method of moments will break down numerically (a digital computer cannot provide numerically stable solutions) at low frequencies. The theory behind the transmission line model breaks down at high frequencies. However,

both techniques should provide good results over a fairly large common frequency range. In particular, the upper frequency limitation of the transmission line model will be investigated. Here, the method of moments solution should be valid and accurate.

In Chapter 2 the transmission line model is described in detail and a solution is derived for the terminal currents. In Chapter 3 the basic principles behind the method of moments technique are discussed. As mentioned earlier, two computer codes have been selected to provide the method of moments solution. Although both codes use the method of moments technique, each takes a slightly different approach to the solution and some of the differences between the two codes are discussed. The structure used for the majority of the data generation and the reasons for its selection are discussed in Chapter 4. A great deal of data was collected for this structure, for several different cases. The validity of the transmission line results is explored in detail here. Several special cases are considered in Chapter 5. These cases involve structures slightly different from the structure considered in Chapter 4. These modified structures help to demonstrate several points better than the basic structure. A very important topic is addressed in Chapter 6: the relationship between the common and differential mode currents and their relationship to the total induced current. The findings presented in Chapters 4 and 5 show an amazing accuracy for the transmission line model predictions

of differential mode currents over a considerable frequency range. These results demonstrate the integrity of this efficient model and suggest that it can provide accurate predictions when applied properly to cases which are within its limits of application.

CHAPTER 2

THE TRANSMISSION LINE MODEL

The purpose of this chapter is to describe the transmission line model mathematically. But first, the parameters which physically describe the structure must be defined. In Chapter 4 a two wire transmission line is analyzed in some detail; therefore, the model described here will be specialized to two wires. (Refer to FIGURE 2-1(a).) As discussed in Chapter 1, the structure consists of two parallel wires terminated at each end with complex loads Z_0 and Z_L. The line has length L, which is defined as being the distance between terminal planes. The load is not part of the physical line and makes up no part of the length. The distance between the centers of the wires is the wire separation, d. The radius of the wires, r, has no effect on the measurement of the separation between the wires because of the "thin wire" assumption, which implies that the radius (diameter) is insignificant when discussing the location of the wires. The radius is only used in the calculation of per-unit-length capacitance and inductance, and the characteristic resistance of the line, which are discussed later.

The orientation of the transmission line with respect to the Cartesian coordinate system is shown in FIGURE 2-1(b). The structure lies in the x-y plane (z=0). The bottom wire starts at the origin

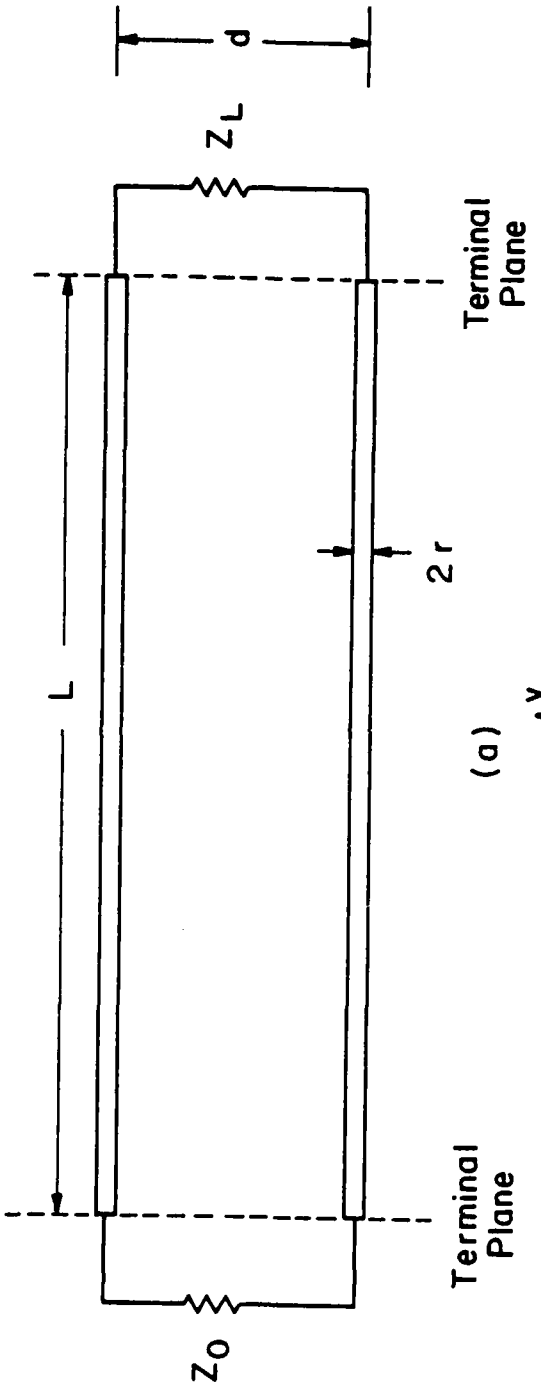

FIGURE 2-1

and extends along the positive x-axis for a distance L. The top wire starts at a distance d on the positive y-axis and extends out in the positive x direction a distance L to the point x=L, y=d, z=0.

Only certain structures are capable of supporting a TEM mode of propagation. These structures always have at least two conductors (coaxial line, parallel plate waveguide, two wire transmission line). One of the most basic and important assumptions of transmission line theory is that only the TEM mode propagates down the line. The restrictions on frequency and wire separation are directly related to this assumption. As mentioned in Chapter 1, the electrical separation (physical separation as a portion of a wavelength) must be small enough so that only the TEM mode propagates and all higher order modes are cut off. The TEM assumption assures that in any plane transverse to the longitudinal path of the transmission lines, static electromagnetic field conditions are satisfied. This is very important in that it allows the calculation of a per-unit-length capacitance and a per-unit-length inductance. A unique voltage can then be defined between the conductors at a point, x, anywhere along the line. Also a unique current, equal but oppositely directed in each of the two conductors (the current in the top wire, flowing in one direction, is equal to the current in the bottom wire, flowing in the opposite direction), can be defined at any point x, along the line.

The property of currents being equal and opposite is referred to as a "differential mode". (See FIGURE 2-2(a).) Equal currents that flow in the same direction are referred to as "common mode" currents (See FIGURE 2-2(b)). Given any arbitrary pair of currents flowing at the same position x on the line, these currents can be decomposed algebraically into common and differential mode currents (see FIGURE 2-2(c)). The top current, $I_1(x)$, is equal to the sum of the common and differential mode currents. The bottom current, $I_2(x)$, is equal to the common mode current minus the differential mode current. Transmission line theory assumes and predicts only differential mode currents due to the TEM assumption.

Based on the previous description, the following is a presentation of the derivation of the transmission line equations and the solution for the terminal currents. This derivation follows a standard and accepted format such as that presented in [1], [2], and [3]. In the following development, the transmission line wires are assumed to be non-insulated, perfect conductors immersed in a homogeneous, lossless medium.

Faraday's law, in the integral, sinusoidal steady state (time-harmonic) form provides the first step in the derivation of the transmission line equations. Consider a Δx section (see FIGURE 2-3(a)) of the line. A differential surface in the x-y plane, with the unit

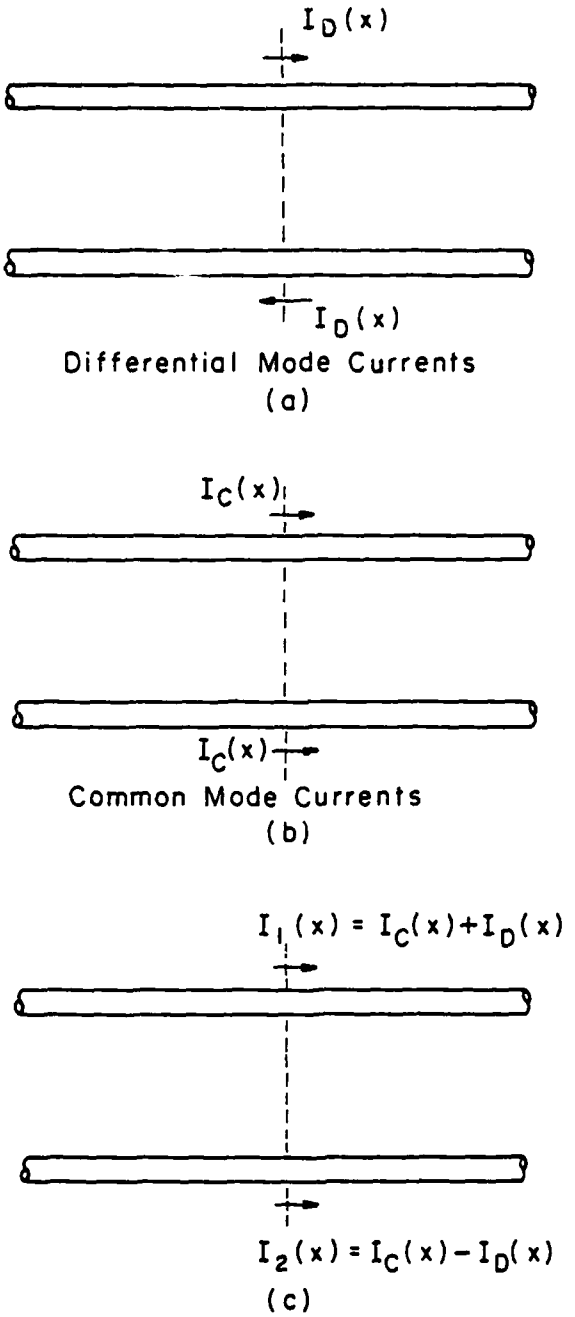
$I_D(x)$
$I_D(x)$
Differential Mode Currents
(a)
$I_C(x)$
$I_C(x)$
Common Mode Currents
(b)
$I_1(x) = I_C(x) + I_D(x)$
$I_2(x) = I_C(x) - I_D(x)$
(c)

FIGURE 2-2

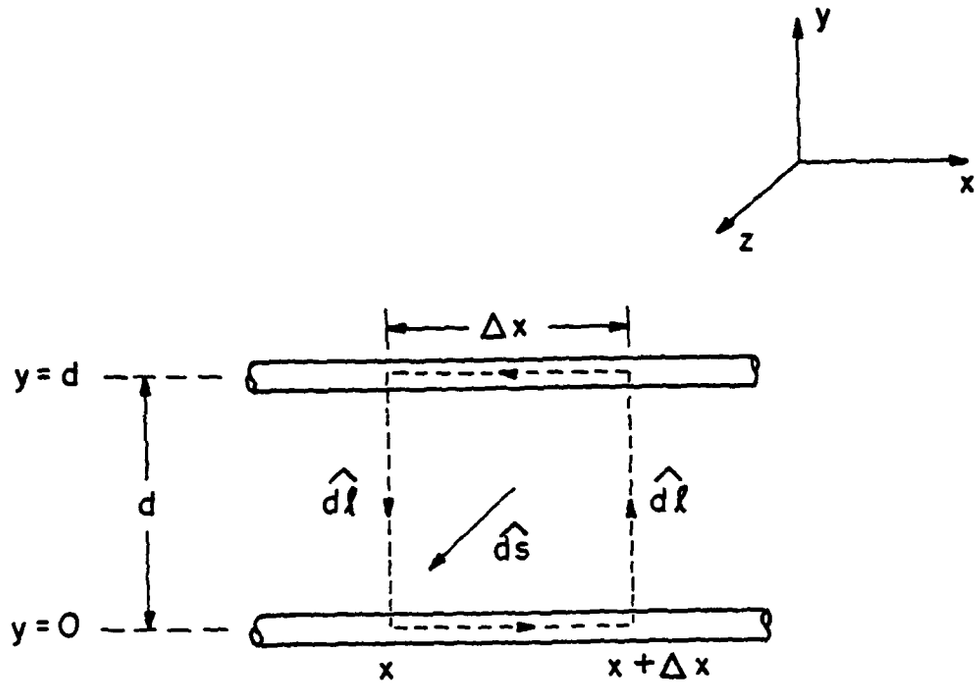
y
x
z
Δx
y = d
d
dℓ̂
dℓ̂
ds̄
y = 0
x
x + Δx

(a)

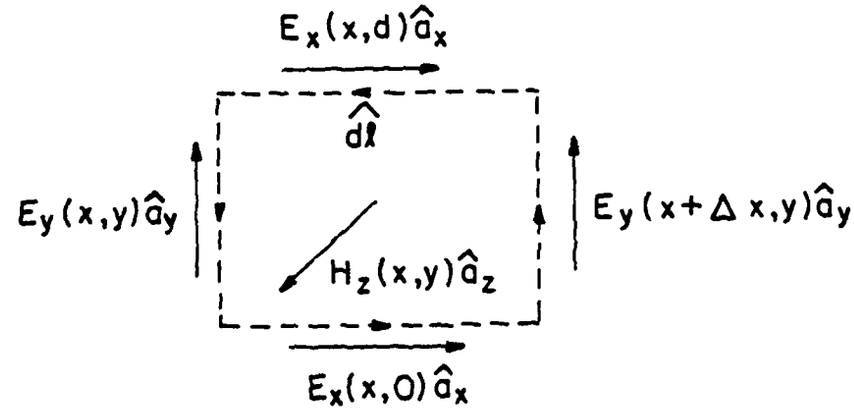
$E_x(x,d)\hat{a}_x$
dℓ̂
$E_y(x,y)\hat{a}_y$
$E_y(x+\Delta x,y)\hat{a}_y$
$H_z(x,y)\hat{a}_z$
$E_x(x,0)\hat{a}_x$

(b)

FIGURE 2-3

vector, $\hat{ds}$, normal to the surface, is defined by the closed contour ℓ. The direction of the contour is represented by the unit vector, $\hat{d\ell}$, which is related to $\hat{ds}$ by the right-hand rule. The closed contour integration on the left-hand side of Faraday's law,

$$\oint_c \vec{E} \cdot \hat{d\ell} = - j\omega\mu \int_s \vec{H} \cdot \hat{ds} \tag{2-1}$$

can be broken up into four line integrals. (See FIGURE 2-3(b).)

$$\oint_c \vec{E} \cdot \hat{d\ell} = \int_x^{x+\Delta x} E_x(x,0)dx + \int_0^d E_y(x+\Delta x,y)dy + \int_{x+\Delta x}^{x} E_x(x,d)dx + \int_d^0 E_y(x,y)dy \tag{2-2}$$

The surface integration on the right-hand side becomes

$$-j\omega\mu \int_s \vec{H} \cdot \hat{ds} = - j\omega\mu \int_x^{x+\Delta x} \int_{y=0}^{d} H_z(x,y)dxdy \tag{2-3}$$

By the assumption of perfect electric conductors, the electric field in the x direction must be zero at y=0 and y=d. Therefore, both line integrals involving E_x will be zero.

Voltage on the transmission line is defined as (see FIGURE 2-4)

$$V(x) = -\int_\ell \vec{E} \cdot d\ell = -\int_0^d E_y(x,y)dy = \int_d^0 E_y(x,y)dy \tag{2-4}$$

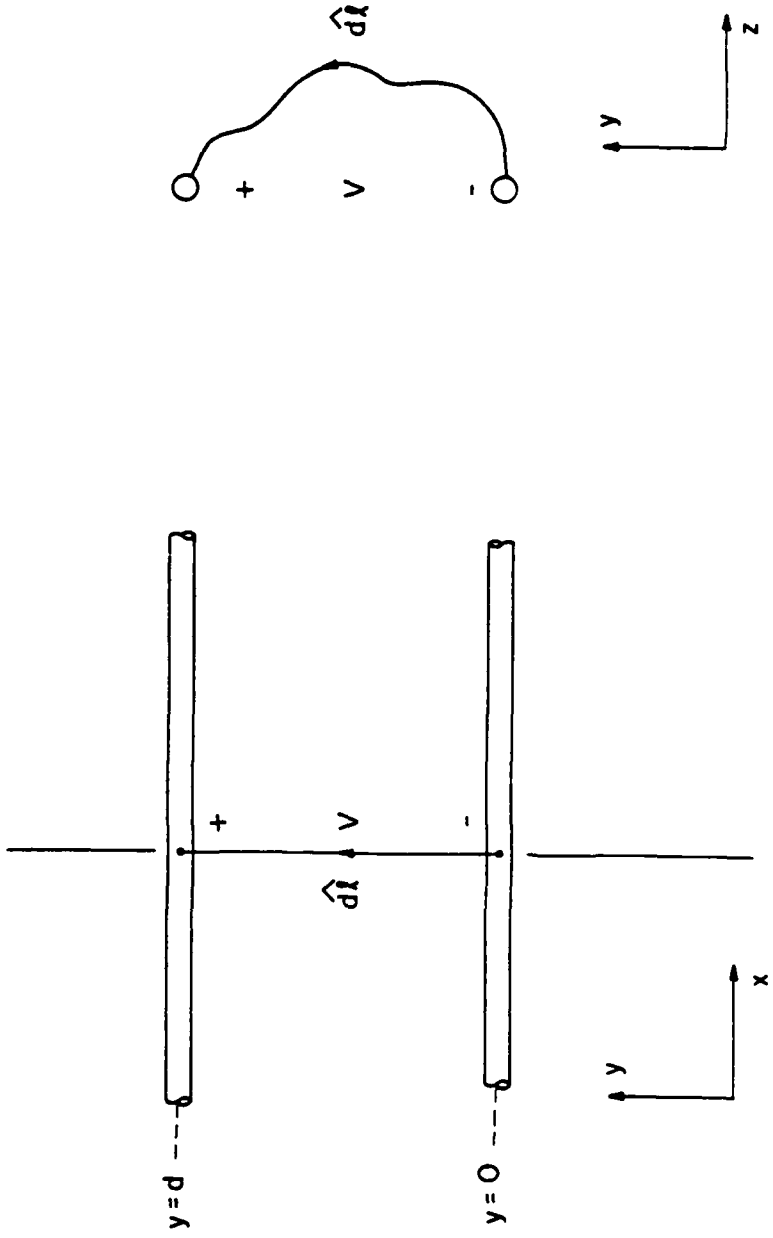

FIGURE 2-4

for some fixed value of x. The voltage at x + Δx becomes

$$- V(x+\Delta x) = \int_0^d E_y(x+\Delta x, y)dy \qquad (2\text{-}5)$$

Equation (2-1) now has the form

$$V(x+\Delta x) - V(x) = j\omega\mu \int_x^{x+\Delta x} \int_{y=0}^d H_z(x,y)dxdy \qquad (2\text{-}6)$$

Now, considering the left-hand side again, and dividing by Δx

$$\lim_{\Delta x \to 0} \left[\frac{V(x+\Delta x) - V(x)}{\Delta x} \right] = \frac{d}{dx} V(x) \qquad (2\text{-}7)$$

which gives the relationship

$$\frac{d}{dx} V(x) = j\omega\mu \int_0^d H_z(x,y)dy \qquad (2\text{-}8)$$

The H field, or H_z, can be seen as being the sum of an incident and a scattered field,

$$H_z = H_z^i + H_z^s \qquad (2\text{-}9)$$

Now the current on the top wire can be defined in terms of the transverse scattered H field. (See FIGURE 2-5.)

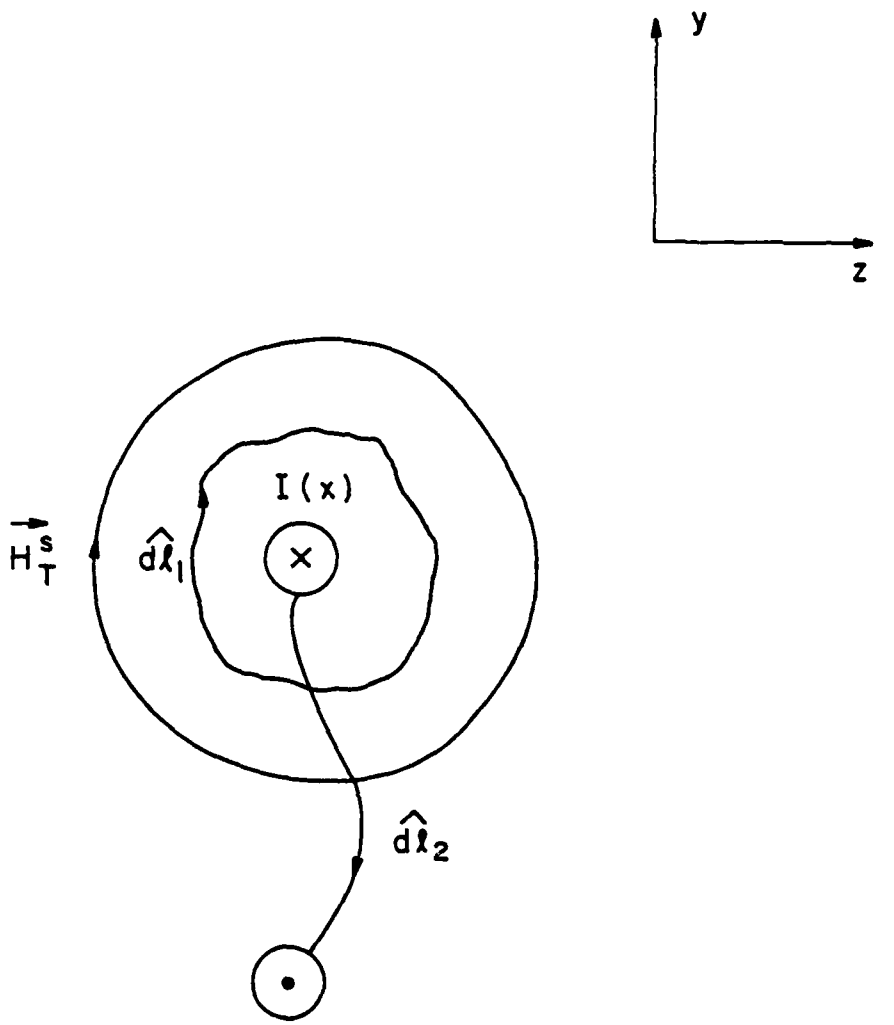

FIGURE 2-5

$$I(x) = \oint_C \vec{H}_T^s \cdot d\hat{\ell} \tag{2-10}$$

Also, the per-unit-length flux linkage can be defined in terms of $\vec{H}_T^s$

$$\psi(x) = \int_\ell \mu \vec{H}_T^s \cdot (\hat{a}_x \times d\hat{\ell}_2) \tag{2-11}$$

where $\hat{a}_x$ represents the direction of I(x). By definition [9], the per-unit-length inductance, ℓ, is

$$\ell = \frac{\psi(x)}{I(x)} = \frac{\int_\ell \mu \vec{H}_T^s \cdot (\hat{a}_x \times d\hat{\ell}_2)}{\oint_C \vec{H}_T^s \cdot d\hat{\ell}_1} \tag{2-12}$$

Applying (2-9) to equation (2-8) we obtain

$$\frac{d}{dx} V(x) = j\omega\mu \int_0^d H_z^i(x,y)dy + j\omega\mu \int_0^d H_z^s(x,y)dy \tag{2-13}$$

Equation (2-11) can be written as

$$- \psi(x) = - \ell I(x) = \mu \int_0^d H_z^s dy \tag{2-14}$$

where H_z^s equals $- H_T^s$ at z=0. Substituting equation (2-14) into equation (2-13) yields the first transmission line equation.

$$\frac{d}{dx} V(x) + j\omega\ell I(x) = j\omega\mu \int_0^d H_z^i(x,y)dy \tag{2-15}$$

The concept of continuity of current (conservation of charge) implies the following relation.

$$\oint_s \vec{J} \cdot \hat{ds} = - j\omega \int_v \rho dv \qquad (2\text{-}16)$$

Examining a differential volume (see FIGURE 2-6(a)), the left-hand side of (2-16) can be divided into two surface integrations, with normal surface vectors shown in FIGURE 2-6(b).

$$\oint_s \vec{J} \cdot \hat{ds} = \int_{s_e} \vec{J} \cdot \hat{ds}_e + \int_{s_c} \vec{J} \cdot \hat{ds}_c \qquad (2\text{-}17)$$

The integral involving the surface s_e (endcap surfaces) represents the axial conduction current. This current flows in one end of the segment and out of the other end; or more properly, it represents the currents flowing onto and off of the segment, just off the surface of the conductor (since perfect conductors are assumed), in the direction of the unit vector $\hat{ds}_e$ (see FIGURE 2-7(a)). This term can be represented as the difference between the current leaving the segment at $x+\Delta x$ and the current entering the segment at x.

$$I(x+\Delta x) - I(x) = \int_{s_e} \vec{J} \cdot \hat{ds}_e \qquad (2\text{-}18)$$

The second integration term, involving s_c (circumferential or cylindrical surface) represents the transverse conduction current

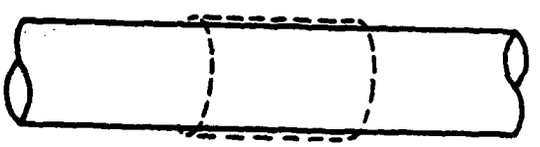

(a)

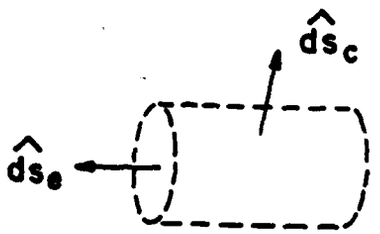

(b)

FIGURE 2-6

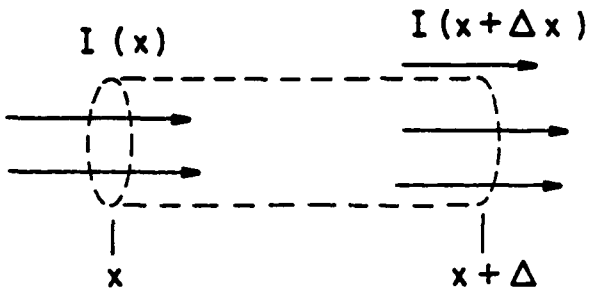

Conduction Current

(a)

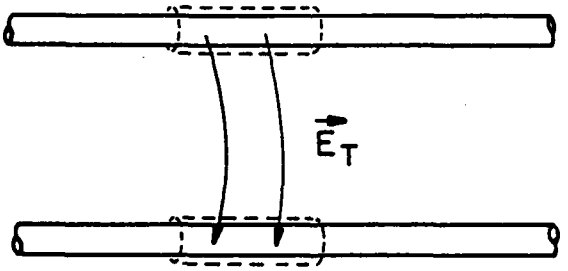

Transverse Conduction Current

(b)

FIGURE 2-7

(see FIGURE 2-7(b)).

$$\int_{s_c} \vec{J} \cdot \hat{ds}_c = \sigma \int_{s_c} \vec{E}_T \cdot \hat{ds}_c \qquad (2\text{-}19)$$

where σ is the conductivity of the medium and E_T is the E field transverse to the conductors. The assumption of a lossless medium allows us to neglect this term.

The integral on the right-hand side of (2-16) represents the total charge enclosed by the differential volume.

$$\int_v \rho dv = Q \qquad (2\text{-}20)$$

where ρ is the charge density and Q is the total charge enclosed. A cross section of the differential segment of transmission line is shown in FIGURE 2-8. Here, Q can also be defined in terms of the scattered E field,

$$Q = \varepsilon \int_x^{x+\Delta x} \int_c (\vec{E}_T^s \cdot \hat{a}_n) d\ell_2 dx \qquad (2\text{-}21)$$

where the contour, c, is just off the surface of the conductor. As defined by equation (2-4), the voltage due to the scattered field is

$$V^s(x) = - \int_0^d \vec{E}_T^s \cdot \hat{d\ell}_1 \qquad (2\text{-}22)$$

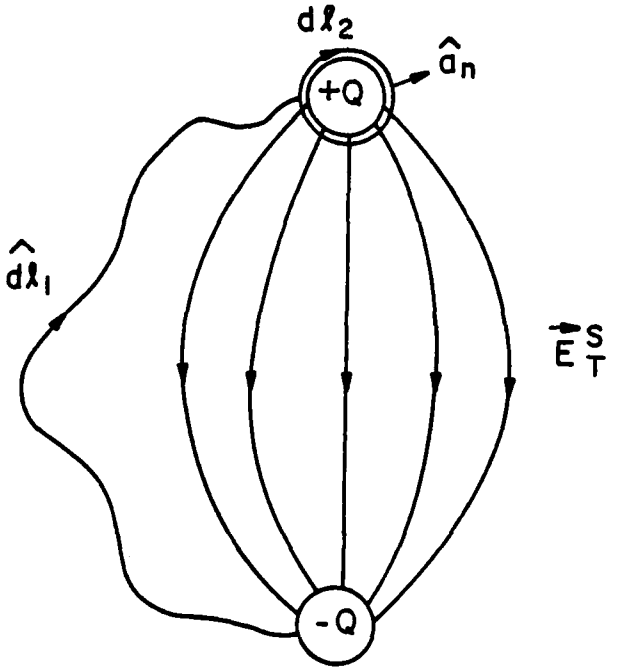

FIGURE 2-8

By definition [9], the per-unit-length capacitance is

$$c = \frac{Q}{\Delta x V^s(x)} = \frac{\Delta x \, \epsilon \int_c (\vec{E}_T^s \cdot \hat{a}_n) d\ell_2}{-\int_0^d \vec{E}_T^s \cdot d\hat{\ell}_1} \qquad (2\text{-}23)$$

so

$$Q = \Delta x \; c \; V^s(x) \qquad (2\text{-}24)$$

With the substitution of equation (2-24) for the right-hand side of (2-16), we obtain

$$I(x+\Delta x) - I(x) = - j\Delta x \; \omega c \; V^s(x) \qquad (2\text{-}25)$$

Dividing both sides by Δx gives

$$\frac{I(x+\Delta x) - I(x)}{\Delta x} = - j\omega c \; V^s(x) \qquad (2\text{-}26)$$

As with V(x) before, the limit as $\Delta x \to 0$ of the left-hand side is $\frac{d}{dx} I(x)$.

The total voltage has not yet been represented in the above equations. $V^s(x)$ represents only the voltage due to the scattered field. The total voltage is the sum of the voltage due to the incident field and the voltage due to the scattered field.

$$V^s(x) = V(x) - V^i(x) \tag{2-27}$$

By definition (equation (2-4)),

$$- V^i(x) = \int_0^d E_y^i(x,y)dy \tag{2-28}$$

Substitution of (2-28) and (2-27) yields the following from (2-26).

$$\frac{d}{dx} I(x) = - j\omega c\, V(x) - j\omega c \int_0^d E_y^i(x,y)dy \tag{2-29}$$

This is the second transmission line equation.

The two transmission line equations can easily be put in a form suitable for solution by state variable methods.

$$\frac{d}{dx} V(x) = - j\omega \ell\, I(x) + V_s(x) \tag{2-30}$$

$$\frac{d}{dx} I(x) = - j\omega c\, V(x) + I_s(x) \tag{2-31}$$

where

$$V_s(x) = j\omega\mu \int_0^d H_z^i(x,y)dy \tag{2-32}$$

$$I_s(x) = - j\omega c \int_0^d E_y^i(x,y)dy \tag{2-33}$$

If we define $Z=j\omega\ell$ and $Y=j\omega c$ the following equation is in state variable form.

$$\begin{bmatrix}\dot{V}(x)\\ \dot{I}(x)\end{bmatrix} = \begin{bmatrix}0 & -Z\\ -Y & 0\end{bmatrix}\begin{bmatrix}V(x)\\ I(x)\end{bmatrix} + \begin{bmatrix}V_s(x)\\ I_s(x)\end{bmatrix} \tag{2-34}$$

This has the same form as the more general equation,

$$\underline{\dot{X}}(t) = \underset{\sim}{A}\,\underline{X}(t) + \underline{F}(t) \tag{2-35}$$

often encountered in linear system theory. Here, $\underline{X}(t)$ is the state vector whose entries are the system states and $\underline{F}(t)$ is the forcing vector whose entries are the system inputs.

The state variable solution as presented in [4] is

$$\underline{X}(t) = \underset{\sim}{e}^{A(t-t_0)}\,\underline{X}(t_0) + \int_{t_0}^{t} \underset{\sim}{e}^{A(t-\tau)}\,F(\tau)\,d\tau \tag{2-36}$$

In transmission line theory,

$$\underset{\sim}{e}^{A(t)} \triangleq \underset{\sim}{\phi}(x) \tag{2-37}$$

where $\underset{\sim}{\phi}(x)$ is the chain parameter matrix. It serves to relate voltages and currents at different positions on the line. For a loss-

less transmission line [8]

$$\underset{\sim}{\phi}(x) = \begin{bmatrix} \phi_{11}(x) & \phi_{12}(x) \\ \phi_{21}(x) & \phi_{22}(x) \end{bmatrix} = \begin{bmatrix} \cos(\beta x) & - jv\ell \sin(\beta x) \\ - jvc \sin(\beta x) & \cos(\beta x) \end{bmatrix} \quad (2\text{-}38)$$

where

$$\beta = \frac{2\pi}{\lambda}$$

and is the propagation constant (λ = wavelength), v is the velocity of light, and ℓ and c are the per-unit-length capacitance and inductance respectively, as defined earlier.

Specializing (2-36) to the two wire transmission line model, the following relation is obtained

$$\begin{bmatrix} V(x) \\ I(x) \end{bmatrix} = \begin{bmatrix} \\ \underset{\sim}{\phi}(x) \\ \\ \end{bmatrix} \begin{bmatrix} V(0) \\ I(0) \end{bmatrix} + \int_0^x \begin{bmatrix} \\ \underset{\sim}{\phi}(x-\tau) \\ \\ \end{bmatrix} \begin{bmatrix} V_s(\tau) \\ I_s(\tau) \end{bmatrix} d\tau \quad (2\text{-}39)$$

Writing separate equations for V(x) and I(x) gives:

$$V(x) = \cos(\beta x)\, V(0) - jv\ell \sin(\beta x)\, I(0) + V_s'(x) \quad (2\text{-}40)$$

$$I(x) = - jvc \sin(\beta x)\, V(0) + \cos(\beta x)\, I(0) + I_s'(x) \quad (2\text{-}41)$$

where

$$V_s'(x) = \int_0^x [\cos(\beta(x-\tau))V_s(\tau) - jv\ell \sin(\beta(x-\tau))I_s(\tau)]d\tau \qquad (2\text{-}42)$$

$$I_s'(x) = \int_0^x [- jvc \sin(\beta(x-\tau))V_s(\tau) + \cos(\beta(x-\tau))I_s(\tau)]d\tau \qquad (2\text{-}43)$$

In order to solve the system of equations, (2-40) and (2-41), the terminal conditions must be specified to relate V(0) and I(0), and V(x) and I(x). If we let x=L, the line length, then V(L) is related to I(L) by the load at x=L, Z_L.

$$V(L) = Z_L I(L) \qquad (2\text{-}44)$$

(See FIGURE 2-9.) V(0) is related to I(0) by the load at x=0, Z_0.

$$V(0) = - Z_0 I(0) \qquad (2\text{-}45)$$

Substituting (2-44) and (2-45) into (2-40) and (2-41),

$$I(L) = \frac{1}{Z_L} [- \cos(\beta L)Z_0 I(0) - jv\ell \sin(\beta L)I(0) + V_s'(L)] \qquad (2\text{-}46)$$

$$I(L) = jvc \sin(\beta L)Z_0 I(0) + \cos(\beta L)I(0) + I_s'(L) \qquad (2\text{-}47)$$

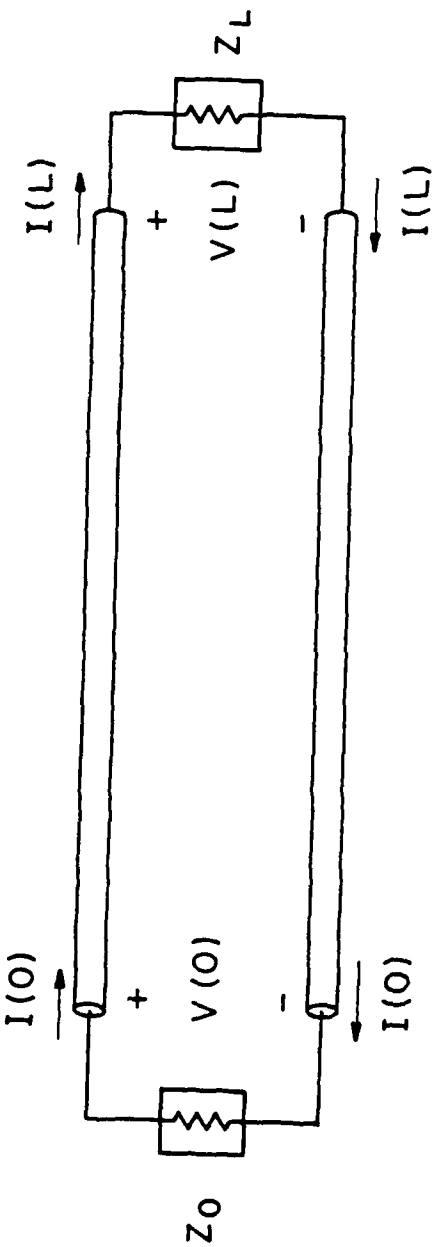

FIGURE 2-9

Setting (2-46) and (2-47) equal and solving for I(0) gives the following, which is equivalent to the form presented in [1] specialized to the two-conductor case:

$$I(0) = \frac{V_s'(L) - Z_L I_s'(L)}{(Z_0 + Z_L)\cos(\beta L) + j(v\ell + vcZ_0Z_L)\sin(\beta L)} \qquad (2\text{-}48)$$

In Chapter 4 the loads, Z_0 and Z_L, will be equal and resistive. This allows us to define a load resistor R.

$$R = Z_0 = Z_L \qquad (2\text{-}49)$$

Also, the characteristic resistance of the line, R_c, can be defined as [8]

$$R_c = v\ell = \frac{1}{vc} \qquad (2\text{-}50)$$

Equation (2-48) can now be written in the form

$$I(0) = \frac{V_s'(L) - R\, I_s'(L)}{2(R\cos(\beta L)) + j(R_c + \frac{R^2}{R_c})\sin(\beta L)} \qquad (2\text{-}51)$$

With the substitution of the result of (2-51) for I(0) (and R I(0) for V(0)) into equation (2-41), the transmission line solution for the differential mode current at any point along the line can be obtained, including x=L, as given by equation (2-46) or (2-47).

The forcing functions $V_s'(x)$ and $I_s'(x)$ contain the terms $V_s(x)$ and $I_s(x)$, given by equations (2-32) and (2-33), which represent sources induced by an incident field. One common way of supplying this incident field is to specify a uniform plane wave excitation. A uniform plane wave (see FIGURE 2-10) has the property that both the electric field vector, $\vec{E}$, and the magnetic field vector, $\vec{H}$, are transverse to the direction of propagation, represented by the vector $\vec{P}$. These vectors are related by the following vector expression.

$$\vec{E} \times \vec{H} = \vec{P} \qquad (2\text{-}52)$$

This is TEM propagation, as discussed earlier.

The details of how to get from an incident uniform plane wave to the E and H field components needed for $V_s(x)$ and $I_s(x)$ are provided in Appendix I. A computer program was written to generate transmission line terminal current predictions for the two wire structure, when excited by an incident plane wave. A description of this program is given in Appendix II and a listing is given in Appendix III.

Although the equations involved in going from an incident plane wave to a prediction of the current entering a load appear somewhat formidable and quite cumbersome (and indeed they can be), greatly simplified forms are presented in Chapter 4 for the special cases con-

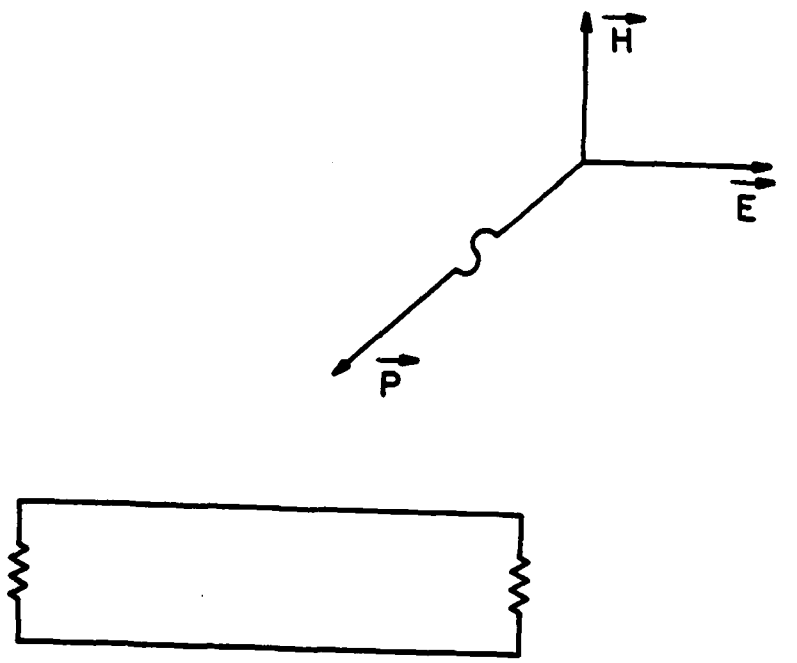

FIGURE 2-10

sidered there. These forms allow more insight into the relationship between incident field excitation and load currents.

CHAPTER 3

THE METHOD OF MOMENTS FORMULATION

The transmission line model provides a very efficient technique for predicting the terminal currents induced by an incident field. Although the theory behind this model is well known, the limits of its validity have not yet been established. Experimental data for a transmission line excited by an incident field are very difficult to obtain. To properly measure the induced currents, at relevant frequencies, would probably require the use of an anechoic chamber. Unfortunately, this type of facility is rarely available for these kinds of measurements. However, in lieu of experimental data, a numerical solution technique called the "method of moments" has been used in Chapters 4 and 5 to generate a set of baseline data with which the transmission line model predictions can be compared.

The method of moments has gained wide acceptance and credibility in recent years. Several user-oriented computer programs have been developed to solve problems in electromagnetics [10] (particularly in the area of electromagnetic compatability), since Harrington [11] specialized the technique to electromagnetic problems. While the method of moments can give very accurate results, the cost (computer time and memory) of this accuracy can be substantial, as mentioned in Chapter 1. This is why computationally efficient models, like the transmission line model, are very important.

One reason that the method of moments technique is so expensive is that very few assumptions are made. One significant assumption, however, in both of the formulations presented later in this chapter is that of "thin wires". In addition to the implications discussed in earlier chapters for the thin wire assumption, it has an important effect on the enforcement of E field boundary conditions. This will be discussed further in a moment.

In the method of moments technique the current distribution over the entire structure is solved for by enforcing the boundary condition that the tangential E field should be zero at any point on the structure. Due to the thin wire approximation, this condition is applied only to the axial component of the E field at the surface of the conductors. The method of moments can be thought of in the following way. The structure is divided up into many subsections. The currents on each of the subsections can be put into vector form,

$$I = \begin{bmatrix} I_1 \\ I_2 \\ \vdots \\ I_n \end{bmatrix} \qquad (3\text{-}1)$$

where I_i (i=1,2,...,n) is the current on the i^{th} segment (subsection). The voltage of each segment can be treated in the same fashion [10].

$$\underline{V} = \begin{bmatrix} V_1 \\ V_2 \\ \vdots \\ V_n \end{bmatrix} \tag{3-2}$$

These voltages and currents can then be related by a generalized impedance matrix, which essentially characterizes the structure.

$$[\underline{V}] = [\underset{\sim}{Z}][\underline{I}] \tag{3-3}$$

The values of the entries in the voltage vector are supplied by the excitation (incident field) for scattering problems. Standard matrix analysis techniques can now be used to solve for the current vector.

$$[\underline{I}] = [\underset{\sim}{Z}]^{-1} [\underline{V}] \tag{3-4}$$

Loading can be accounted for by adding the value of the load to the value of the impedance for the corresponding segment on the diagonal of the impedance matrix. Losses in the conductors can be handled in the same way, adding a load to every segment. A description of the

method of moments in terms of linear operators is given in Chapter 1 of [11].

Basically, this technique allows the complex integro-differential equations that are normally used to characterize the current on this type of structure to be put into matrix form and solved as a linear system. The current on each segment must be represented by some function, referred to as an expansion function. One of the major differences in various formulations of the method of moments is the choice of expansion functions. A second major difference is the choice of testing functions. The testing functions are used to enforce the tangential E field boundary condition. The two method of moments programs to be discussed here employ different expansion and testing functions. The second program discussed uses a special procedure referred to as Galerkin's method where the expansion and testing functions are the same.

The first computer program to be discussed is entitled WRSMOM, and was written by D. E. Warren. WRSMOM is a program that was designed specifically for configurations of straight thin wires [10]. It is based on the formulation presented in Chapter 4 of [11]. The program employs the "pulse expansion and point matching" technique. This refers to the current expansion functions and the E field testing functions discussed earlier. In this technique, the current is assumed

to be constant over each segment; or in other words, the current on each segment is expanded as a piecewise constant pulse. (See FIGURE 3-1(a).) The tangential E field boundary condition is enforced only at the "matchpoint" (hence "point matching") located at the center of each segment. The testing function is therefore a form of the dirac (or delta) function. The program output includes the current array, which is the same as the current vector discussed earlier. Each entry in this vector gives the magnitude and phase of the pulse representing the complex current over the corresponding subsection.

Due to the way in which charge and current are represented on the structure, it is important that the segment length (or zone size) remains fairly consistent. Although segments of varying lengths can be used, only small changes in length between adjacent subsections are acceptable. To maintain the thin wire assumption, the zone size should be several times greater than the radius of the wire (at least five times the radius [12]). Also, ten to forty subsections per wire wavelength are recommended for accuracy in [12].

The pulse expansion and point matching technique is fairly well known and popular because it is, conceptually, the most straightforward formulation. Also, this is the technique first specialized to electromagnetic problems by Harrington. However, other formulations using more sophisticated expansion and testing functions can in some cases give

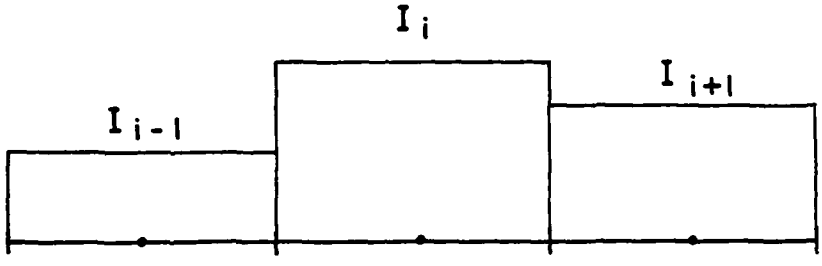

(a)

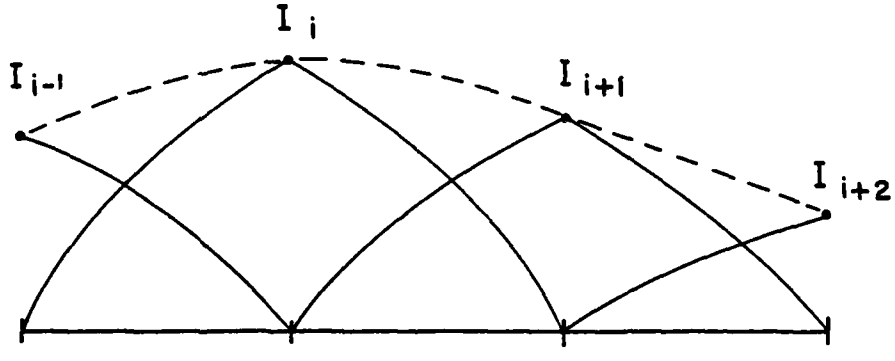

(b)

FIGURE 3-1

more accurate results and better convergence. One such computer code is OSMOM (this is not the name given it by the author, but is one that is commonly used) written by J. H. Richmond at Ohio State University [13], [14]. Richmond's code has gained a great deal of respect and a general acceptance from users of the method of moments [10]. In fact, several individuals have used the code as a basis for modified versions. The program is noted for handling wire junctions and corners very well. This makes it well suited for application to the (transmission line) structures considered in the next few chapters. The expansion functions used in OSMOM are piecewise sinusoidal (sometimes referred to as sinusoidal triangles). (See FIGURE 3-1(b).) These functions are defined as follows:

$$I_i(x) = \frac{\sin\beta(x - x_{i-1})}{\sin\beta(x_i - x_{i-1})}, \quad x_{i-1} \leq x \leq x_i$$
$$= \frac{\sin\beta(x_{i+1} - x)}{\sin\beta(x_{i+1} - x_i)}, \quad x_i \leq x \leq x_{i+1} \tag{3-5}$$

where β is the propagation constant defined in Chapter 2. Here $I_i(x)$ is the current approximation for an x-directed current (axial current on an x-directed wire), where each expansion function spans two segments and adjacent functions overlap. The i^{th} entry in the current vector is the complex amplitude of the corresponding piecewise sinusoidal expansion function. A wire which is divided into n subsections will have n+1 entries in the current vector, one entry for the begin-

ning and end of each segment (of course the end of one segment is the beginning of the next).

OSMOM uses a special technique, referred to as Galerkin's method, so the testing functions are the same as the expansion functions, as was mentioned earlier. Lumped loads can be accounted for by adding a diagonal matrix of loads to the generalized impedance matrix. This is the same as with WRSMOM except that the loads are placed at the end-points of adjoining segments (which correspond to the expansion function peaks) instead of at the centers of the segments. Excitation voltages, which are derived in the program from the plane wave incident field (as with WRSMOM), are also positioned at the peaks of the sinusoidal triangles. Because of the type of expansion function and the Galerkin technique, consistent zone size is not as critical as with the pulse expansion and point matching procedure. However, the restrictions placed on subsection length by the thin wire assumption still apply. For the sake of comparison, the same zone structure will be used for both WRSMOM and OSMOM, applying the more stringent requirements of the pulse expansion and point matching technique to both, whenever possible.

In general, Galerkin's method seems to give accurate results with fewer subsections and better convergence than pulse expansion and point matching. In addition, sinusoidal triangles seem to be

very effective as expansion functions.

The transmission line structure presents some modeling problems which particularly tax the method of moments and especially the pulse expansion, point matching technique. With the method of moments, the terminal loads now become part of the physical structure and must be modeled as wires containing lumped loading. Thus, the structure is made up of two long wires and two very short wires. In order to preserve any consistency in zone length and at the same time maintain a reasonable matrix size (a reasonable number of zones), very few zones can be used to model the terminal wires. As suggested by [15], in certain cases the matchpoints of the collocation (point matching) technique cannot be spaced sufficiently dense to accurately sample the E field. This problem is compounded when the incident field is such that the only excitation voltages (in the voltage vector) are located in the loads. In this case the highly localized driving field is very poorly represented. In addition, if the current magnitude changes rapidly near the termination, the pulse expansion formulation cannot adequately model the rapidly changing subsection currents. These factors are extremely important since we are interested in an accurate prediction of the currents entering the loads.

To summarize, we should expect the Galerkin's method formulation (with sinusoidal triangles) to give much better accuracy and conver-

gence than the pulse expansion, point matching technique for transmission line structures with close wire separation, when the same zone configuration is used for both solutions. The sinusoidal expansion functions allow the tangential E field to be more adequately represented in and near the terminal wires than do the highly localized matchpoints of the collocation technique. This is especially true in the corners where the transmission lines meet the terminal wires and it is impossible to place a matchpoint. For these reasons, the transmission line results will only be compared with predictions made by OSMOM in Chapter 4. However, WRSMOM will be used, along with OSMOM in Chapter 5, where several special cases are considered.

CHAPTER 4

PREDICTION ACCURACY OF THE TRANSMISSION LINE MODEL

In the last few chapters we have been discussing solution techniques for the terminal currents of a general two wire transmission line. The structure was described by its physical dimensions of length, wire separation and wire radius and by the terminal loads. In this chapter, specific values will be chosen for these parameters and predictions made by the different methods of solution will be compared in detail. It may be helpful to keep in mind that the method of moments solution should establish a set of baseline data. These data have been generated by a rigorous solution technique and are accepted among experts in the field as the "correct" solution. The transmission line model provides a much more efficient means of prediction. The effort here is intended to validate the transmission line results by comparison with the baseline data set produced by the method of moments.

The dimensions of the structure used for analysis in this chapter were carefully selected. It would be an impossible task to evaluate all configurations of transmission line networks. With the wide variety of wire gauges, lengths of lines, separations between wires, and wire bundling techniques, even defining an "average" structure is quite subjective. However, several characteristics common to all transmission

lines help guide the selection of dimensions. As was discussed in Chapter 1, the separation between the wires should be many times smaller than the overall length of the line. For a line with a length of one meter, a wire separation of one centimeter more than satisfies this requirement. The wire radius is assumed to be many times smaller than the separation. Selecting the wire radius to be one tenth of a millimeter more than satisfies this requirement and also assures the validity of the thin wire assumption. This radius corresponds approximately to 32 gauge wire, which is in the range of gauges commonly used for lines carrying low level signals. The wire separation could represent the distance between two conductors in a cable bundle or a conductor at a height of five millimeters over a ground plane (using image theory). While this separation may be wide for some applications, remember that the transmission line results will improve with closer separations. Given the parameters of radius and separation, the selected length of one meter is convenient and allows for the observation of terminal current predictions with a line that is both electrically long and electrically short over the range of frequencies being investigated. All of the physical dimensions have now been defined. The line length is one meter; the wire separation is one centimeter; and, the radius is one tenth of one millimeter giving a radius that is one hundred times smaller than the separation, and a separation that is one hundred times smaller than the line length.

The only parameters left undefined are the load impedances. For the sake of simplicity, the loads at each termination will be equal and resistive. This still leaves quite a range of loading conditions. The choices can be narrowed by looking at three cases: loads much smaller than the characteristic resistance of the line, loads much larger than the characteristic resistance and loads equal to the characteristic resistance (the latter are referred to as matched loads). The characteristic resistance of the present line under discussion is 552.2262 ohms as given by equation (2-50); so, this is the value to be used for the "matched" case. The selection of the other two loading conditions is again, highly subjective. The choices of 50 ohms for the "low impedance" case and 10K ohms for the "high impedance" case represent nominal input impedances for typical electronic devices. The important point with respect to these latter two choices is that one is many times smaller than, and one is many times larger than, the characteristic resistance of the line. Other choices in those ranges should give results similar to those obtained for the selected values.

At this point the structure has been completely defined for solution by the transmission line model. One step remains, however, in defining the structure for solution by the method of moments. Each wire must be divided into subsections, as described in Chapter 3. If the terminal wires are characterized by one segment each, using equal

length segments on the remainder of the structure creates more than 200 total subsections. This would require solving a system of 202 simultaneous equations and unknowns. This is a very large problem even with the best matrix analysis techniques. Numerical noise and round-off problems might make the accuracy of the result questionable, also. From a standpoint of economics (computer time and memory) and numerical stability, a structure with 50 total subsections is much more reasonable. Again characterizing the terminal wire as one segment and dividing each transmission line wire into 24 equal segments gives a structure with a total of 50 subsections.

In Chapter 2 it was pointed out that the transmission line model solves for the differential mode current, because of the TEM assumption. However, the method of moments solves for the total current. For a valid comparison between the two solutions, the differential mode current must be extracted from the total current given by the method of moments. This is a simple algebraic manipulation. We are interested in the currents entering and leaving the load at $x=0$. The output from OSMOM will give a value for the total current, I_T, flowing in the positive x direction on the top wire at x=0 and a value for the total current, I_B, flowing in the positive x direction on the bottom wire at x=0. The total currents can be decomposed into common and differential mode currents by the following matrix equation.

$$\begin{bmatrix} I_C \\ \\ I_D \end{bmatrix} = \begin{bmatrix} \frac{1}{2} & \frac{1}{2} \\ \\ \frac{1}{2} & -\frac{1}{2} \end{bmatrix} \begin{bmatrix} I_T \\ \\ I_B \end{bmatrix} \qquad (4\text{-}1)$$

The differential mode component, I_D, obtained from the method of moments solution by this equation is then compared to the terminal current prediction made by the transmission line model. The relationship between the common mode, differential mode and the total current is discussed in Chapter 6.

Now that the structure has been fully characterized for solution by the transmission line model and by the method of moments, the only parameters yet to be defined are those describing the incident field. As mentioned earlier and described in more detail in Appendix I, the excitation is provided by a uniform plane wave. Each of the method of moments programs and the transmission line program will solve for the currents induced by a plane wave excitation with any angle of incidence and any polarization. Three cases have been selected for study. These cases are representative of all of the possible cases in the following ways. First, each coordinate direction of plane wave propagation is represented by one of the cases. Secondly, in the transmission line model, sources are induced by the incident E field and by the incident H field for an arbitrary angle of incidence. The cases being considered here include an incidence angle and polarization

that induce sources only from the E field, that induce sources only from the H field and one case where both the E field and H field induce distributed sources. For each of the following three cases the orientation of the incident plane wave will be illustrated and a simplified version of the transmission line model solution for I(0), specialized to that case, will be derived. Even though the general formulation of the terminal current solution was used to generate the actual data, these specialized forms provide more insight into the solution.

The first case to be considered has the plane wave incident on the end of the structure. (See FIGURE 4-1.) The plane wave is propagating in the positive x direction and first strikes the transmission line at the end where x=0; thus, it will be referred to as the ENDFIRE case. The E field is oriented in the positive y direction, leaving the H field oriented in the positive z direction. This is the only logical polarization (with the exception of a negative y-directed E field and a negative z-directed H field). Since E_y and H_z are the only field components which induce currents, this polarization gives maximum pickup of both fields by the structure. Rotating the polarization 90 degrees either direction gives zero pickup, and therefore no induced currents. The following is a derivation of the terminal current flowing out of the load, onto the top wire, at x=0, for the ENDFIRE case.

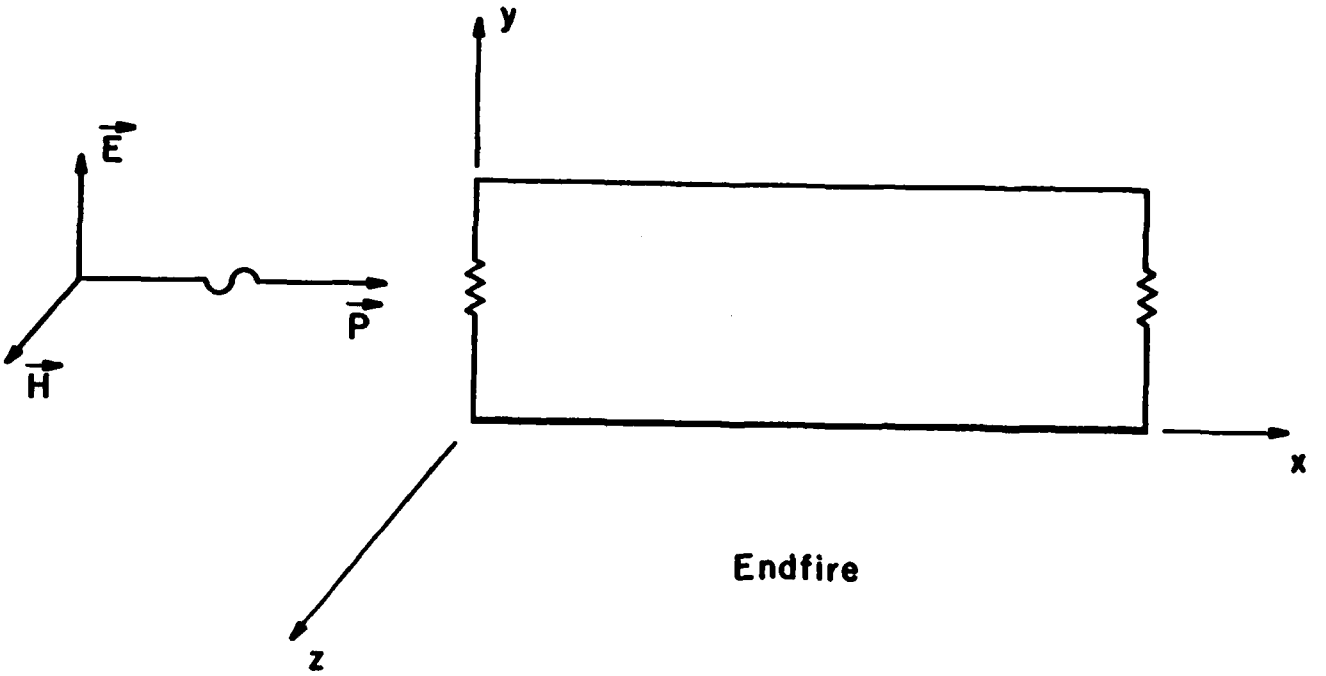

Endfire

FIGURE 4-1

Equations (2-32) and (2-33) provide the induced voltage and current sources respectively in terms of the incident field components, H_z^i and E_y^i. Since the total incident E field is y-directed and the total incident H field is z-directed,

$$E_y = E_m e^{-jkx} \tag{4-2}$$

$$H_z = H_m e^{-jkx} = \frac{E_m}{\eta} e^{-jkx} \tag{4-3}$$

where E_m is the incident E field magnitude and H_m, the incident H field magnitude, is related to E_m by the intrinsic impedance of free space, η, as discussed in Appendix I. The exponential terms indicate that the plane wave is propagating in the positive x direction. From equations (2-32) and (2-33) we obtain

$$V_s(x) = j\omega\mu \int_0^d H_z^i(x,y)dy = j\omega\mu \int_0^d \frac{E_m}{\eta} e^{-jkx}\, dy$$

$$= j\omega\mu \frac{E_m}{\eta} d\, e^{-jkx} \tag{4-4}$$

$$I_s(x) = - j\omega c \int_0^d E_y^i(x,y)dy = - j\omega c \int_0^d E_m\, e^{-jkx} dy$$

$$= - j\omega c\, E_m d\, e^{-jkx} \tag{4-5}$$

Substituting equations (4-4) and (4-5) into equation (2-42) gives

$$V_s'(L) = \int_0^L [\cos(k(L-\tau))V_s(\tau) - jv\ell\sin(k(L-\tau))I_s(\tau)]d\tau$$

$$= \int_0^L [\cos(k(L-\tau))\ j\ \frac{\omega\mu}{\eta}\ E_m d\ e^{-jk\tau} \qquad (4\text{-}6)$$

$$+ jv\ell\sin(k(L-\tau)j\omega c\ E_m d\ e^{-jk\tau}]d\tau$$

Evaluation and simplification of the right-hand side of (4-6), the details of which are given in Appendix IV, yields the following relation.

$$V_s'(L) = j\ E_m d\ \sin(kL) \qquad (4\text{-}7)$$

Substituting equations (4-4) and (4-5) into equation (2-43) gives

$$I_s'(L) = \int_0^L [-\ jvc\ \sin(k(L-\tau))V_s(\tau) + \cos(k(L-\tau))I_s(\tau)]d\tau$$

$$= \int_0^L -\ jvc\ \sin(k(L-\tau))\ j\ \frac{\omega\mu}{\eta}\ E_m d\ e^{-jk\tau}$$

$$-\ \cos(k(L-\tau))\ j\omega c\ E_m d\ e^{-jk\tau}]d\tau \qquad (4\text{-}8)$$

Evaluation and simplification of equation (4-8) (see Appendix IV for the details) yields

$$I_s'(L) = -\ j\ \frac{E_m d}{R_c}\ \sin(kL) \qquad (4\text{-}9)$$

Equations (4-7) and (4-9) can now be substituted into equation (2-51) to obtain

$$I(0) = \frac{j\ E_m d \sin(kL) + j\ E_m d \frac{R}{R_c} \sin(kL)}{2(R\cos(kL)) + j(R_c + \frac{R^2}{R_c}) \sin(kL)} \qquad (4\text{-}10)$$

Multiplying numerator and denominator by R_c and rearranging the numerator,

$$I(0) = \frac{j\ E_m d(R_c + R) \sin(kL)}{2(R\ R_c \cos(kL)) + j(R_c^2 + R^2) \sin(kL)} \qquad (4\text{-}11)$$

The imaginary and real terms in the denominator can never be zero at the same frequency, so I(0) is never singular. However, nulls will occur at frequencies which cause the sine function in the numerator to be zero; sin(kL) equals zero when:

$$kL = n\pi, \qquad n = 0,1,2,... \qquad (4\text{-}12)$$

As defined in an earlier chapter, $k = \frac{\omega}{v}$, giving

$$\frac{\omega}{v} L = n\pi \qquad (4\text{-}13)$$

Substituting 2π times frequency, f, for the radian frequency, ω, and rearranging,

$$f = n\left(\frac{v}{2L}\right) \tag{4-14}$$

Substituting for the velocity of light and line length of one meter gives

$$f = n(150\ \text{MHz}) \tag{4-15}$$

This says that zero nulls will occur at frequencies which are multiples of 150 megahertz, or when the line length is a multiple of a half-wavelength.

At low frequencies, when k becomes small, the cosine function in the denominator will approach one and the imaginary term will become insignificant as sin(kL) approaches zero, so the denominator will become constant. In the numerator, sin(kL) will be approximately kL. Since the numerator will then vary approximately as frequency varies and the denominator will be essentially constant, I(0) will vary approximately as a linear function of frequency.

At high frequencies, I(0) will reach a maximum value at the midpoint between each null, or when

$$kL = n\pi + \frac{\pi}{2} \tag{4-16}$$

which corresponds to

$$f = n(150\ \text{MHz}) + 75\ \text{MHz} \tag{4-17}$$

At these points sin(kL) is equal to one and cos(kL) is equal to zero, and equation (4-11) becomes

$$I(0) = \frac{E_m d(R_c + R)}{(R_c^2 + R^2)} \tag{4-18}$$

giving the maximum current value, which is a constant.

Anticipating the behavior just described, the transmission line program listed in Appendix III was used to generate terminal current predictions for the three loading conditions described earlier. The method of moments solution was produced by the program OSMOM. Transmission line model predictions are represented by the solid curve and OSMOM predictions are represented by the "O's" at discrete points on all plots in this chapter.

PLOTS 4-1(a) and 4-1(b) show the magnitude and phase respectively for terminal currents at x=0 with matched loads and ENDFIRE excitation. The transmission line model results compare quite favorably with the method of moments results over the fairly wide frequency range shown, 10 megahertz to 1 gigahertz. PLOTS 4-2(a) and 4-2(b) show the same

configuration over the lower frequency range of 100 kilohertz to 10 megahertz. Two important characteristics should be pointed out here. First, the linear response of the transmission line model predictions occurs as was anticipated. Secondly, the method of moments technique breaks down numerically, as expected. Predictions by the method of moments could not be obtained for frequencies below those represented and those shown are not particularly good.

PLOTS 4-3(a) and 4-3(b) show the magnitude and phase respectively for the same conditions as PLOTS 4-1(a) and 4-1(b) except that here the low impedance loads are used instead of matched loads. The transmission line model predictions are generally good. However, some slight discrepancies occur between the method of moments results and the transmission line model results as frequency increases. These differences might be caused by reradiation off of the terminal wires, accounted for in the method of moments solution. That is, the method of moments models the loads as part of the physical line, as discussed in Chapter 3. For low impedance loads, relatively large currents flowing on the terminal wires radiate as antennas. This reradiation by the terminal wires is accounted for in the method of moments solution, but not in the transmission line model. This effect is similar to that encountered in [16]. It was noted in [16] that transmission line theory did not predict resonances for currents induced in the terminations of a transmission line where the loads were replaced by

short circuits at both ends. Further, it was inferred that these resonances do exist for the short circuit case (which is an extreme of the low impedance case) as predicted by other solution methods (such as the method of moments). This explanation is enforced by the predictions for higher impedance loads, where discrepancy does not occur. High impedance loads would tend not to radiate as freely as low impedance loads. As the impedance of the loads is increased, eventually the termination will begin to look like an open circuit and the transmission line will behave as two separate wires in free space.

PLOTS 4-4(a) and 4-4(b) are the low frequency predictions for the same low impedance configuration of PLOTS 4-3(a) and 4-3(b). The numerical solution of Method of Moments is inaccurate in this range. PLOTS 4-5(a and b) and 4-6(a and b) show the predictions for high impedance loads. The results are very good as was with the matched case. The plots for the ENDFIRE case are summarized in TABLE 4-1(a).

The second case to be considered has the plane wave incident from the side of the structure (see FIGURE 4-2), this it will be referred to as the SIDEFIRE case. The wave is propagating in the positive y direction striking the bottom wire first. From the transmission line model standpoint, the E field cannot contribute any induced sources because it does not have a y component. However, choosing an x-directed

PLOT 4-1 (A)

EXCITATION: ENDFIRE
LOADING: MATCHED

LINE DIMENSIONS (METERS)

LENGTH	=	1.0
SEPARATION	=	0.01
RADIUS	=	0.0001

TRANSMISSION LINE MODEL — OSMOM ①

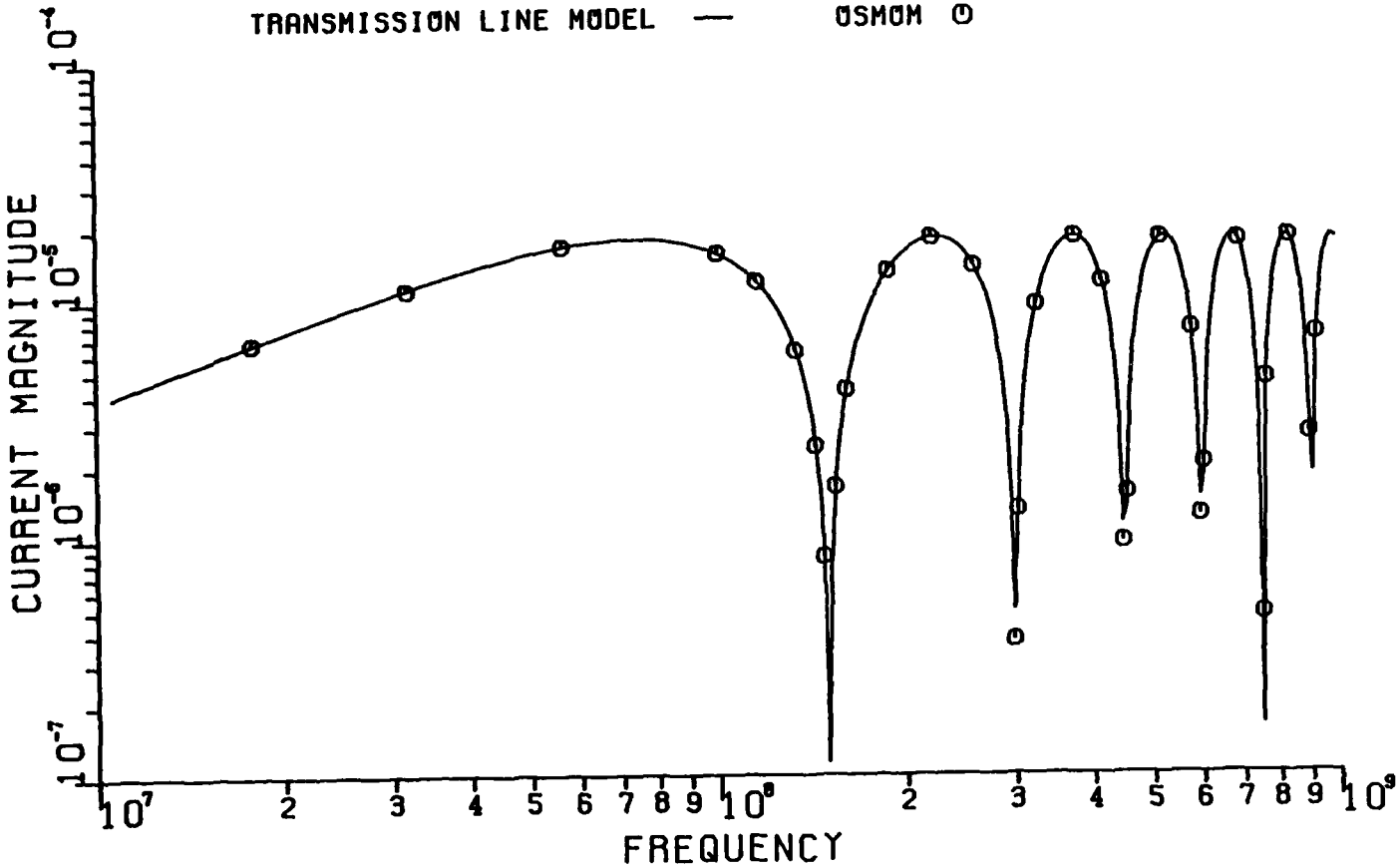

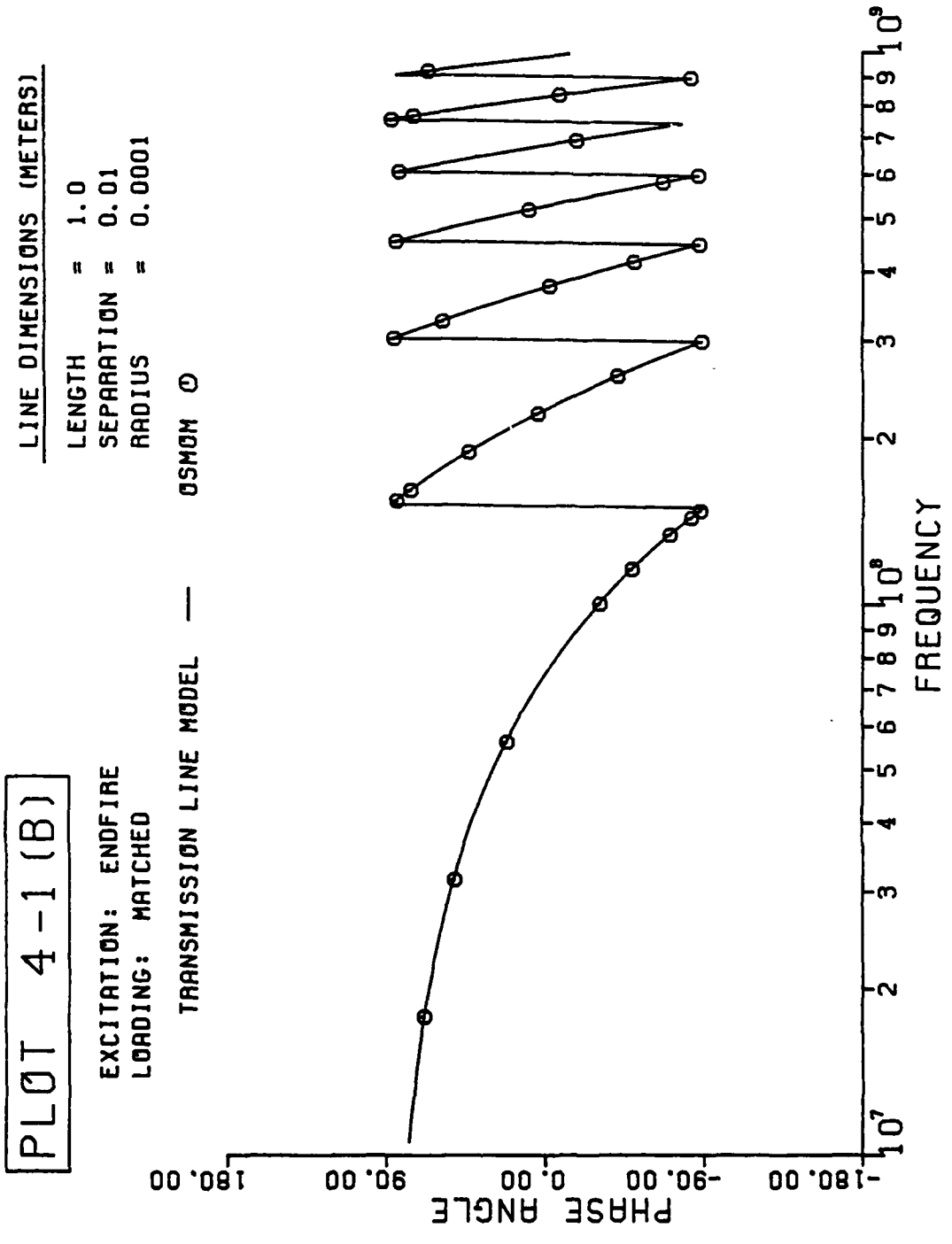
PLOT 4-1 (B)
EXCITATION: ENDFIRE
LOADING: MATCHED
TRANSMISSION LINE MODEL — OSMOM Ø
LINE DIMENSIONS (METERS)
LENGTH = 1.0
SEPARATION = 0.01
RADIUS = 0.0001
PHASE ANGLE
180.00
90.00
0.00
-90.00
-180.00
FREQUENCY
10^7
2
3
4
5
6
7
8
9
10^8
2
3
4
5
6
7
8
9
10^9

PLOT 4-2(A)

EXCITATION: ENDFIRE
LOADING: MATCHED

LINE DIMENSIONS (METERS)

LENGTH	=	1.0
SEPARATION	=	0.01
RADIUS	=	0.0001

TRANSMISSION LINE MODEL —— OSMOM ⊙

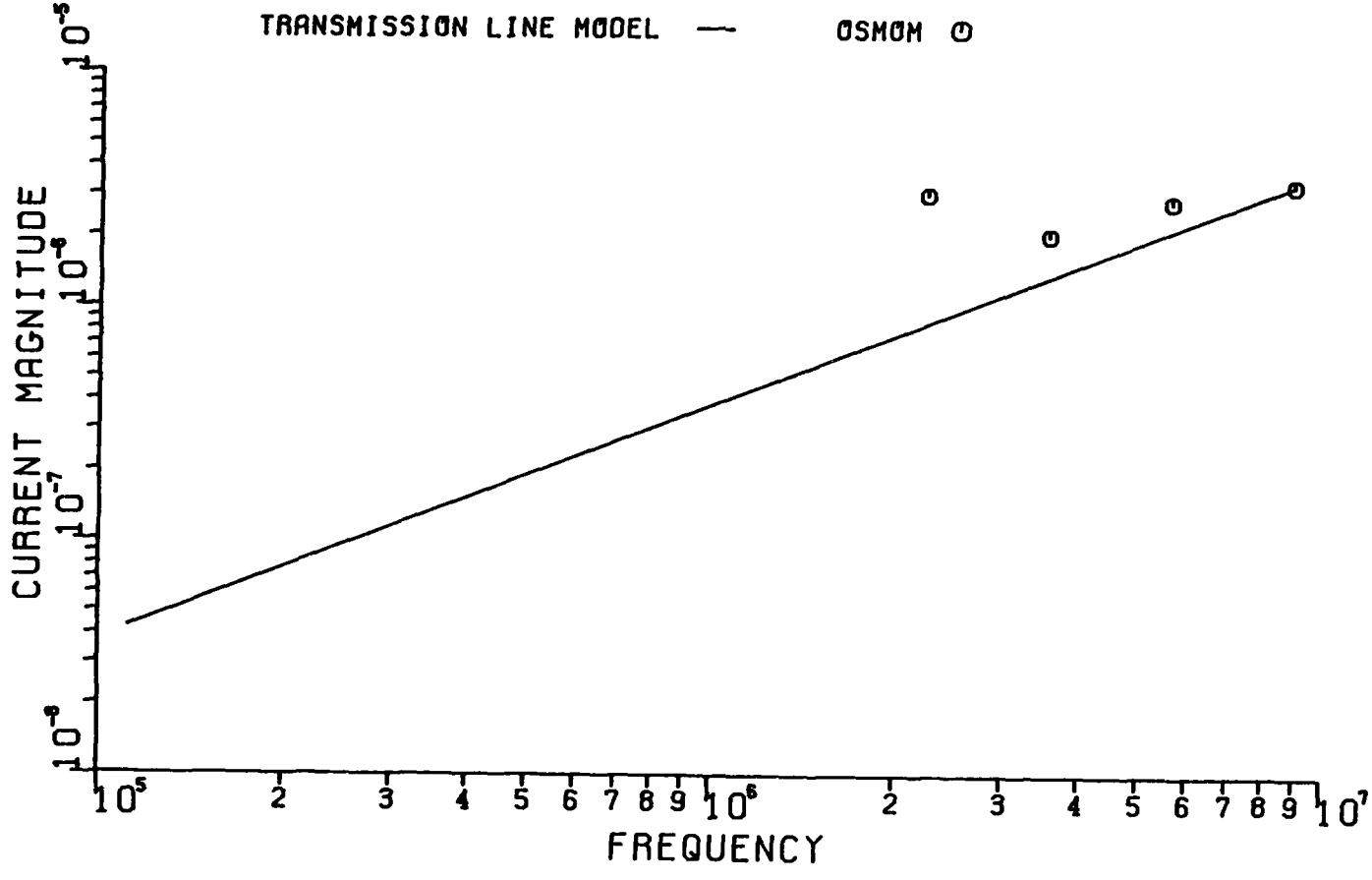

PLOT 4-2(B)

LINE DIMENSIONS (METERS)

LENGTH = 1.0
SEPARATION = 0.01
RADIUS = 0.0001

EXCITATION: ENDFIRE
LOADING: MATCHED

TRANSMISSION LINE MODEL — OSMOM ⊙

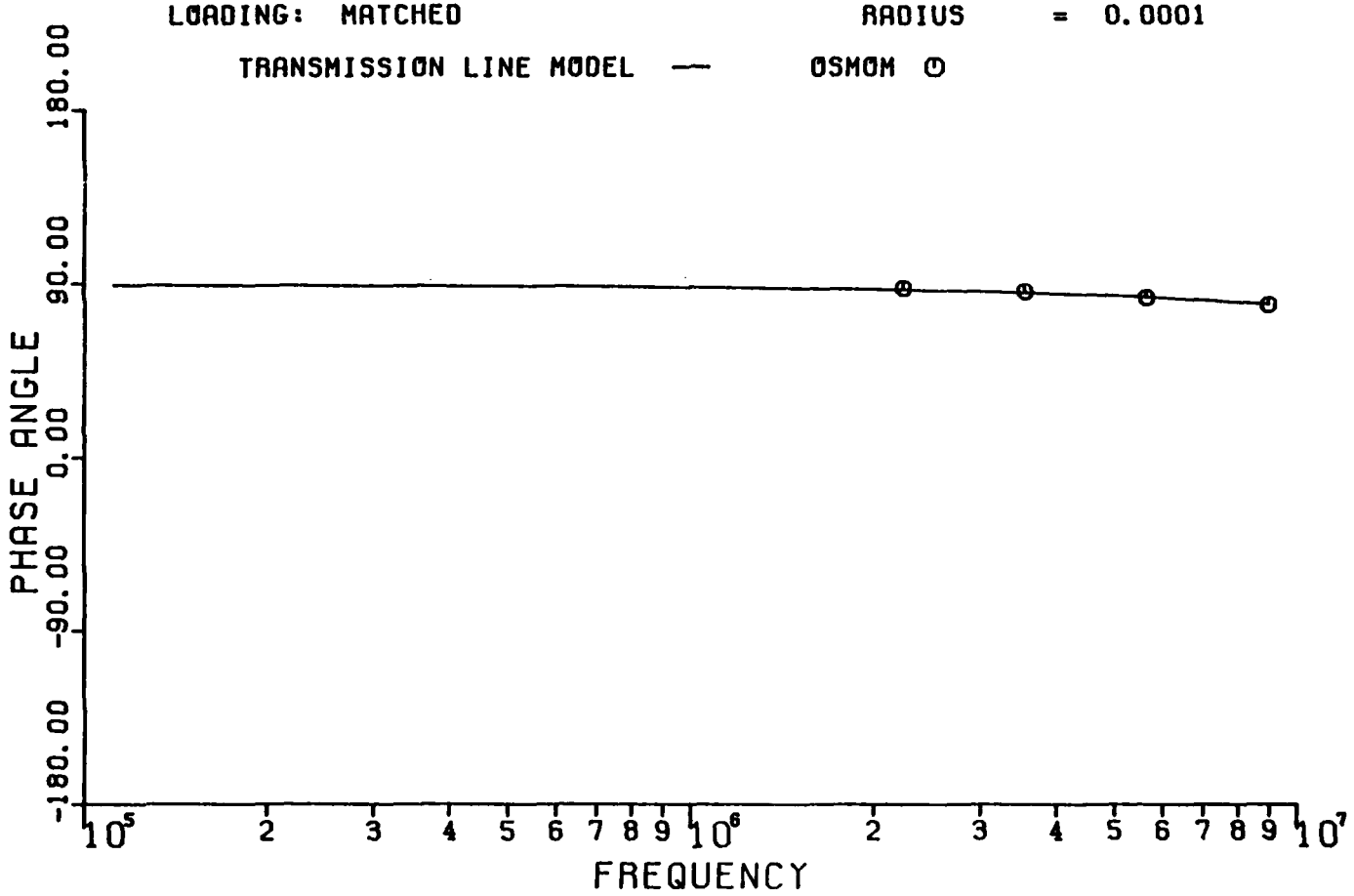

PLOT 4-3(A)

EXCITATION: ENDFIRE
LOADING: LOW IMPEDANCE

LINE DIMENSIONS (METERS)

LENGTH	=	1.0
SEPARATION	=	0.01
RADIUS	=	0.0001

TRANSMISSION LINE MODEL — OSMOM ⊙

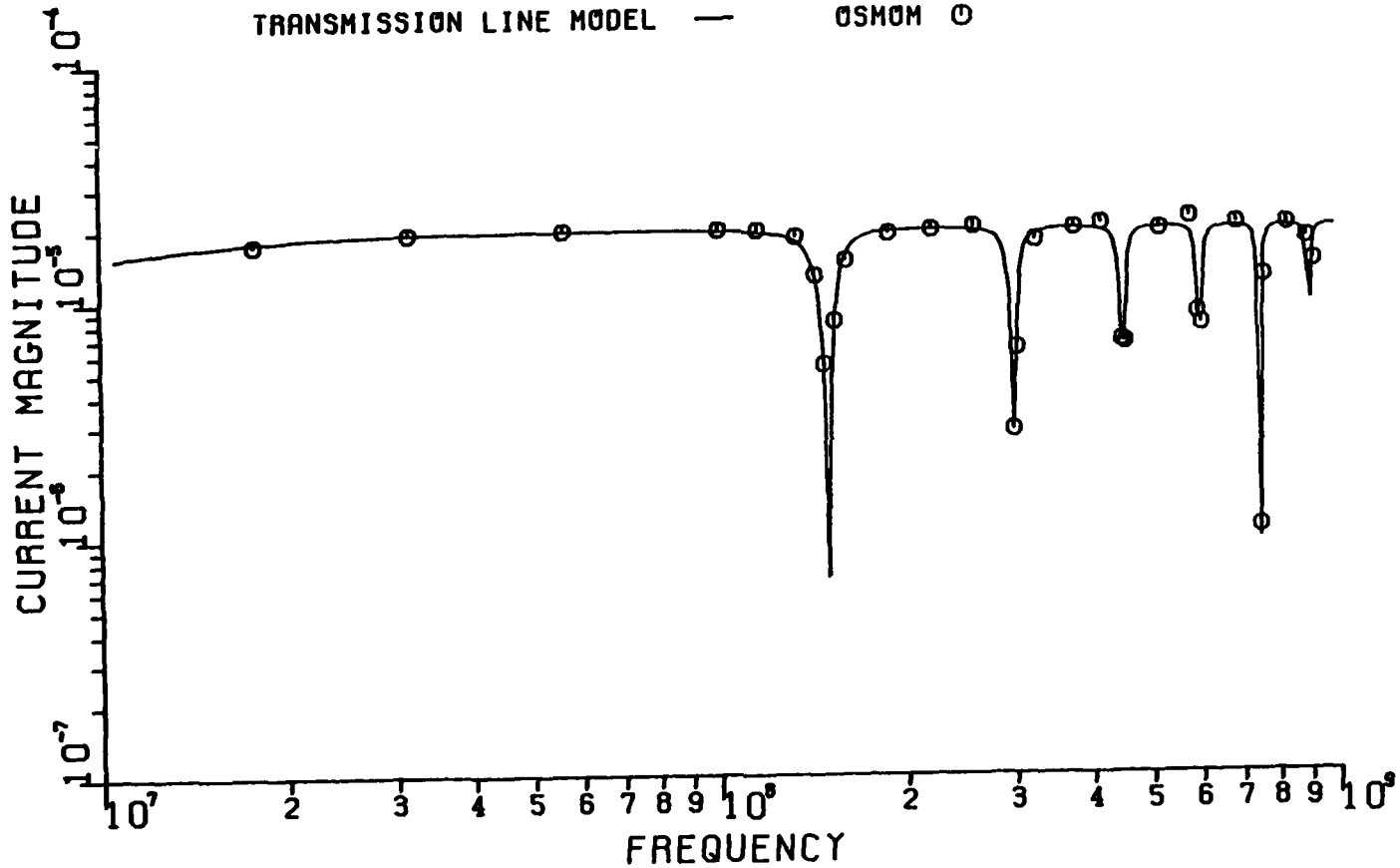

PLOT 4-3(B)

LINE DIMENSIONS (METERS)

LENGTH = 1.0
SEPARATION = 0.01
RADIUS = 0.0001

EXCITATION: ENDFIRE
LOADING: LOW IMPEDANCE

TRANSMISSION LINE MODEL — OSMOM ⊙

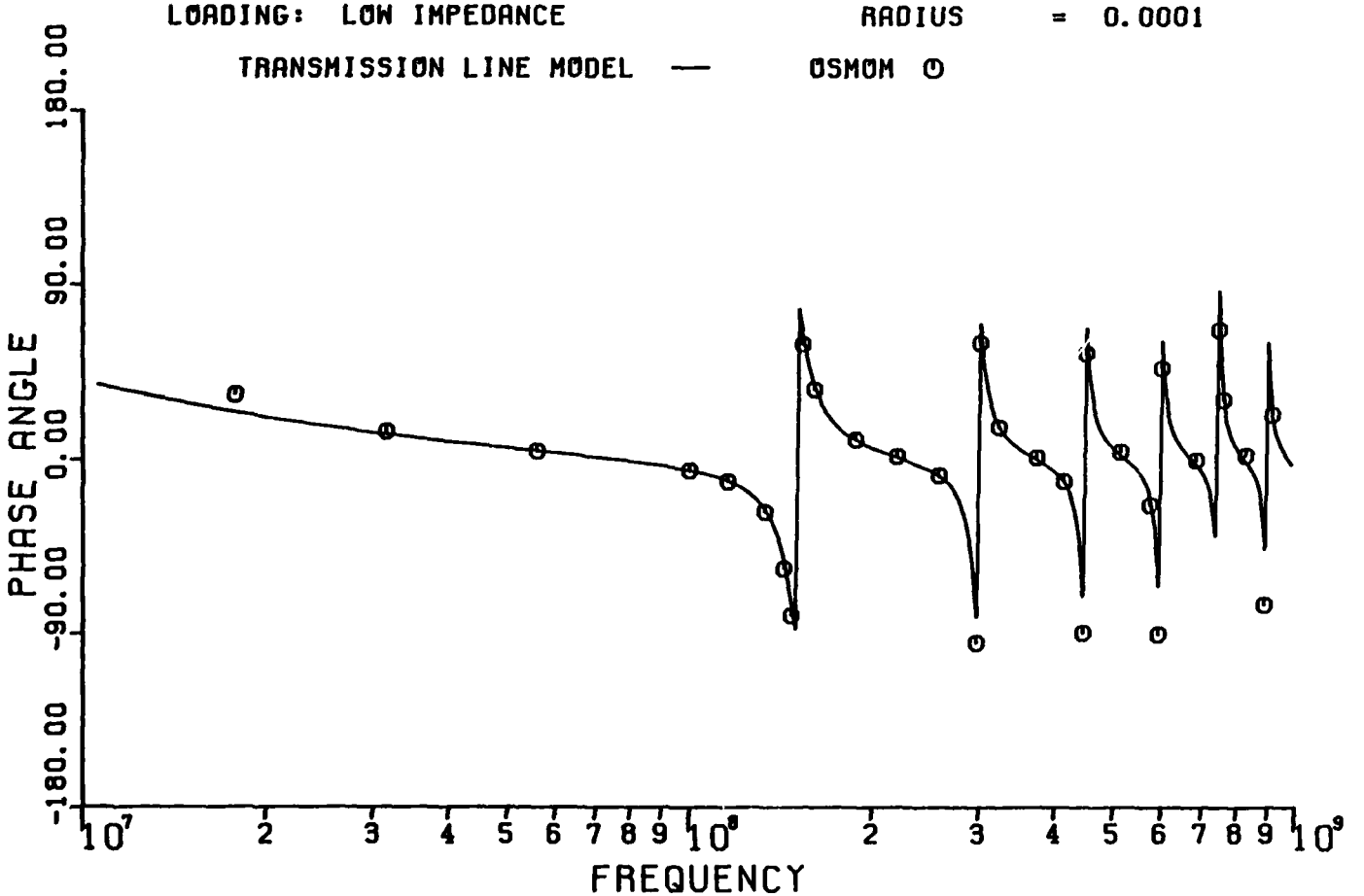

PLOT 4-4 (A)

EXCITATION: ENDFIRE
LOADING: LOW IMPEDANCE

LINE DIMENSIONS (METERS)

LENGTH	=	1.0
SEPARATION	=	0.01
RADIUS	=	0.0001

TRANSMISSION LINE MODEL — OSMOM O

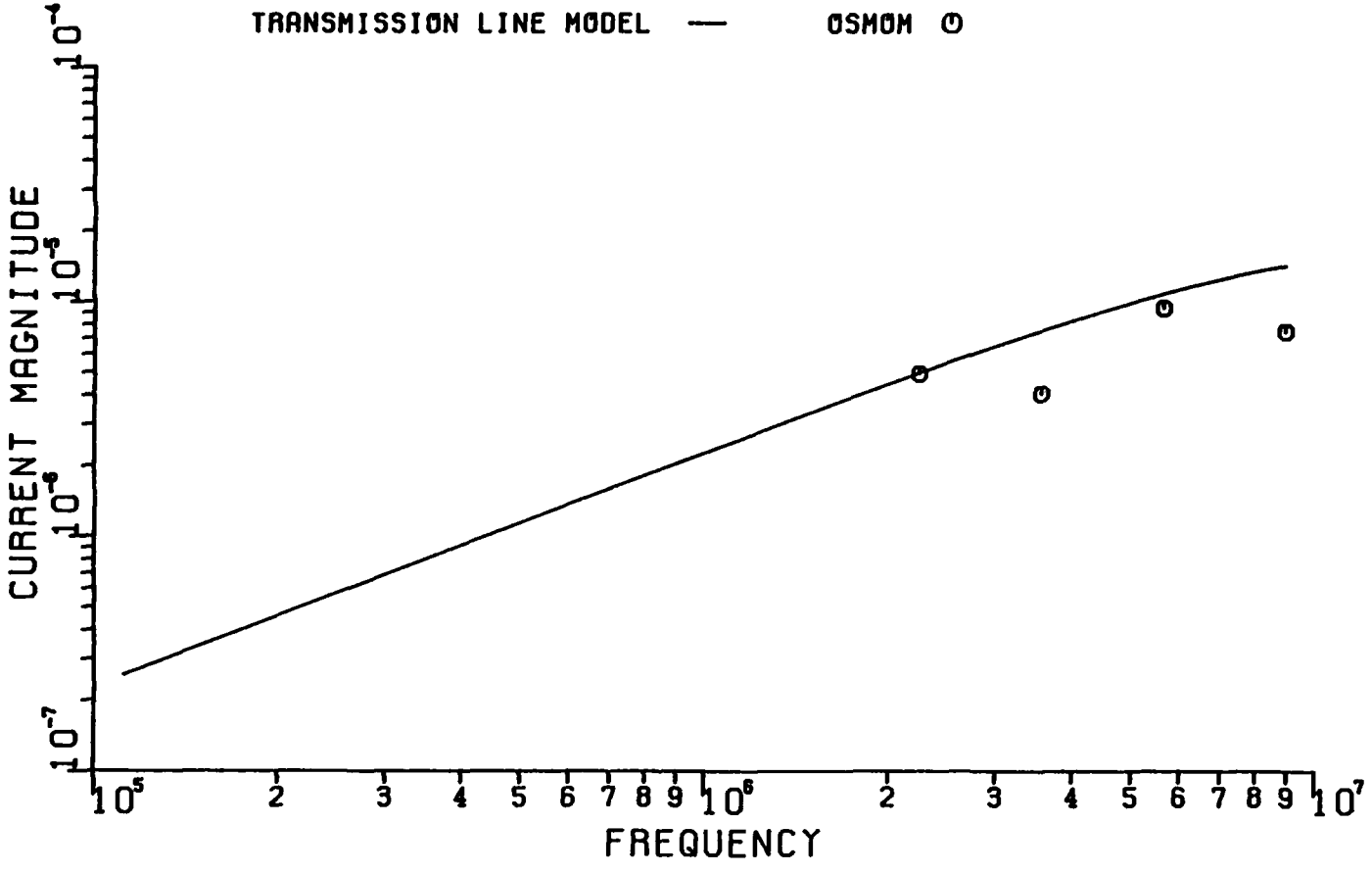

PLOT 4-4(B)

EXCITATION: ENDFIRE
LOADING: LOW IMPEDANCE

LINE DIMENSIONS (METERS)

LENGTH	=	1.0
SEPARATION	=	0.01
RADIUS	=	0.0001

TRANSMISSION LINE MODEL — OSMOM ⊙

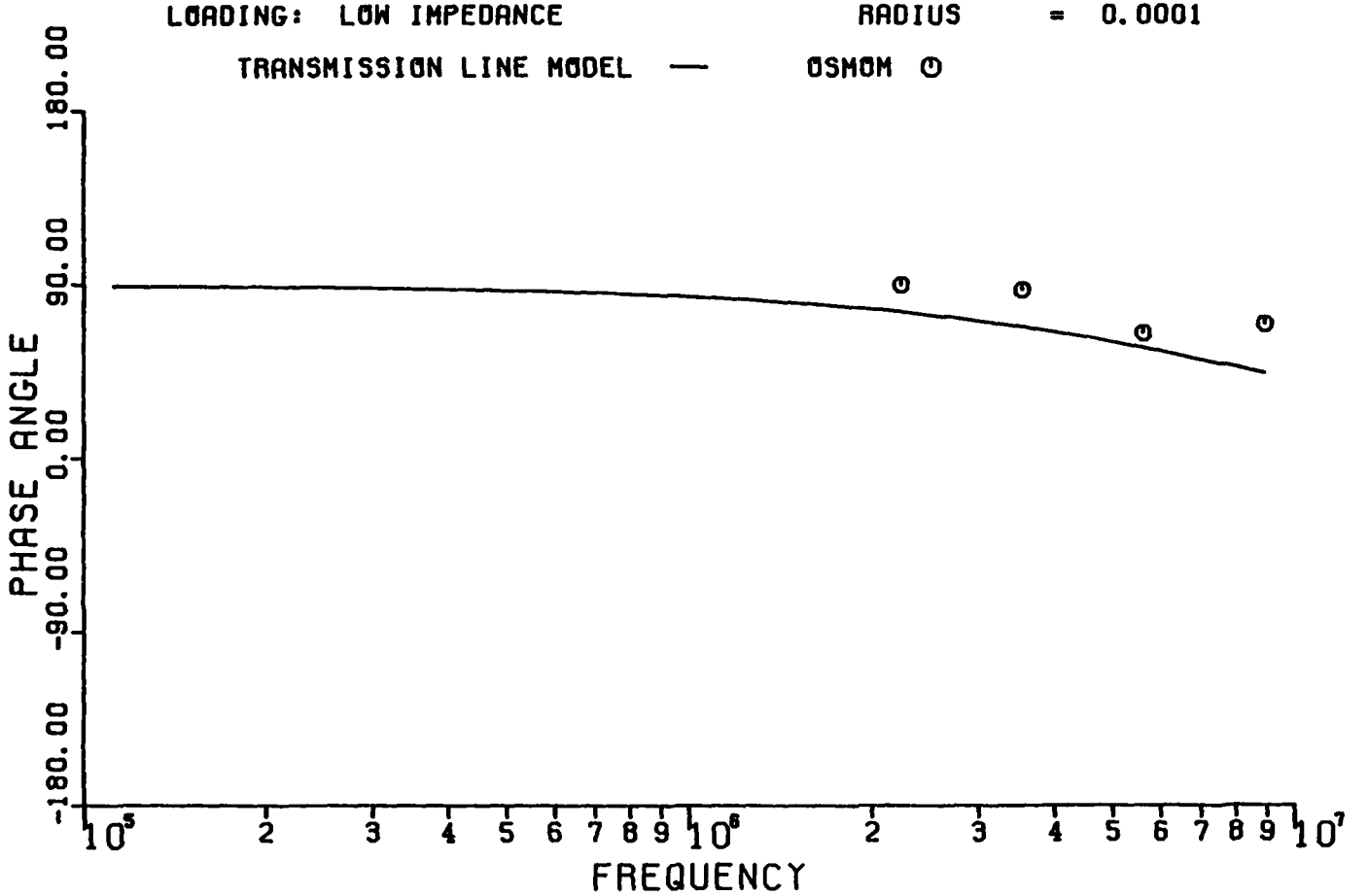

PLOT 4-5(A)

EXCITATION: ENDFIRE
LOADING: HIGH IMPEDANCE

LINE DIMENSIONS (METERS)

LENGTH	=	1.0
SEPARATION	=	0.01
RADIUS	=	0.0001

TRANSMISSION LINE MODEL — OSMOM ⊙

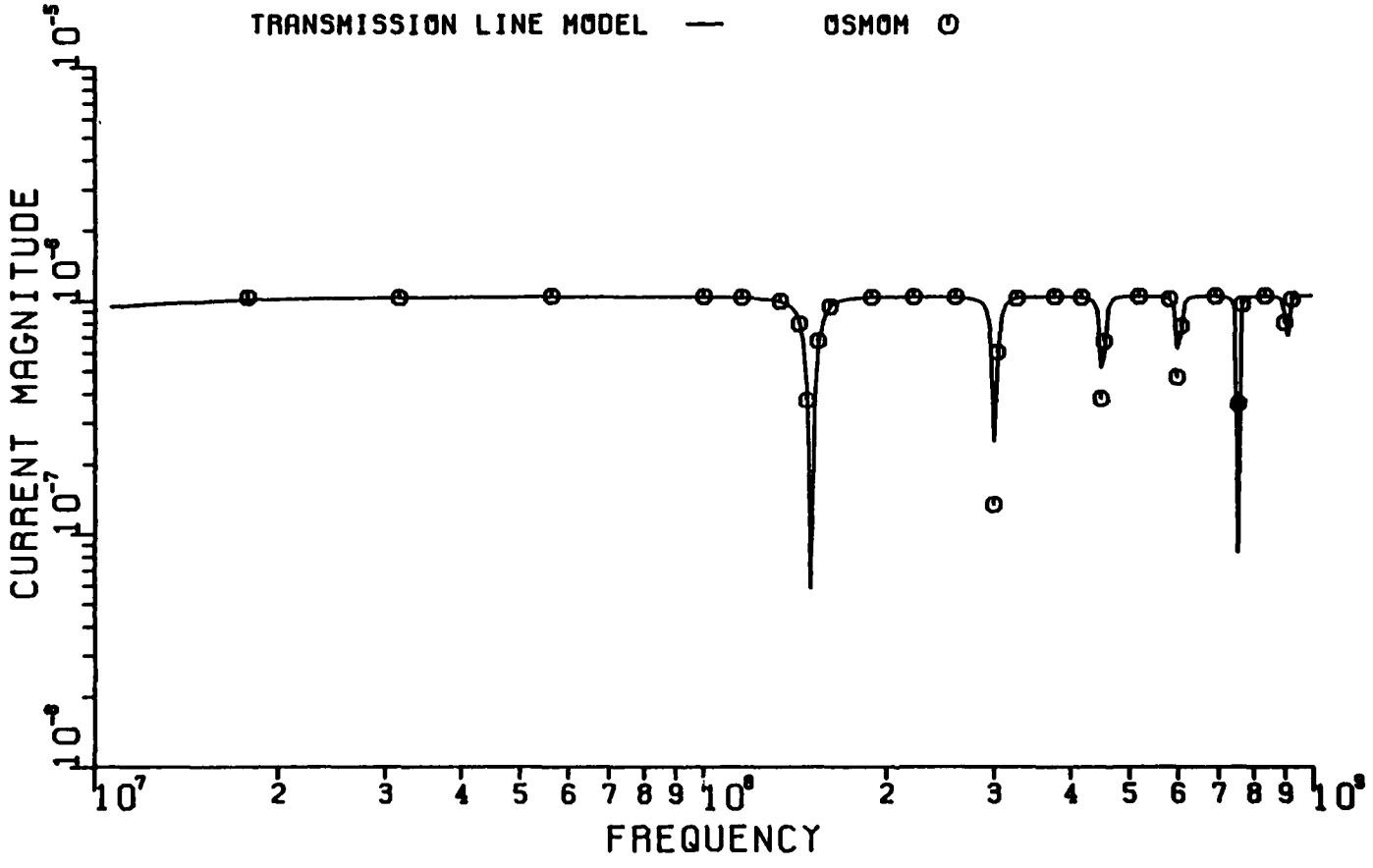

PLOT 4-5 (B)

EXCITATION: ENDFIRE
LOADING: HIGH IMPEDANCE

LINE DIMENSIONS (METERS)

LENGTH	=	1.0
SEPARATION	=	0.01
RADIUS	=	0.0001

TRANSMISSION LINE MODEL — OSMOM ⓪

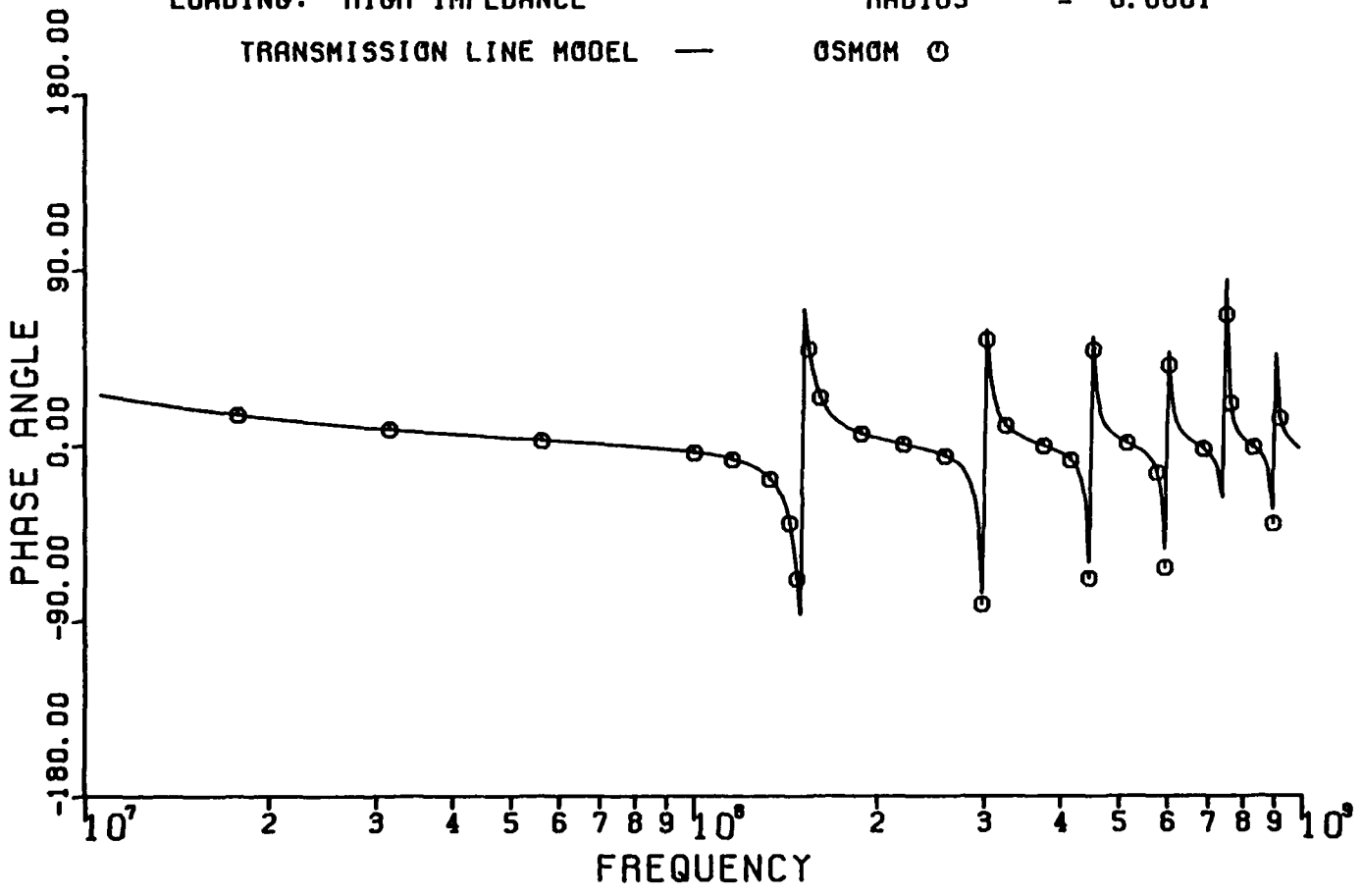

PLOT 4-6 (A)

EXCITATION: ENDFIRE
LOADING: HIGH IMPEDANCE

LINE DIMENSIONS (METERS)

LENGTH	=	1.0
SEPARATION	=	0.01
RADIUS	=	0.0001

TRANSMISSION LINE MODEL — OSMOM ①

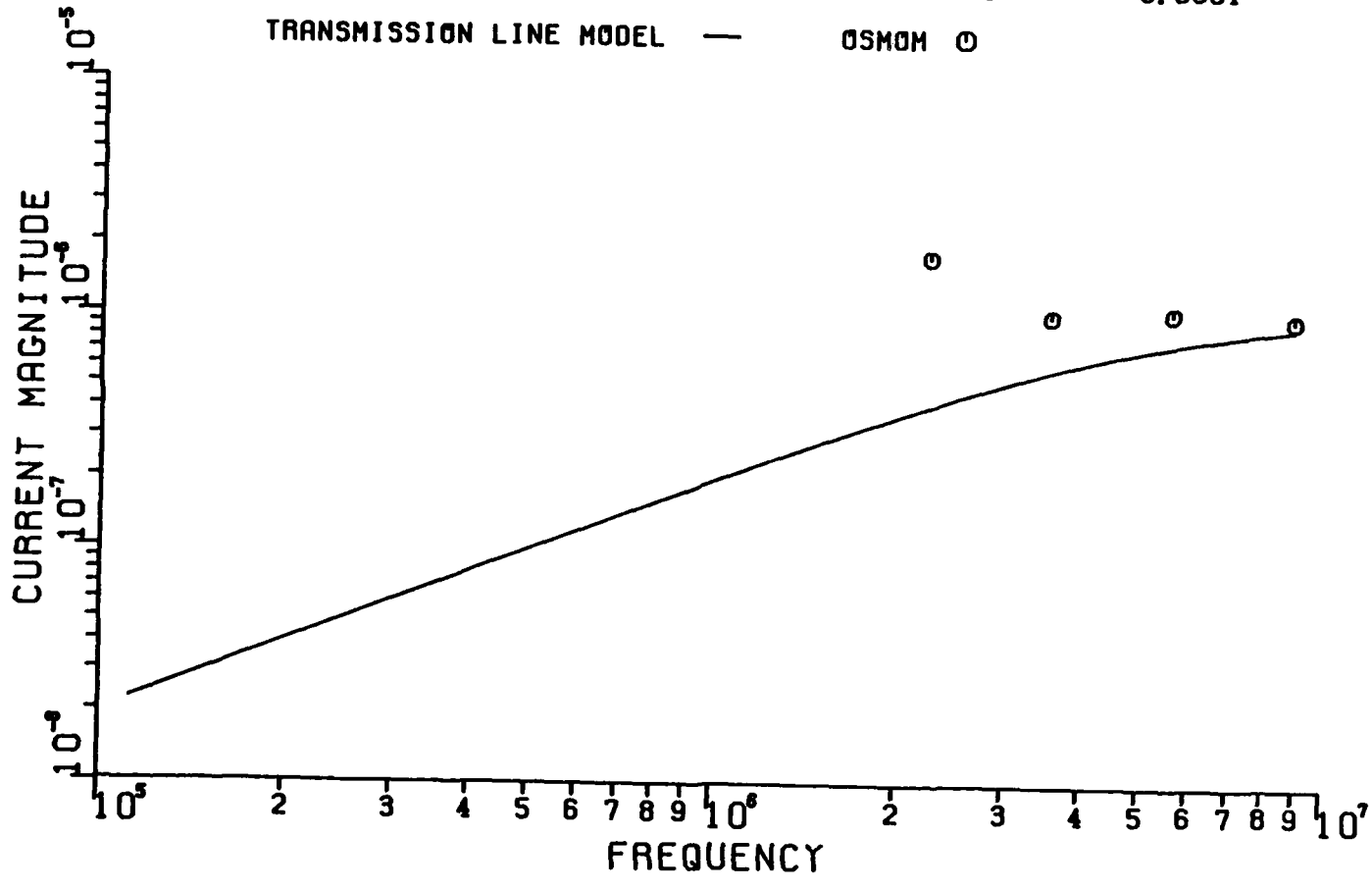

PLOT 4-6(B)

LINE DIMENSIONS (METERS)

LENGTH = 1.0
SEPARATION = 0.01
RADIUS = 0.0001

EXCITATION: ENDFIRE
LOADING: HIGH IMPEDANCE

TRANSMISSION LINE MODEL — OSMOM ⊙

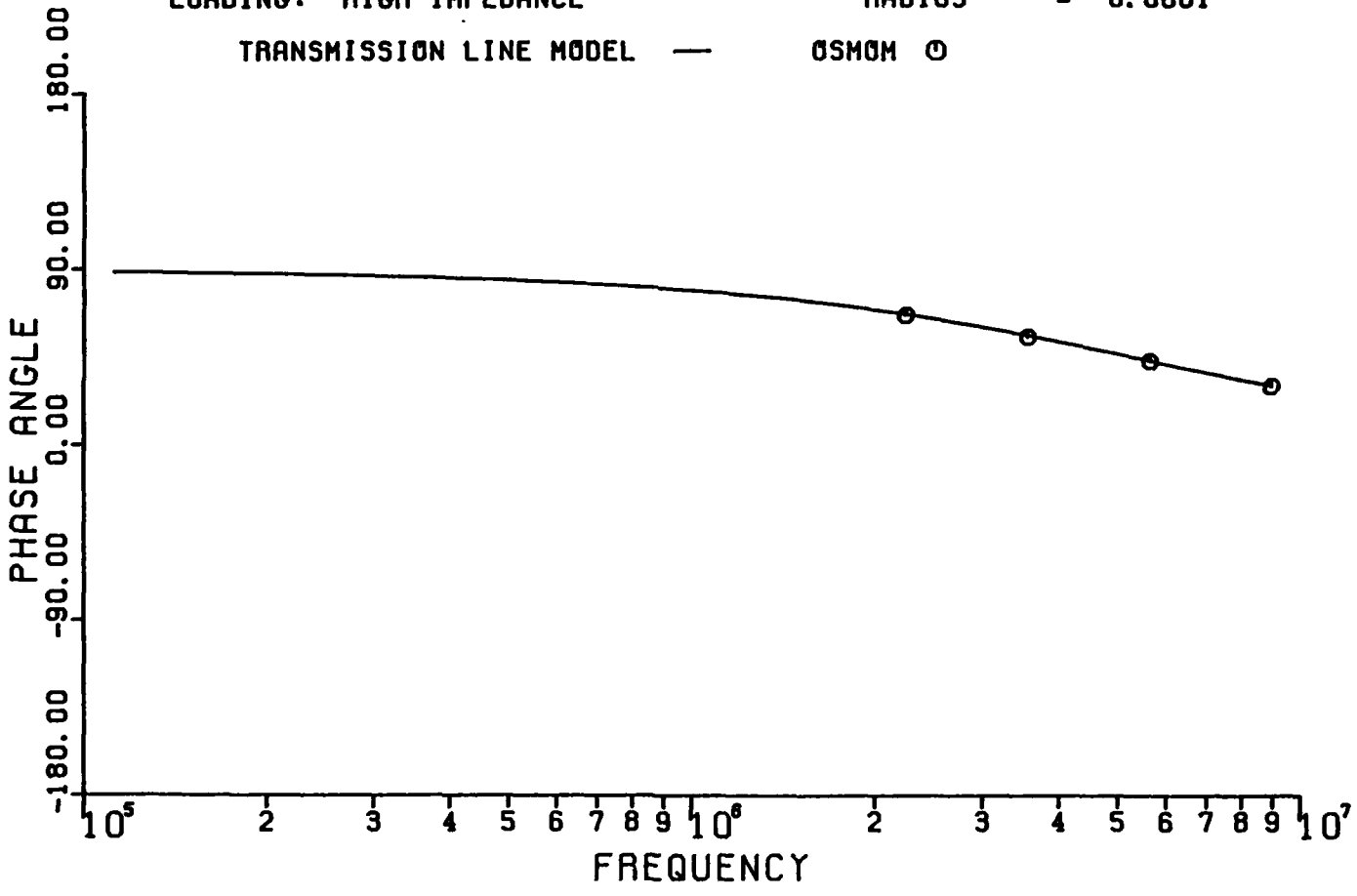

Loading	High Frequency	Low Frequency	
Matched	4-1	4-2	
Low Impedance	4-3	4-4	(a)
High Impedance	4-5	4-6	

ENDFIRE

Loading	High Frequency	Low Frequency	
Matched	4-7	4-8	
Low Impedance	4-9	4-10	(b)
High Impedance	4-5	4-6	

SIDEFIRE

Loading	High Frequency	Low Frequency	
Matched	4-13	4-14	
Low Impedance	4-15	4-16	(c)
High Impedance	4-17	4-18	

BROADSIDE

TABLE 4-1

PLOT 4-7(A)

EXCITATION: SIDEFIRE
LOADING: MATCHED

LINE DIMENSIONS (METERS)

LENGTH	=	1.0
SEPARATION	=	0.01
RADIUS	=	0.0001

TRANSMISSION LINE MODEL — OSMOM ⊙

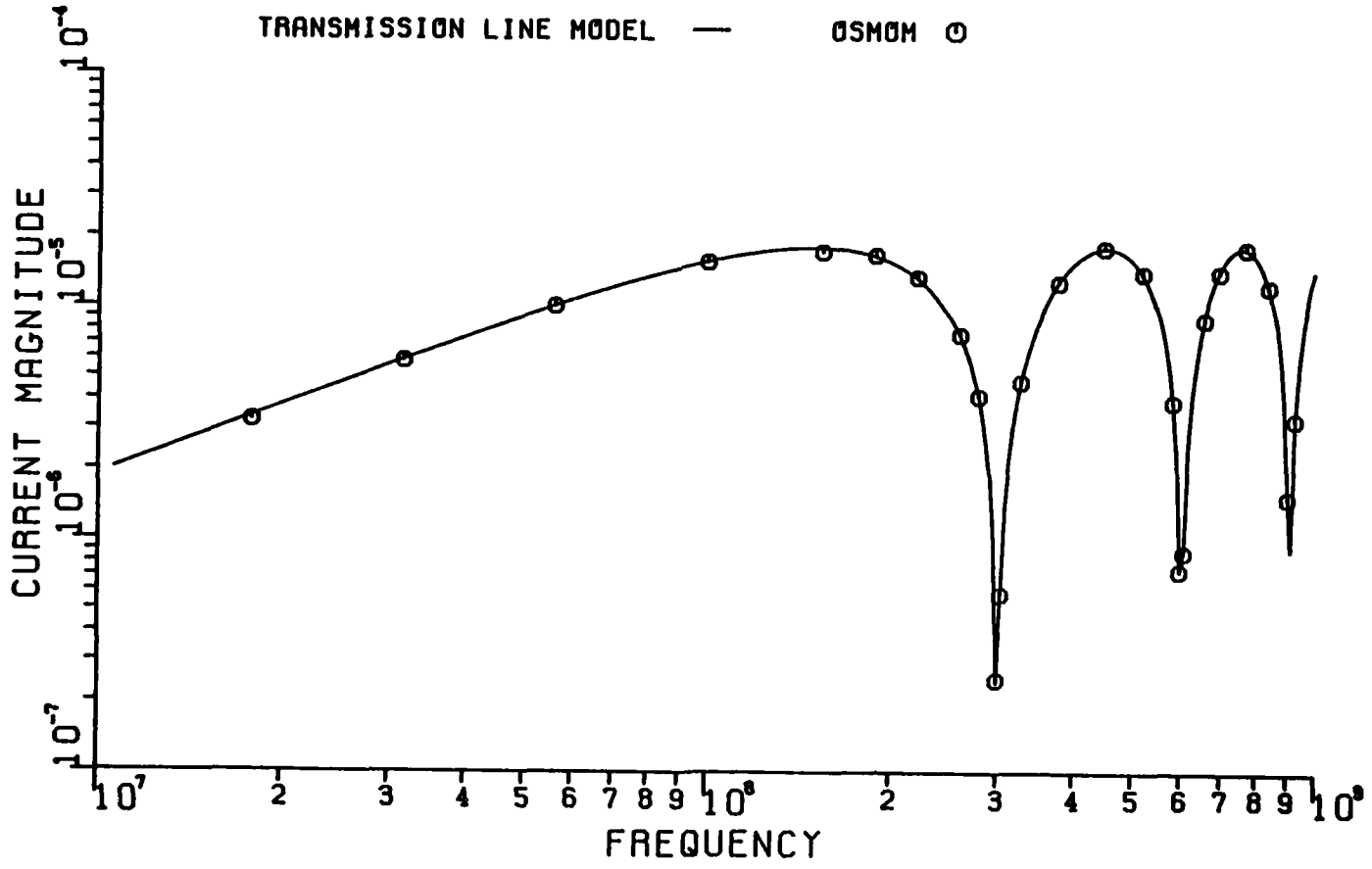

PLOT 4-7(B)

LINE DIMENSIONS (METERS)

LENGTH = 1.0
SEPARATION = 0.01
RADIUS = 0.0001

EXCITATION: SIDEFIRE
LOADING: MATCHED

TRANSMISSION LINE MODEL —— OSMOM ⊙

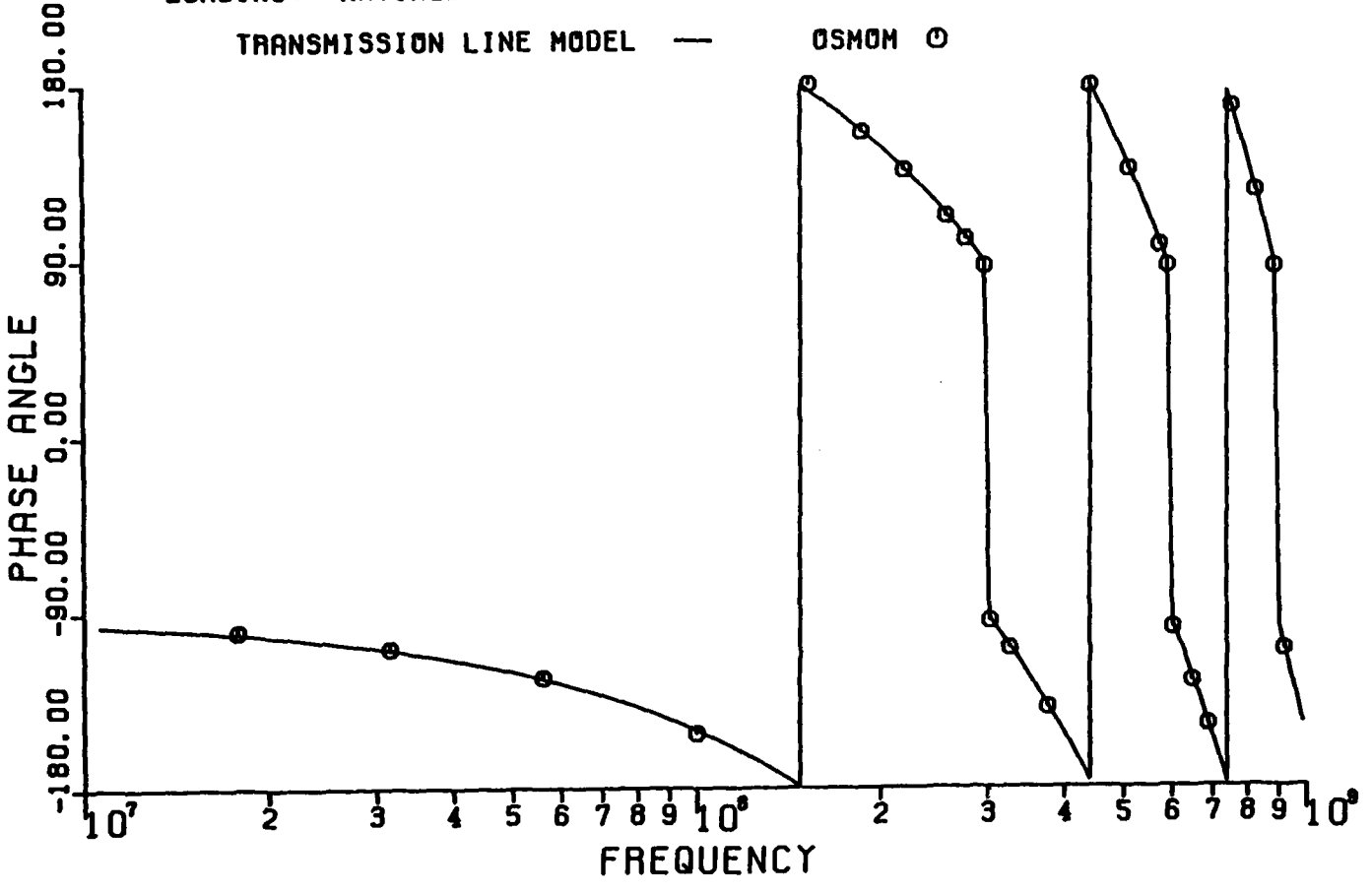

PLOT 4-8(A)

EXCITATION: SIDEFIRE
LOADING: MATCHED

LINE DIMENSIONS (METERS)

LENGTH	=	1.0
SEPARATION	=	0.01
RADIUS	=	0.0001

TRANSMISSION LINE MODEL — OSMOM ⊙

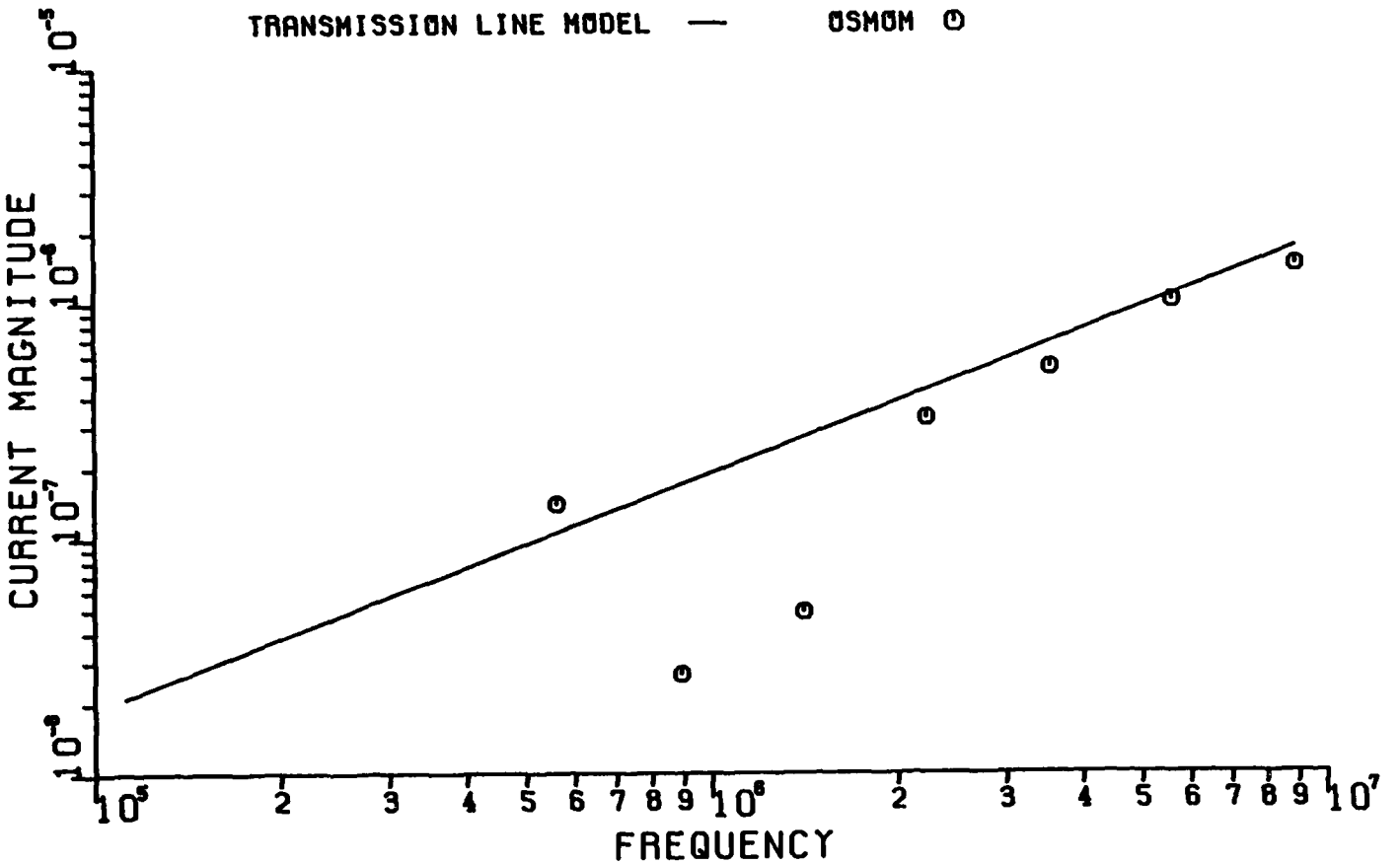

PLOT 4-8(B)

EXCITATION: SIDEFIRE
LOADING: MATCHED

LINE DIMENSIONS (METERS)

LENGTH	=	1.0
SEPARATION	=	0.01
RADIUS	=	0.0001

TRANSMISSION LINE MODEL — OSMOM ⊙

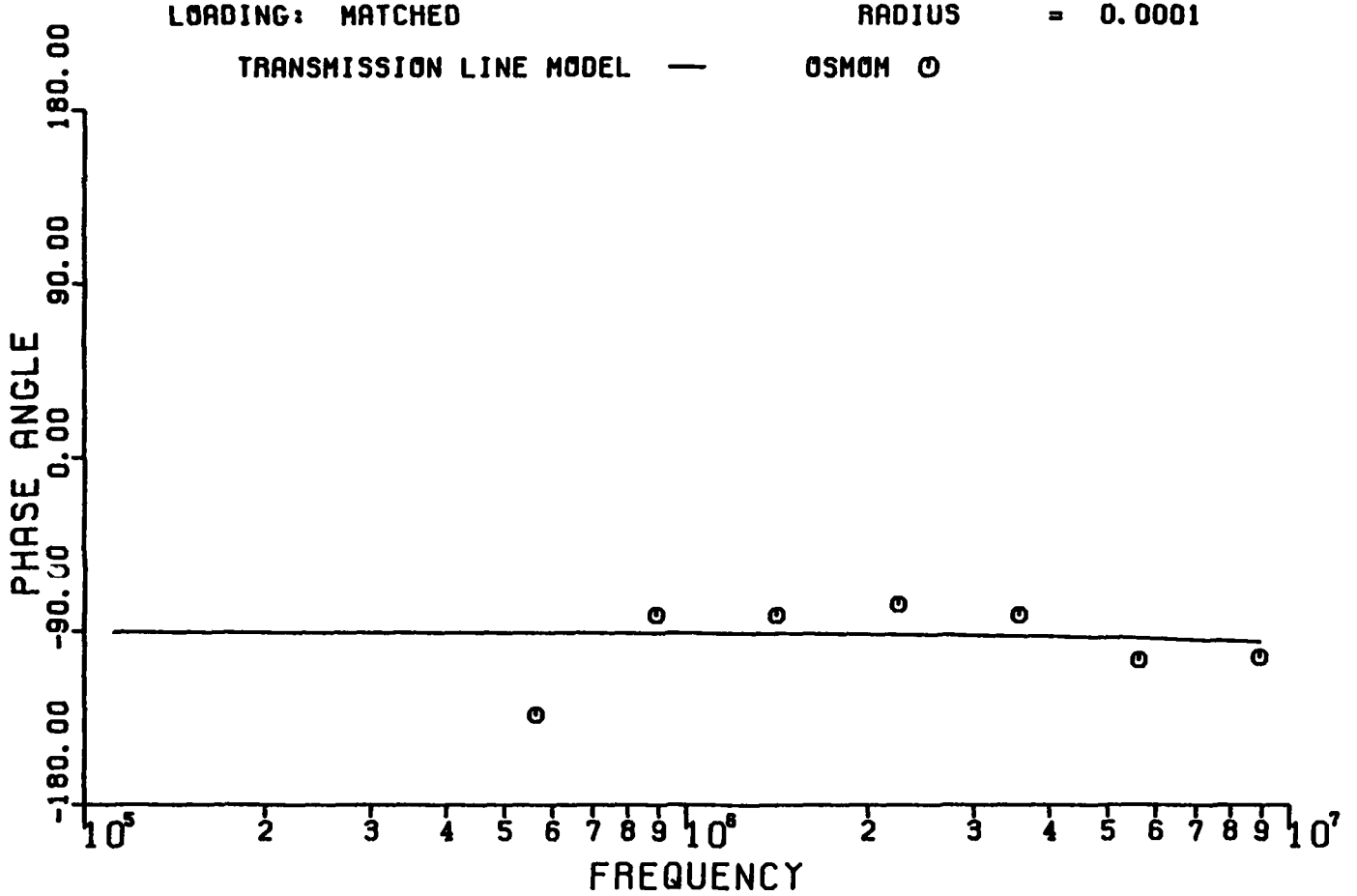

PLOT 4-9(A)

EXCITATION: SIDEFIRE
LOADING: LOW IMPEDANCE

LINE DIMENSIONS (METERS)

LENGTH	=	1.0
SEPARATION	=	0.01
RADIUS	=	0.0001

TRANSMISSION LINE MODEL — OSMOM ⊙

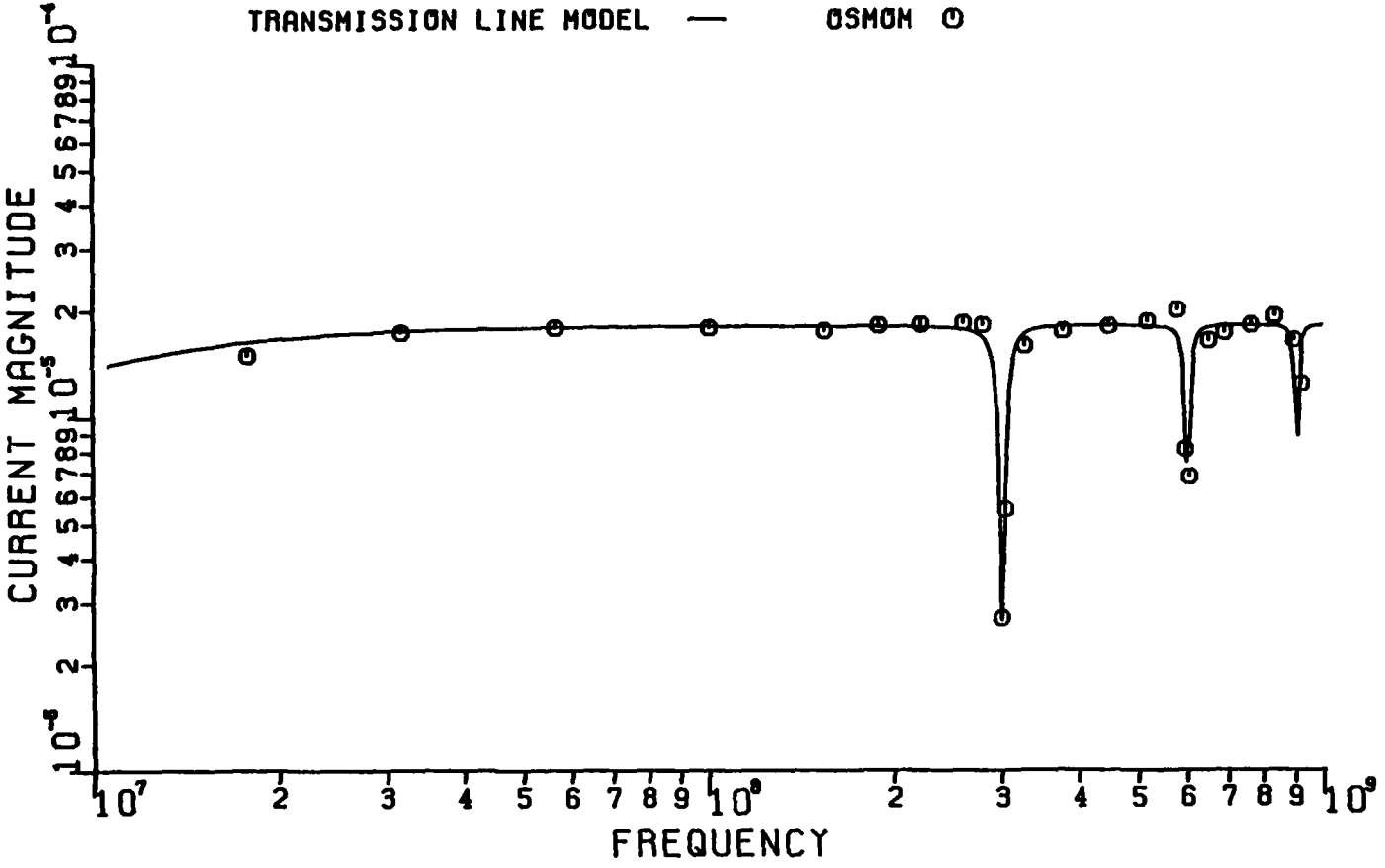

PLOT 4-9(B)

LINE DIMENSIONS (METERS)

LENGTH = 1.0
SEPARATION = 0.01
RADIUS = 0.0001

EXCITATION: SIDEFIRE
LOADING: LOW IMPEDANCE

TRANSMISSION LINE MODEL — OSMOM ⊙

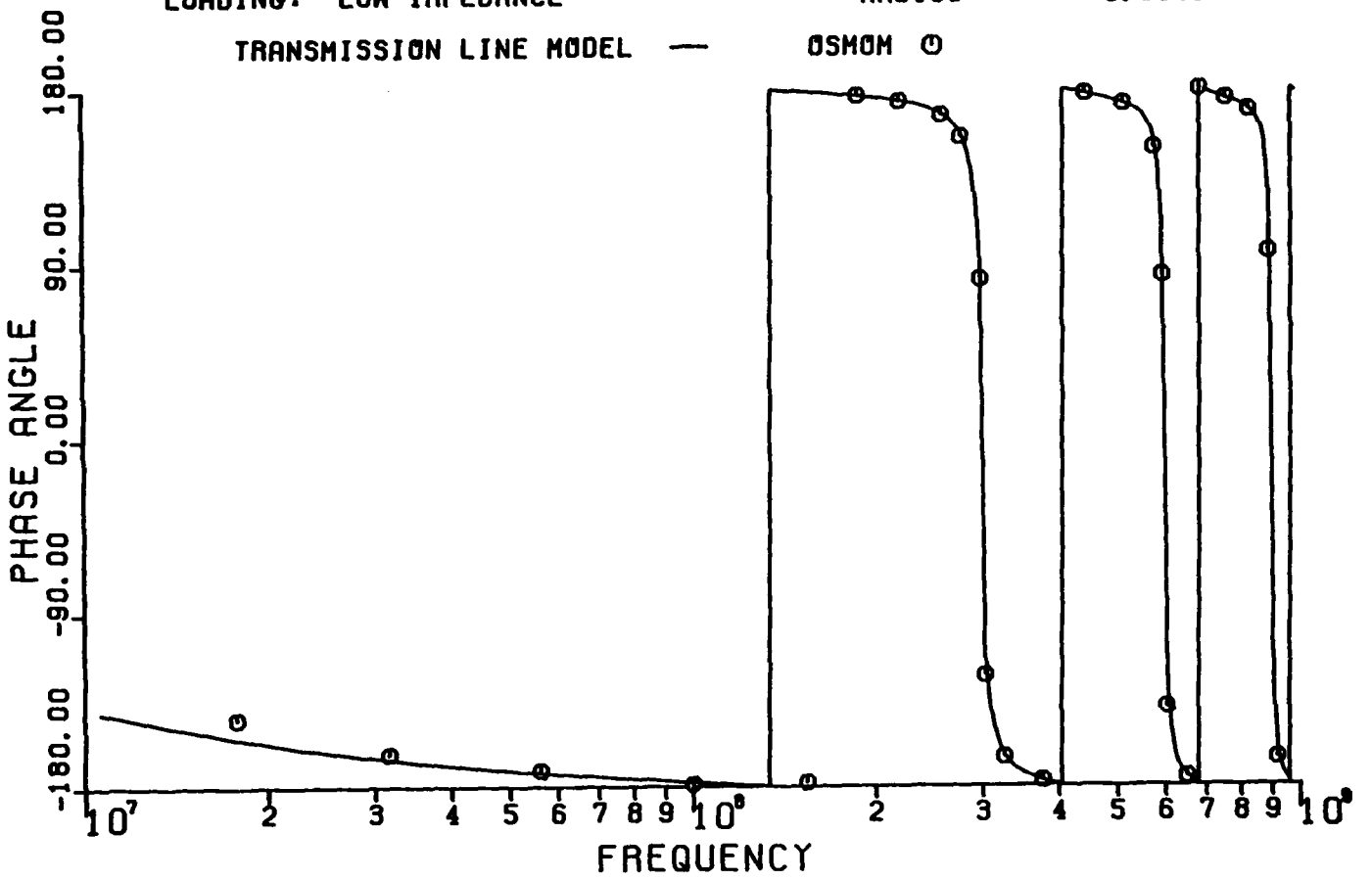

PLOT 4-10(A)

EXCITATION: SIDEFIRE
LOADING: LOW IMPEDANCE

LINE DIMENSIONS (METERS)

LENGTH	=	1.0
SEPARATION	=	0.01
RADIUS	=	0.0001

TRANSMISSION LINE MODEL — OSMOM ⓤ

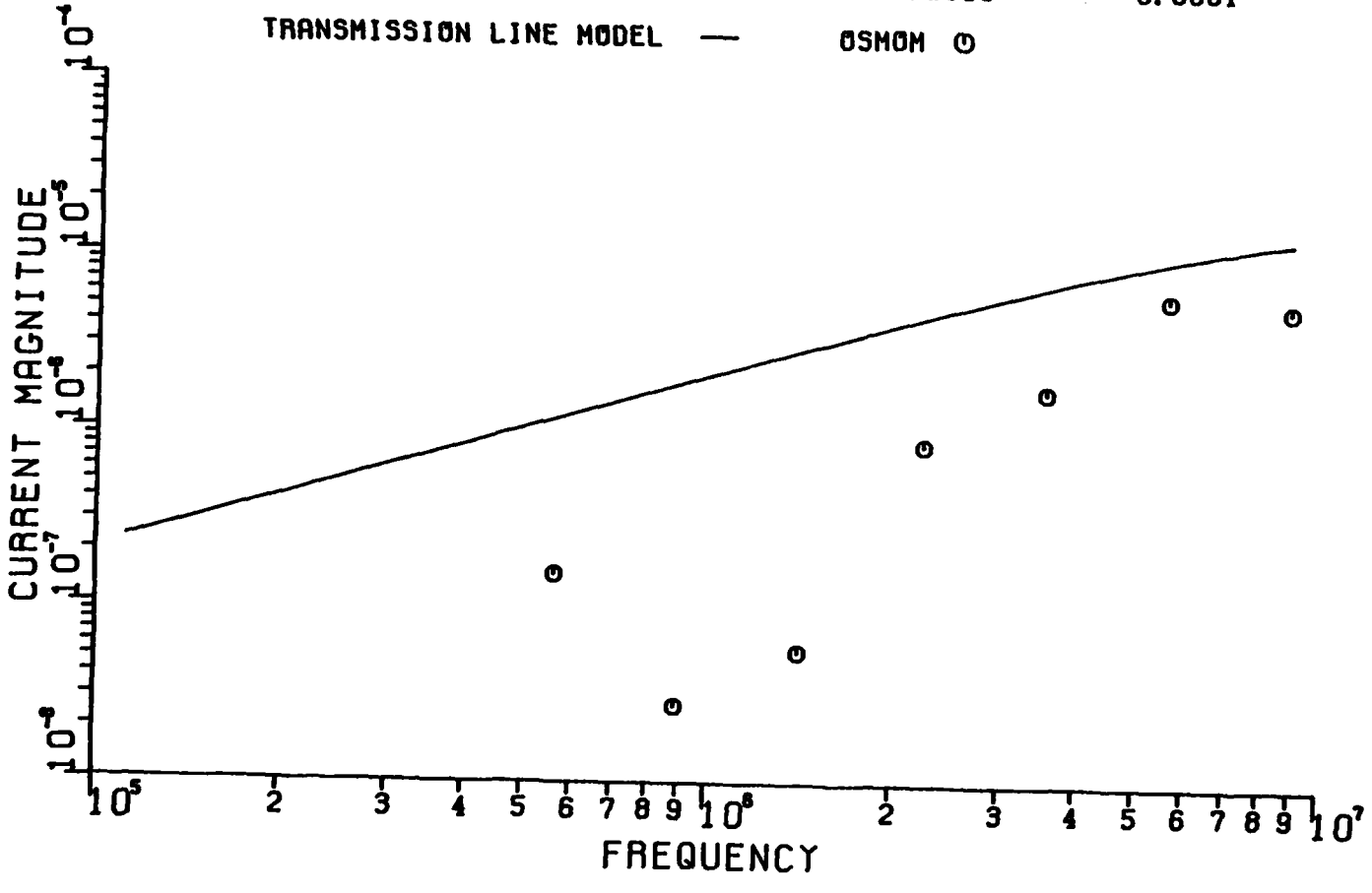

PLOT 4-10(B)

LINE DIMENSIONS (METERS)

LENGTH = 1.0
SEPARATION = 0.01
RADIUS = 0.0001

EXCITATION: SIDEFIRE
LOADING: LOW IMPEDANCE

TRANSMISSION LINE MODEL — OSMOM ⊙

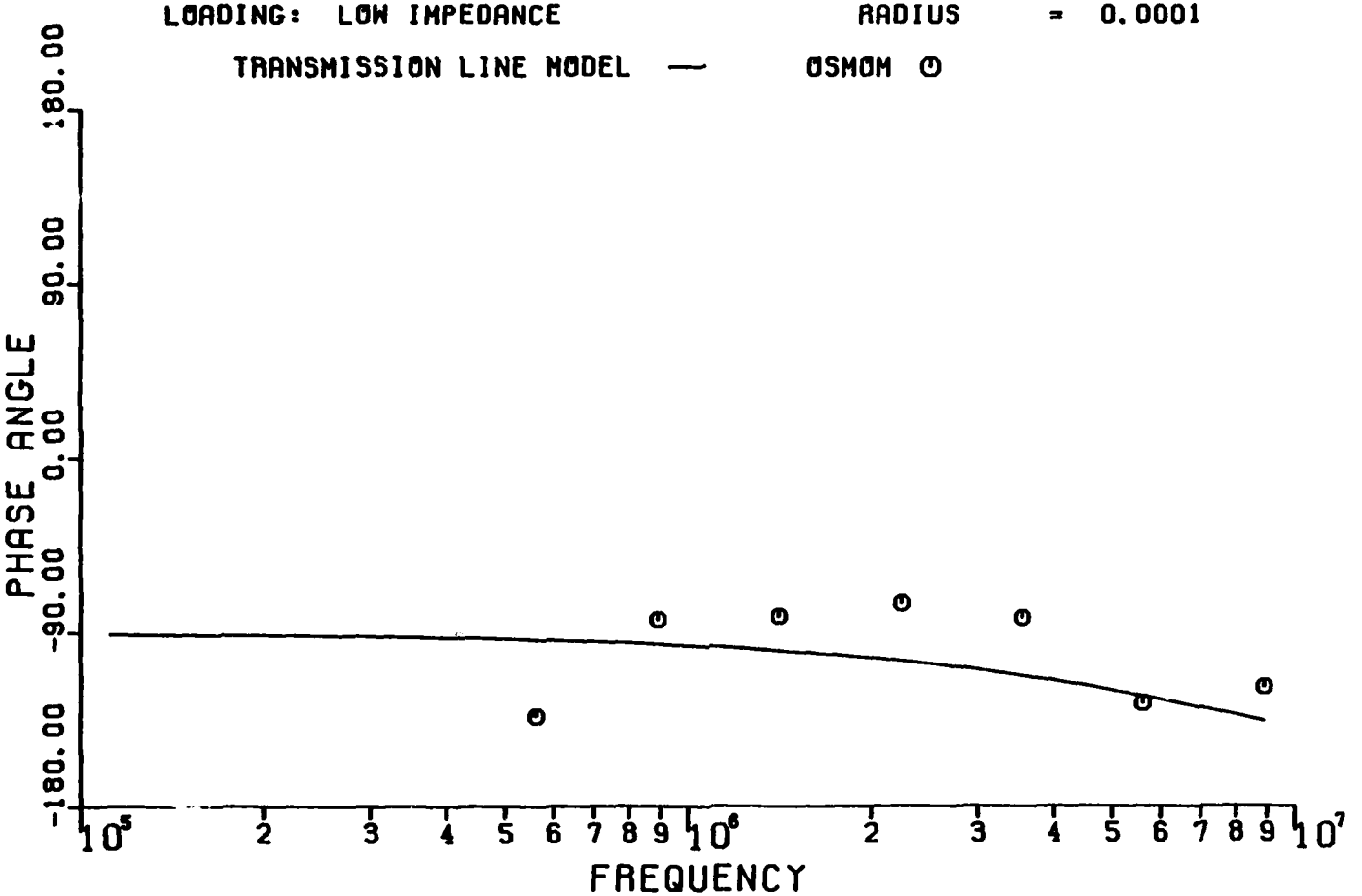

PLOT 4-11 (A)

EXCITATION: SIDEFIRE
LOADING: HIGH IMPEDANCE

LINE DIMENSIONS (METERS)

LENGTH	=	1.0
SEPARATION	=	0.01
RADIUS	=	0.0001

TRANSMISSION LINE MODEL — OSMOH ⓪

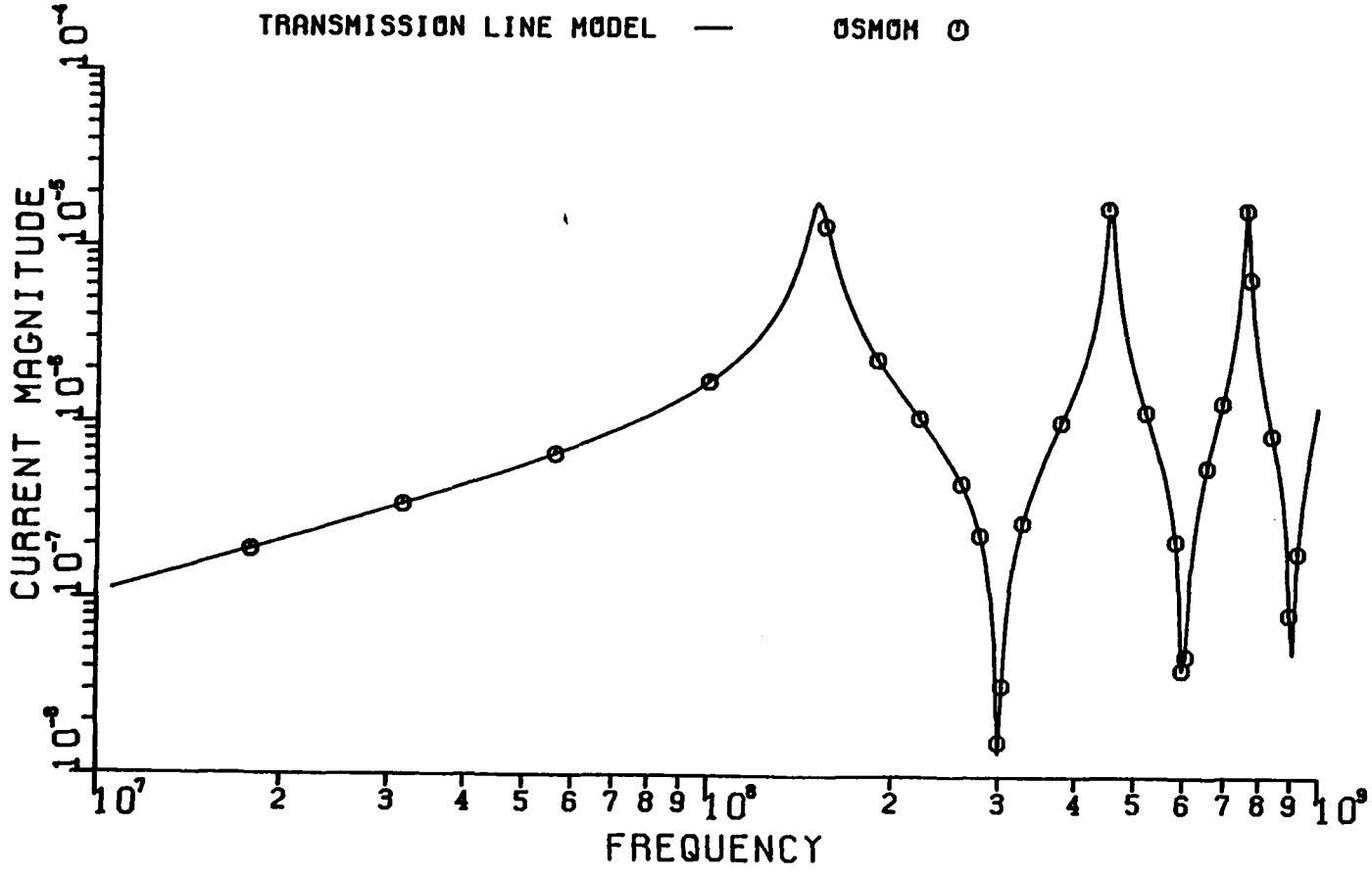

PLOT 4-11 (B)

LINE DIMENSIONS (METERS)

LENGTH = 1.0
SEPARATION = 0.01
RADIUS = 0.0001

EXCITATION: SIDEFIRE
LOADING: HIGH IMPEDANCE

TRANSMISSION LINE MODEL — OSMOM ⊙

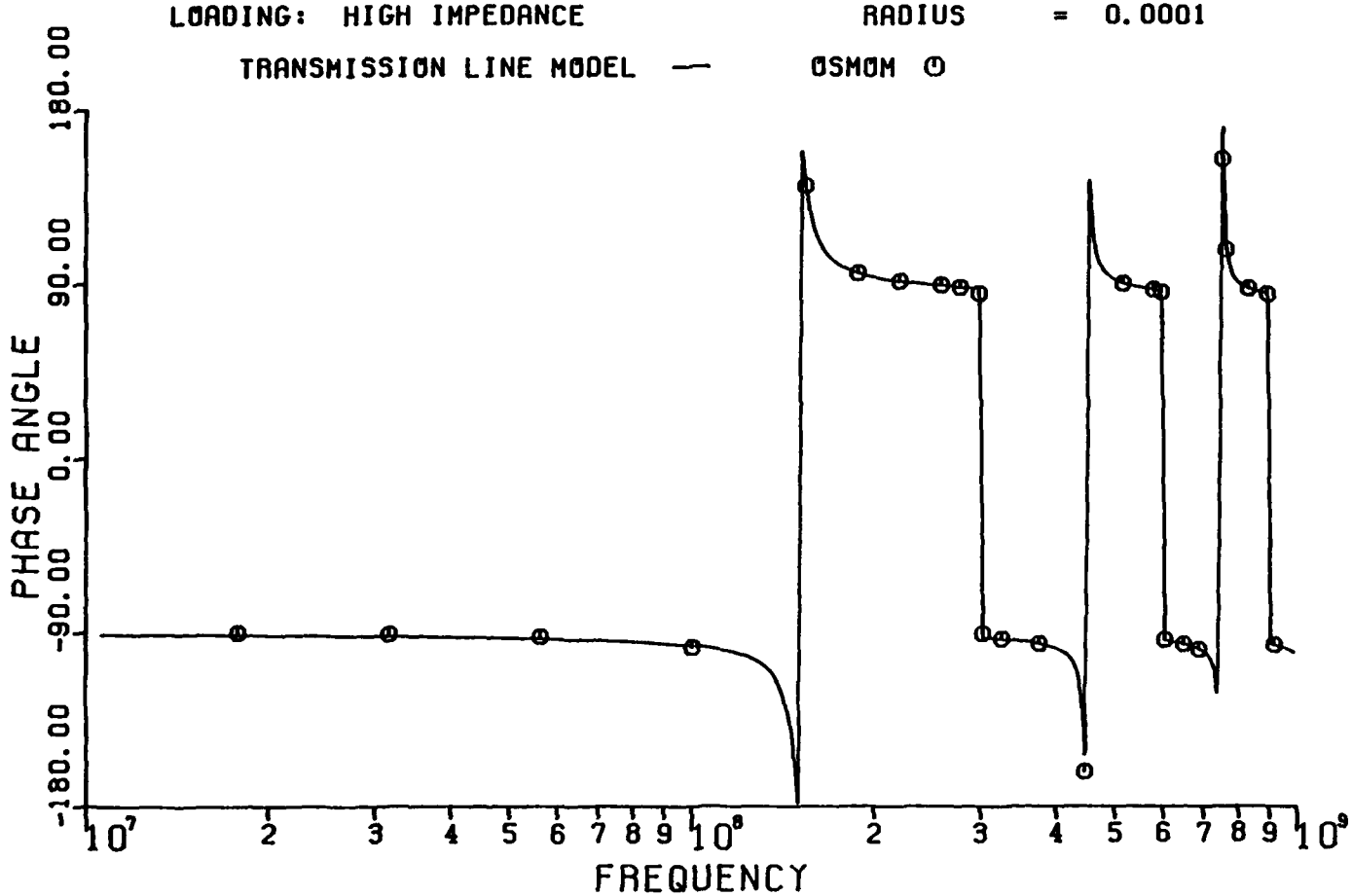

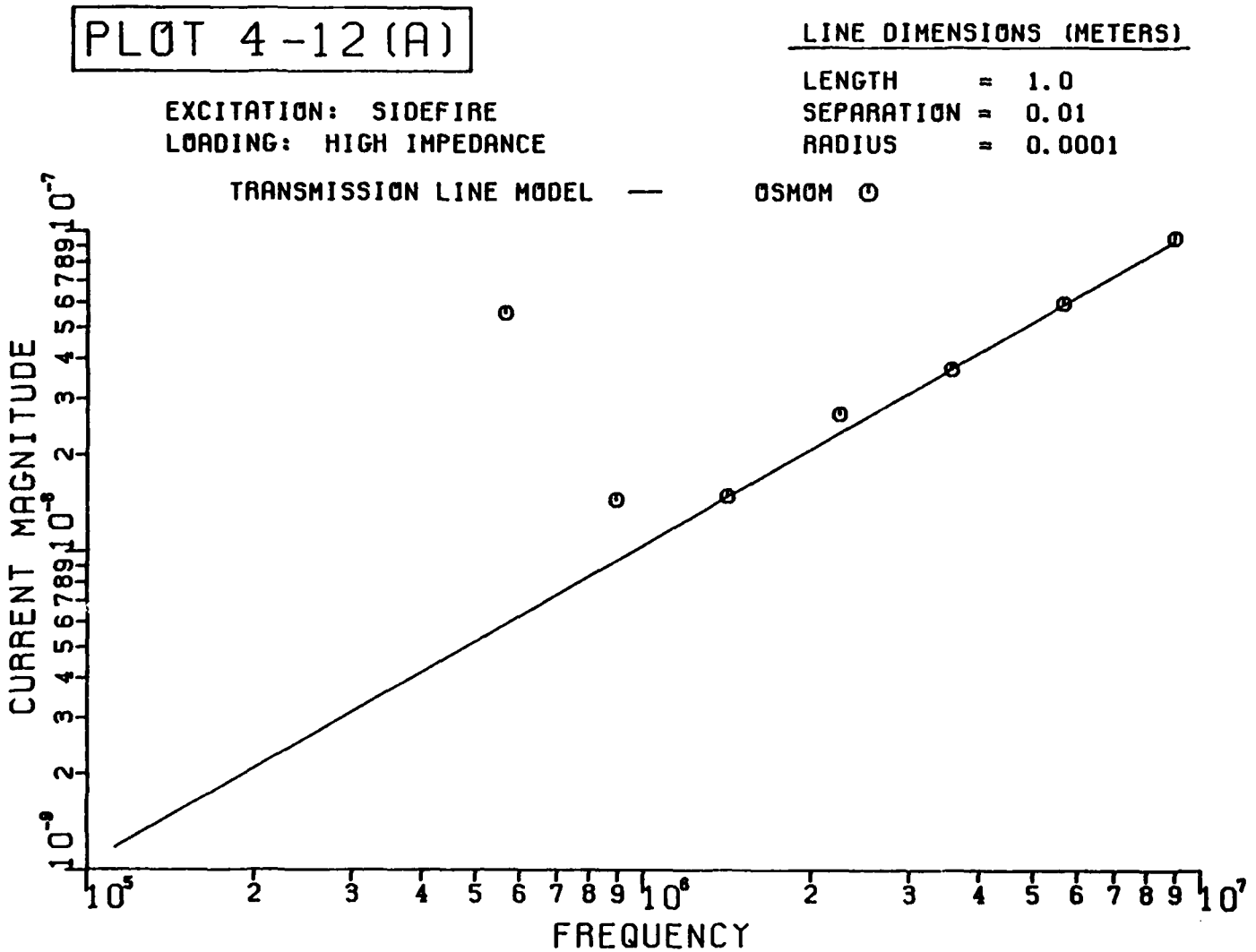
PLØT 4-12(A)
EXCITATION: SIDEFIRE
LOADING: HIGH IMPEDANCE
LINE DIMENSIONS (METERS)
LENGTH = 1.0
SEPARATION = 0.01
RADIUS = 0.0001
TRANSMISSION LINE MODEL — ØSMØM ⊙
CURRENT MAGNITUDE
FREQUENCY
10^-9
10^-8
10^-7
10^5
10^6
10^7

AD-A124 861 BASIC RM TECHNOLOGY ADVANCEMENT FOR C(3) SYSTEMS VOLUME IVA COUPLING OF ... (U) SOUTHEASTERN CENTER FOR ELECTRICAL ENGINEERING EDUCATION INC S..

2/2

UNCLASSIFIED R T ABRAHAM ET AL. NOV 82 F/G 17/2 NL

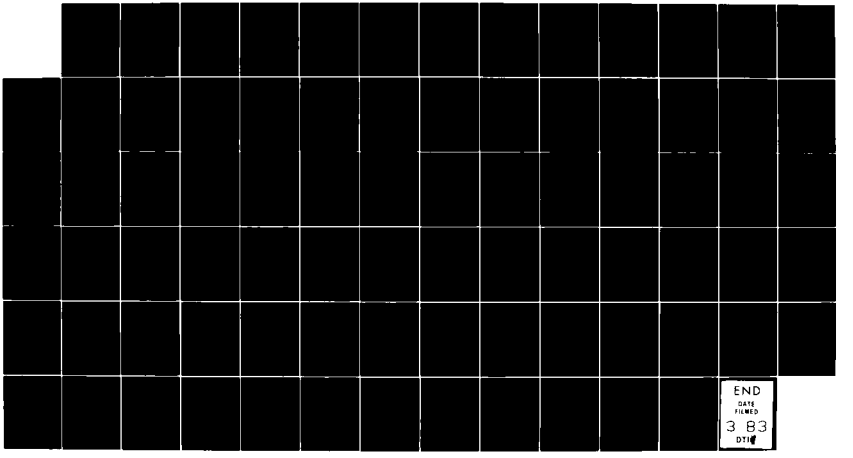

END
DATE FILMED
3 83
DTIC

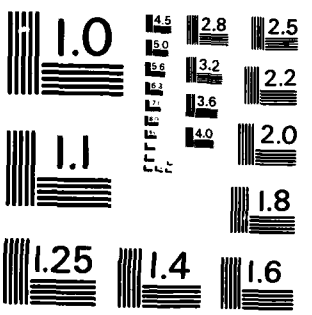

PLOT 4-12(B)

EXCITATION: SIDEFIRE
LOADING: HIGH IMPEDANCE

LINE DIMENSIONS (METERS)

LENGTH	=	1.0
SEPARATION	=	0.01
RADIUS	=	0.0001

TRANSMISSION LINE MODEL — OSMOM ⊙

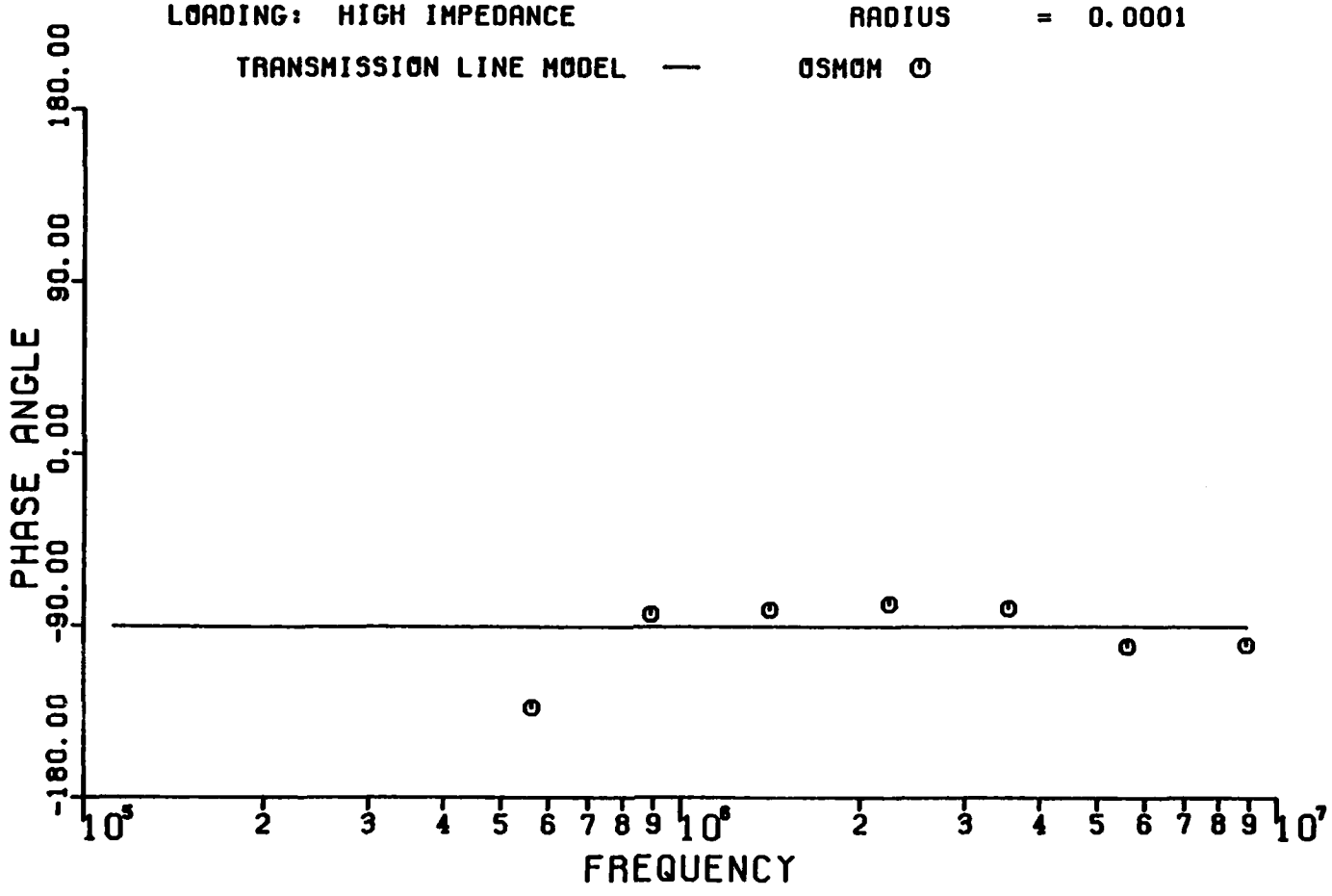

PLOT 4-13(A)

EXCITATION: BROADSIDE
LOADING: MATCHED

LINE DIMENSIONS (METERS)

LENGTH	=	1.0
SEPARATION	=	0.01
RADIUS	=	0.0001

TRANSMISSION LINE MODEL — OSMOM ⊙

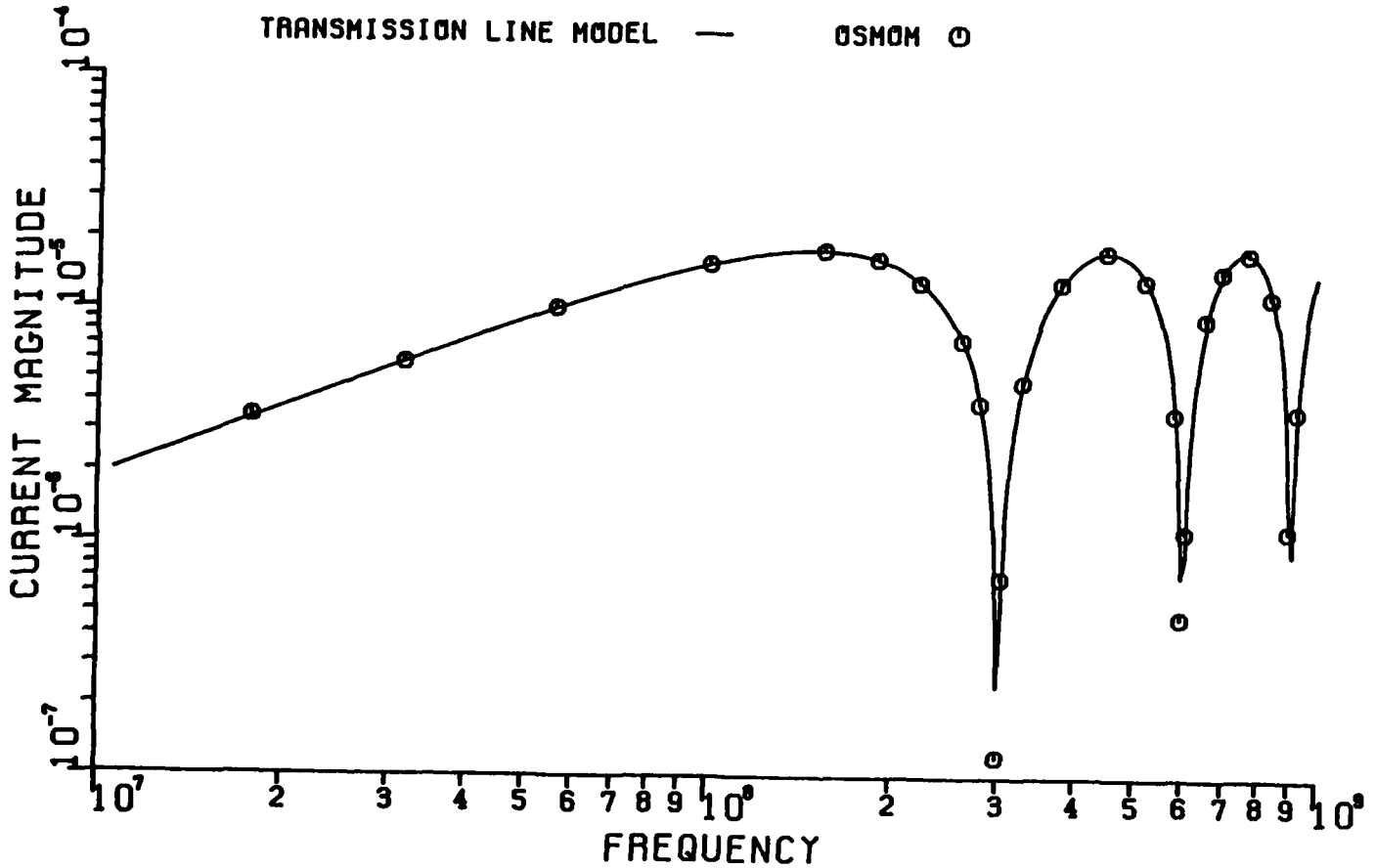

PLOT 4-13(B)

EXCITATION: BROADSIDE
LOADING: MATCHED

LINE DIMENSIONS (METERS)

LENGTH	=	1.0
SEPARATION	=	0.01
RADIUS	=	0.0001

TRANSMISSION LINE MODEL — OSMOM ⊙

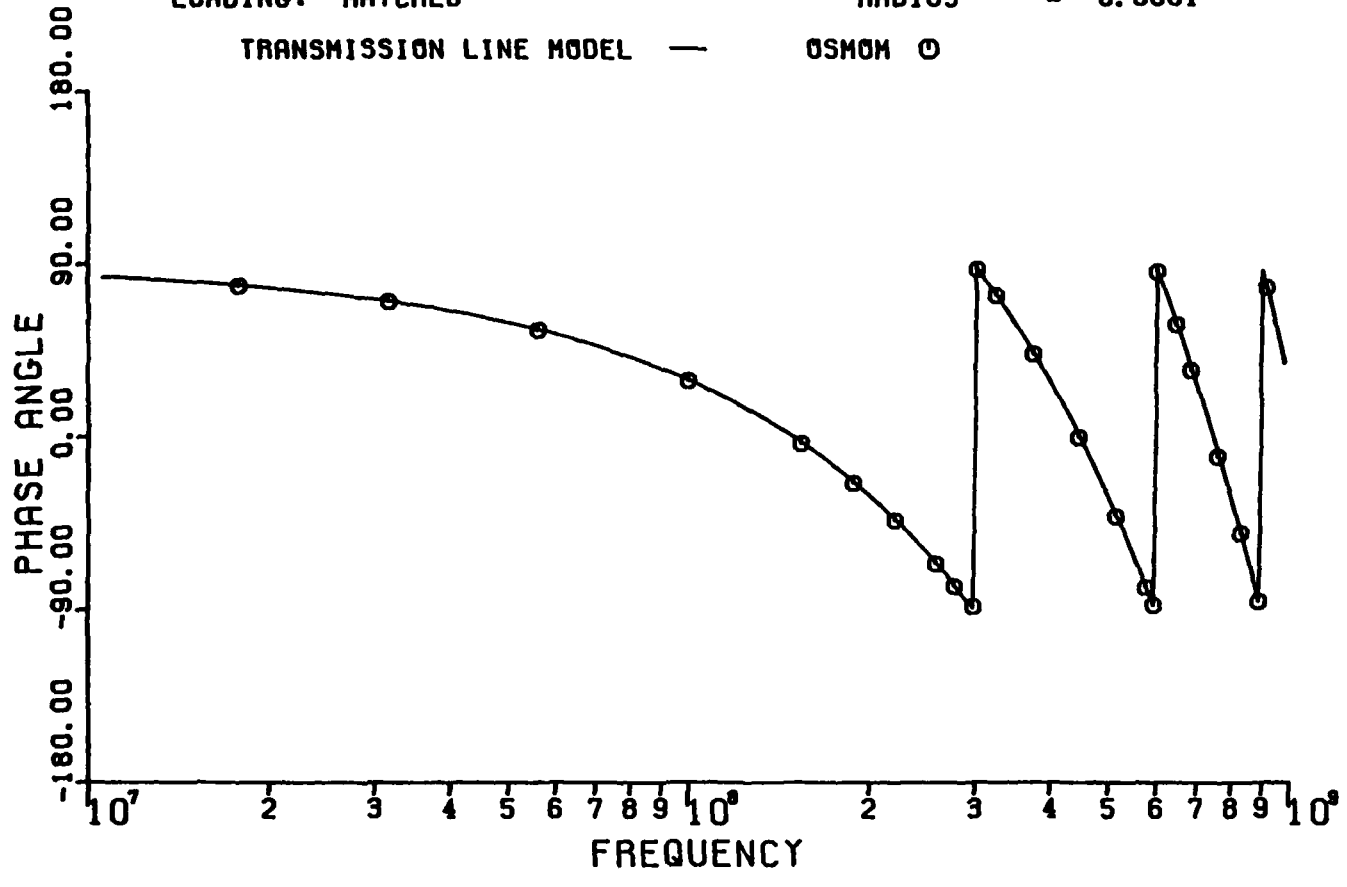

PLOT 4-14(A)

LINE DIMENSIONS (METERS)

LENGTH	=	1.0
SEPARATION	=	0.01
RADIUS	=	0.0001

EXCITATION: BROADSIDE
LOADING: MATCHED

TRANSMISSION LINE MODEL — OSMOM ⊙

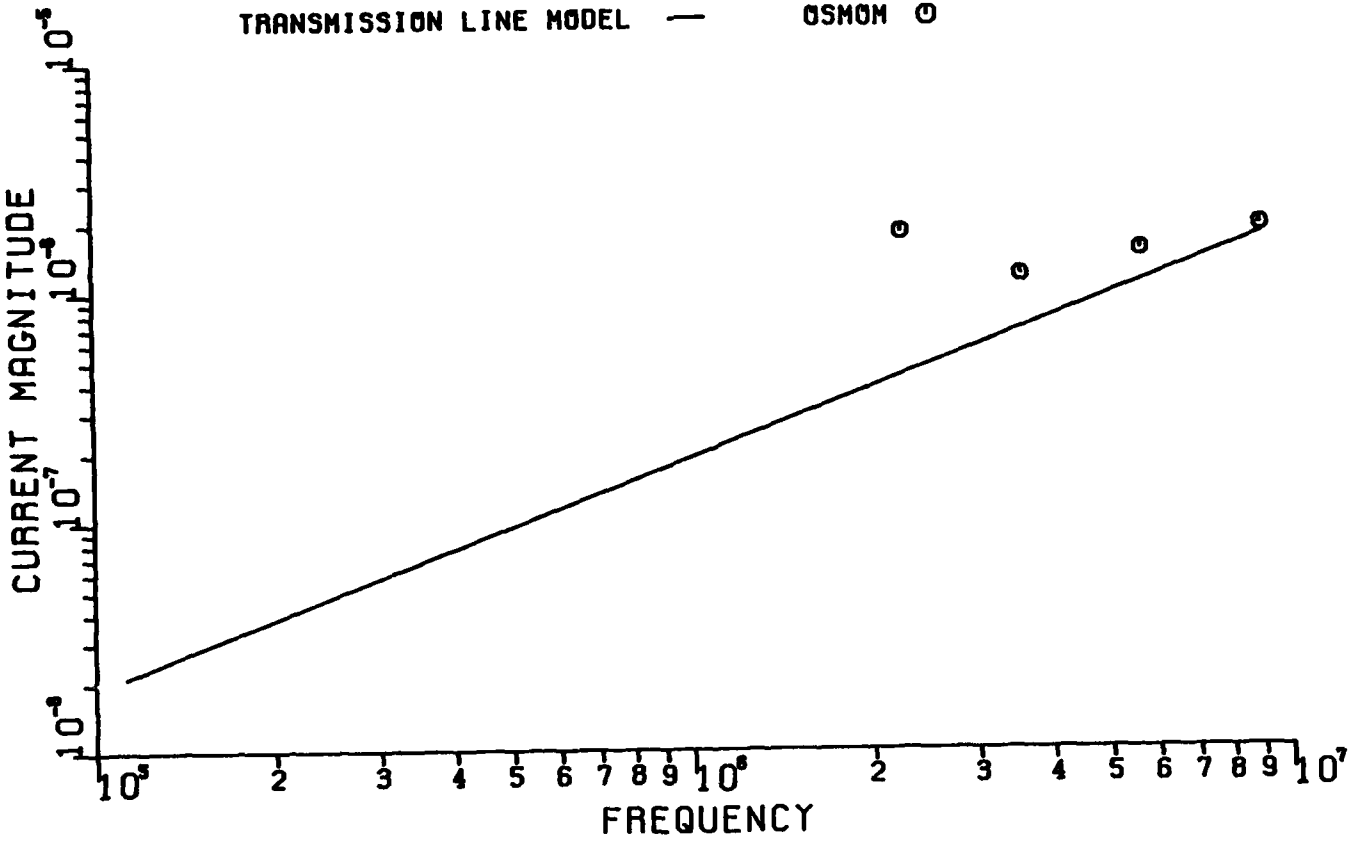

PLOT 4-14(B)

LINE DIMENSIONS (METERS)

LENGTH = 1.0
SEPARATION = 0.01
RADIUS = 0.0001

EXCITATION: BROADSIDE
LOADING: MATCHED

TRANSMISSION LINE MODEL — OSMOM ⊙

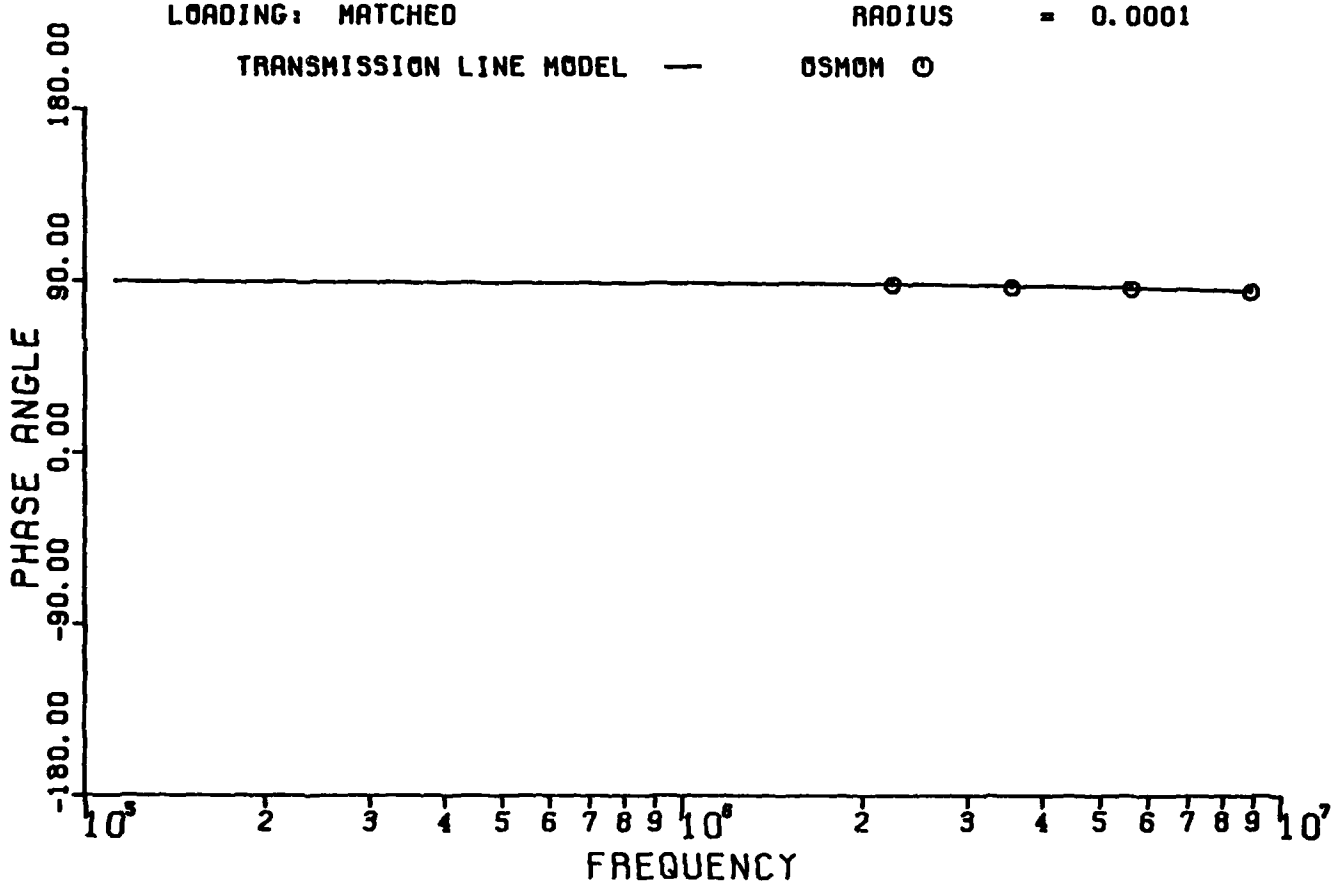

PLOT 4-15(A)

EXCITATION: BROADSIDE
LOADING: LOW IMPEDANCE

LINE DIMENSIONS (METERS)

LENGTH	=	1.0
SEPARATION	=	0.01
RADIUS	=	0.0001

TRANSMISSION LINE MODEL —— OSMOM ⊙

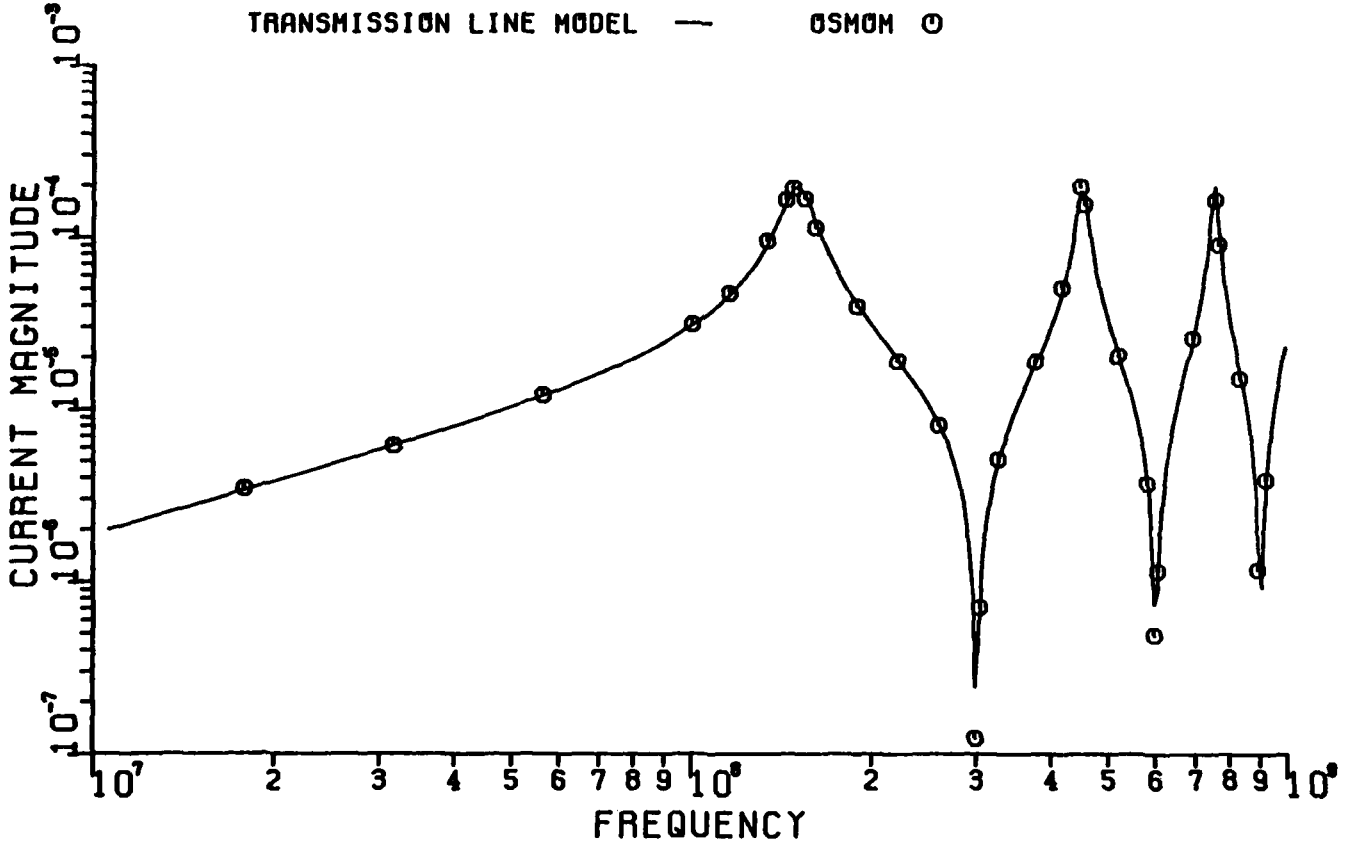

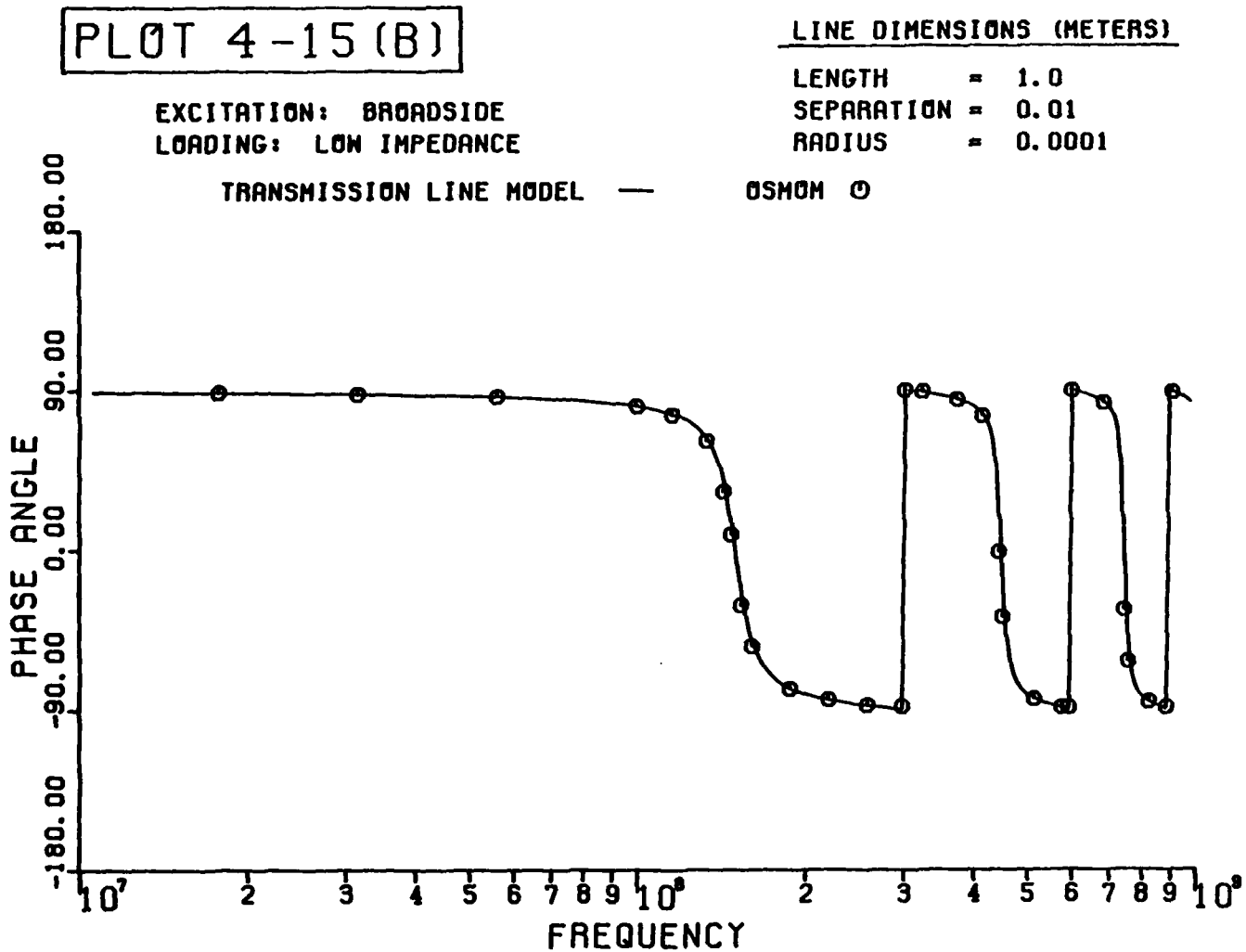
PLOT 4-15(B)
EXCITATION: BROADSIDE
LOADING: LOW IMPEDANCE
LINE DIMENSIONS (METERS)
LENGTH = 1.0
SEPARATION = 0.01
RADIUS = 0.0001
TRANSMISSION LINE MODEL — OSMOM ⊙
PHASE ANGLE
180.00
90.00
0.00
-90.00
-180.00
10⁷ 2 3 4 5 6 7 8 9 10⁸ 2 3 4 5 6 7 8 9 10⁹
FREQUENCY

PLOT 4-16 (A)

EXCITATION: BROADSIDE
LOADING: LOW IMPEDANCE

LINE DIMENSIONS (METERS)

LENGTH	=	1.0
SEPARATION	=	0.01
RADIUS	=	0.0001

TRANSMISSION LINE MODEL — OSMOM ⊙

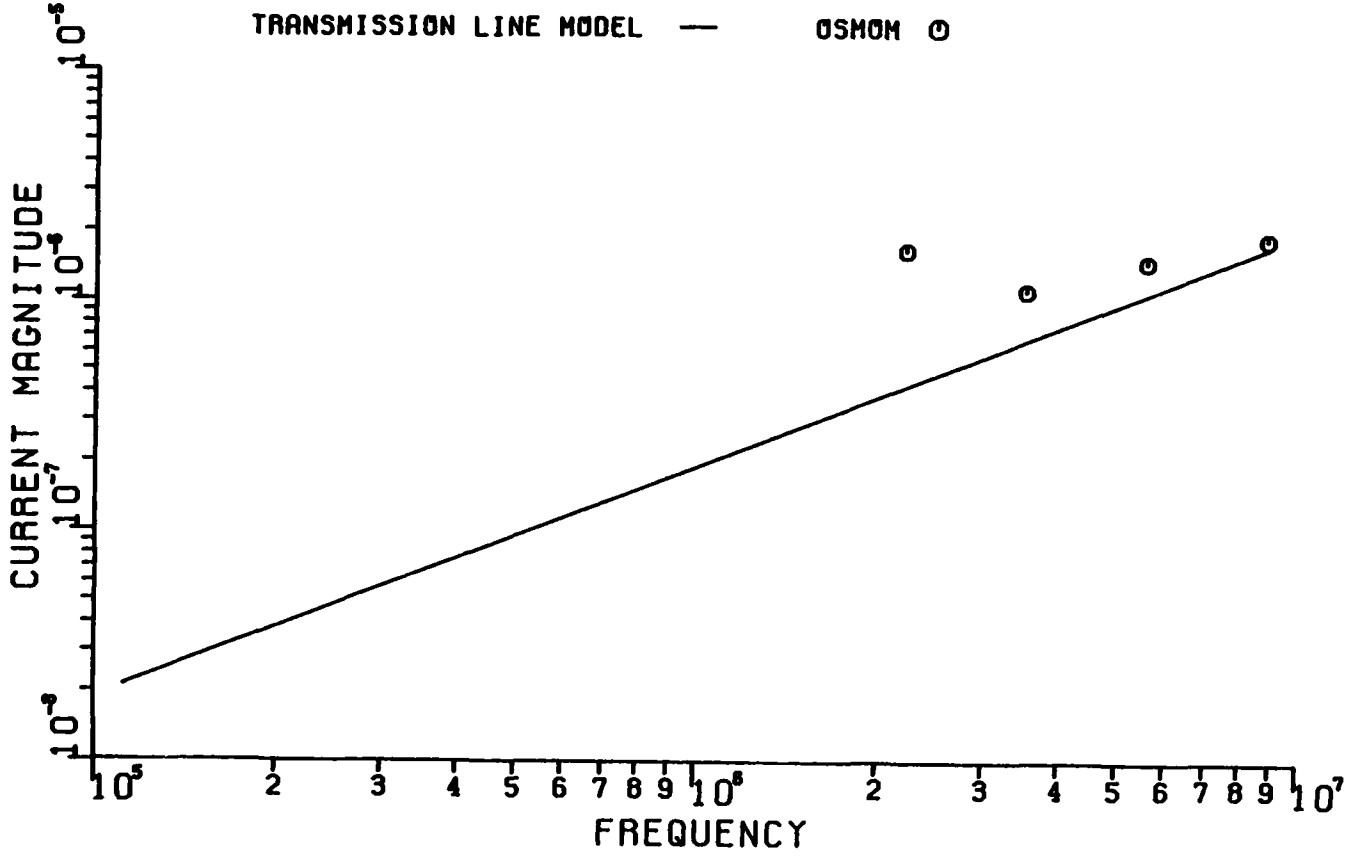

PLOT 4-16 (B)

EXCITATION: BROADSIDE
LOADING: LOW IMPEDANCE

LINE DIMENSIONS (METERS)

LENGTH	=	1.0
SEPARATION	=	0.01
RADIUS	=	0.0001

TRANSMISSION LINE MODEL — OSMOM ⊙

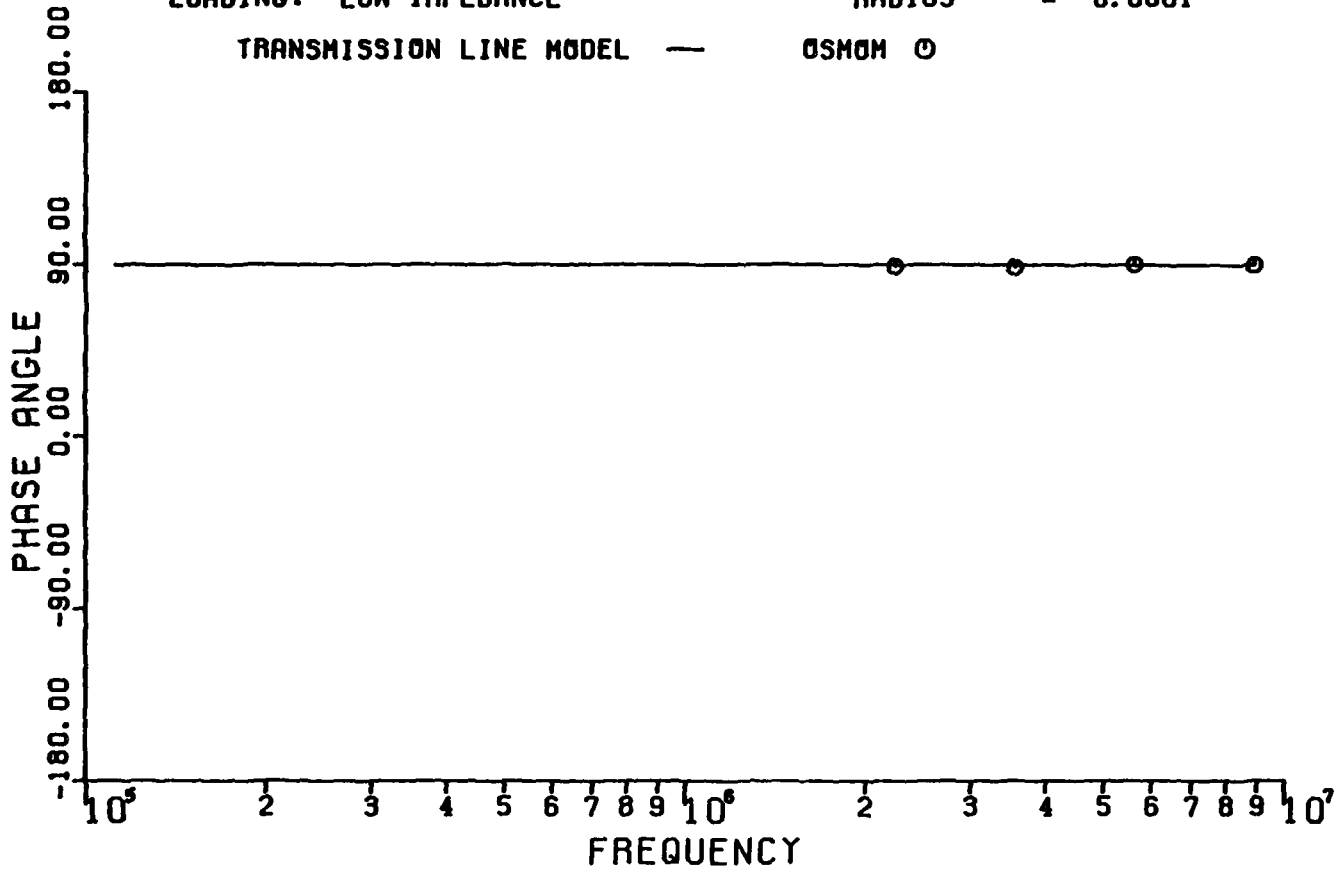

PLØT 4-17(A)

LINE DIMENSIONS (METERS)

LENGTH = 1.0
SEPARATION = 0.01
RADIUS = 0.0001

EXCITATION: BROADSIDE
LOADING: HIGH IMPEDANCE

TRANSMISSION LINE MODEL — OSMOM ⊙

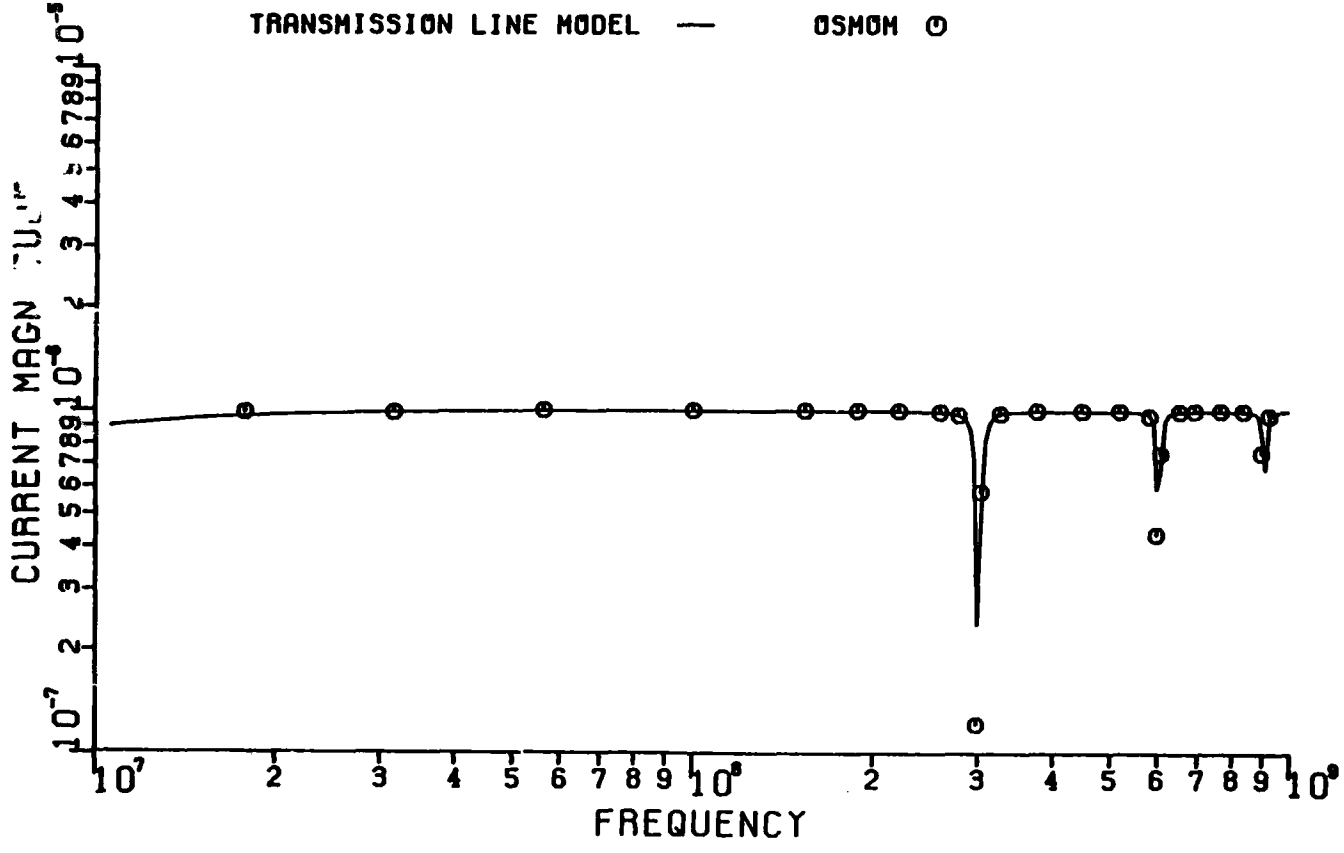

PLOT 4-17(B)

LINE DIMENSIONS (METERS)

LENGTH = 1.0
SEPARATION = 0.01
RADIUS = 0.0001

EXCITATION: BROADSIDE
LOADING: HIGH IMPEDANCE

TRANSMISSION LINE MODEL — OSMOM ①

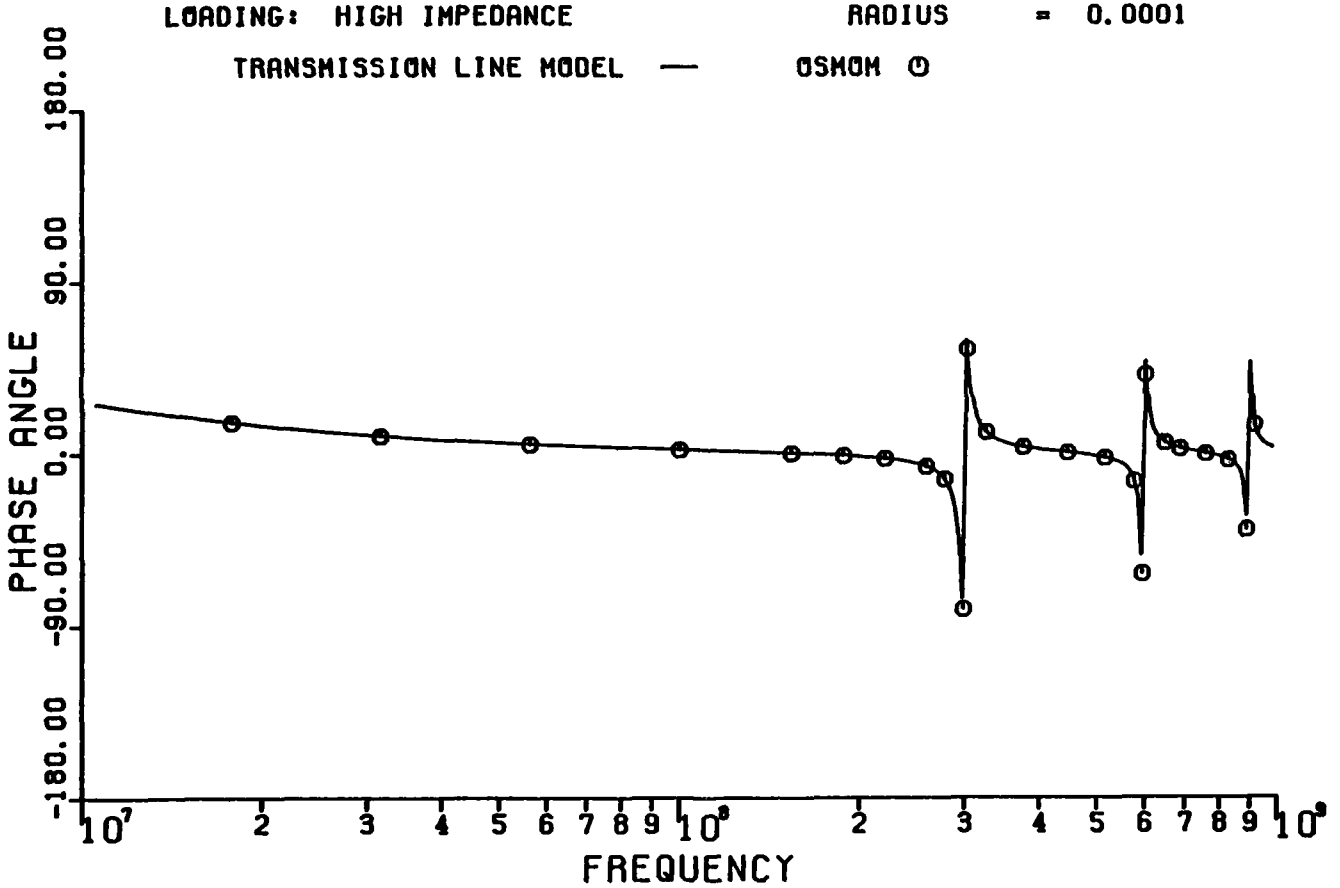

PLØT 4-18(A)

EXCITATION: BROADSIDE
LOADING: HIGH IMPEDANCE

LINE DIMENSIONS (METERS)

LENGTH	=	1.0
SEPARATION	=	0.01
RADIUS	=	0.0001

TRANSMISSION LINE MODEL — ØSMØM ⊙

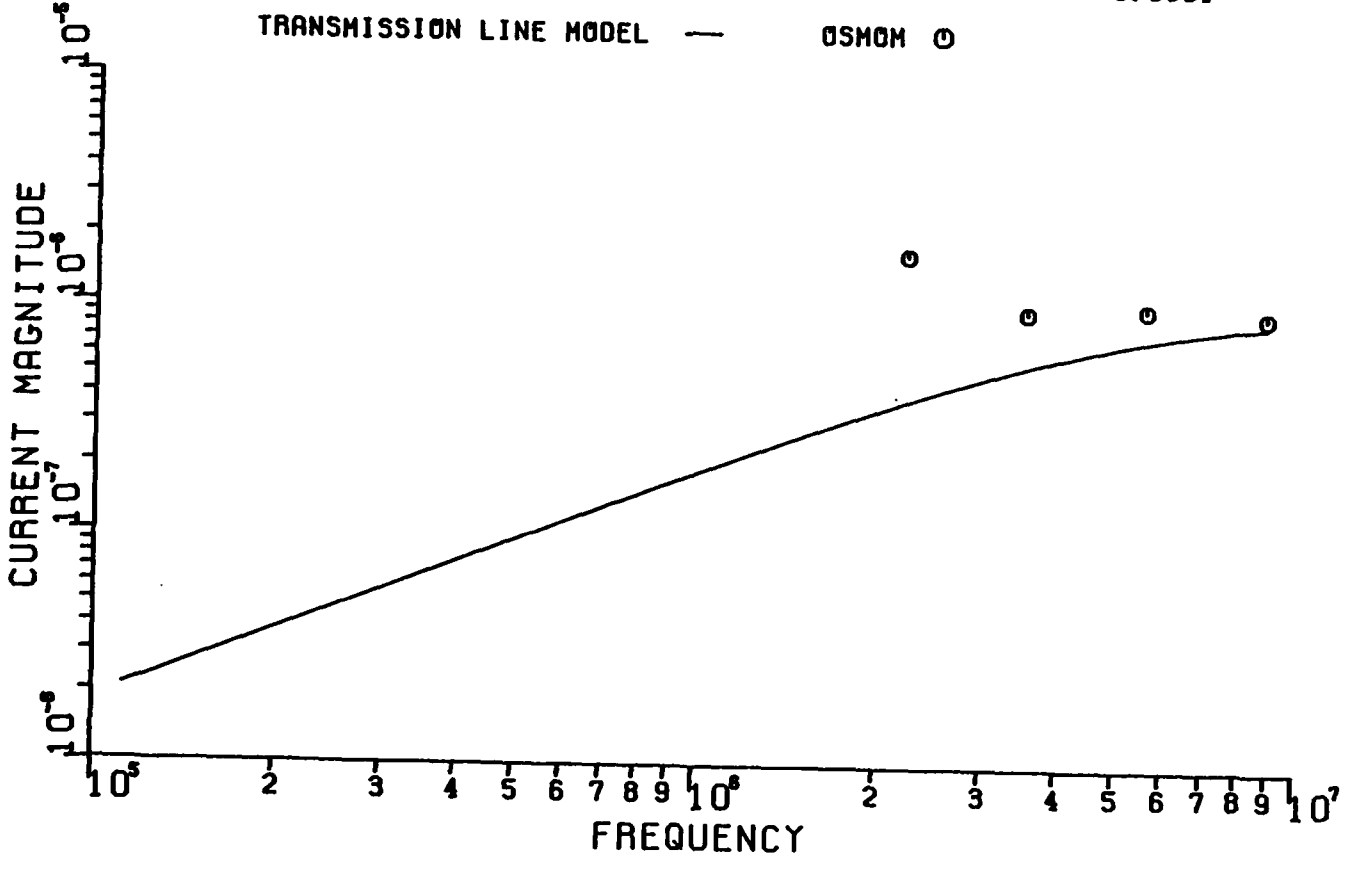

PLOT 4-18(B)

LINE DIMENSIONS (METERS)

LENGTH = 1.0
SEPARATION = 0.01
RADIUS = 0.0001

EXCITATION: BROADSIDE
LOADING: HIGH IMPEDANCE

TRANSMISSION LINE MODEL — OSMOM ⊙

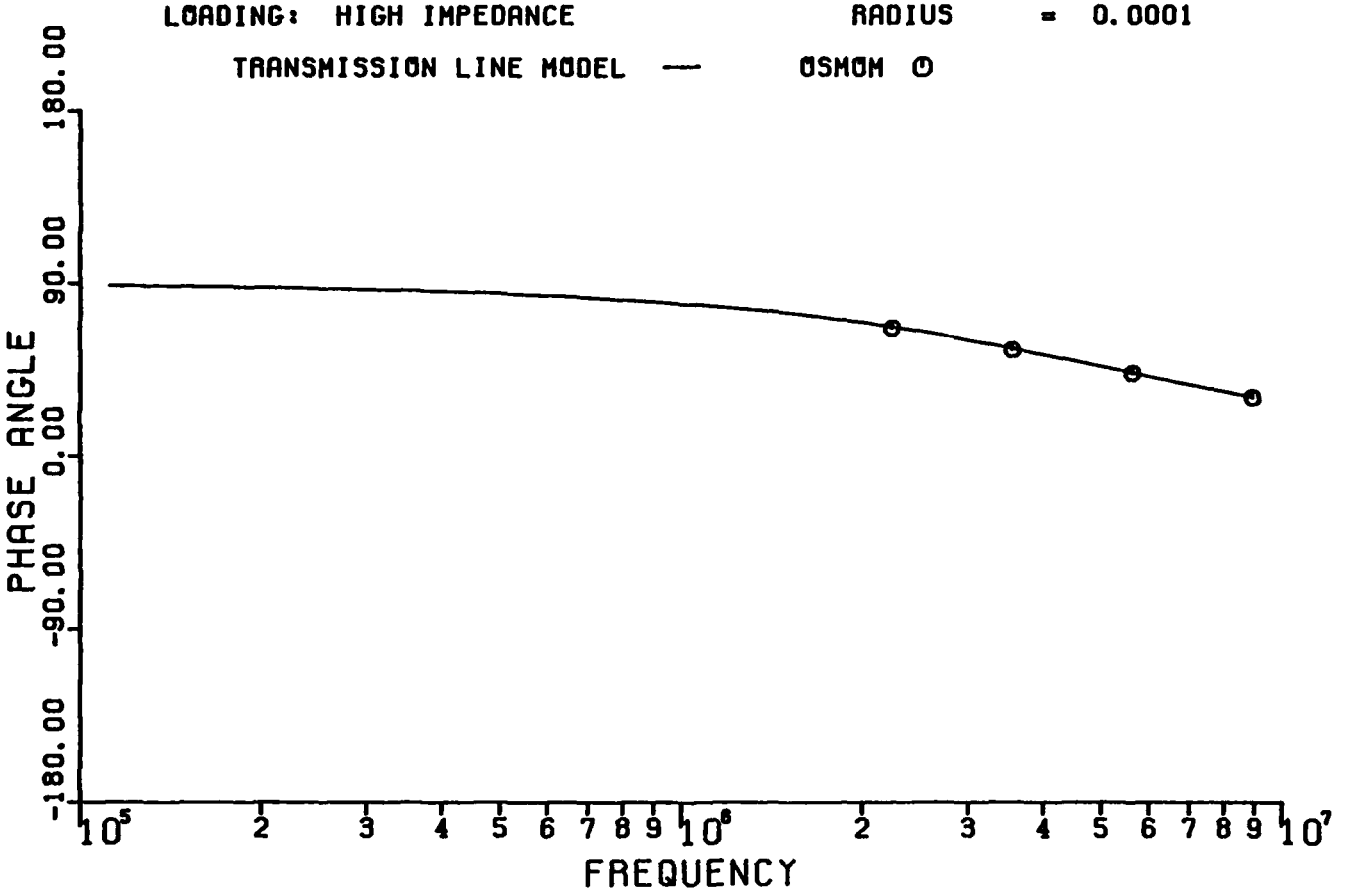

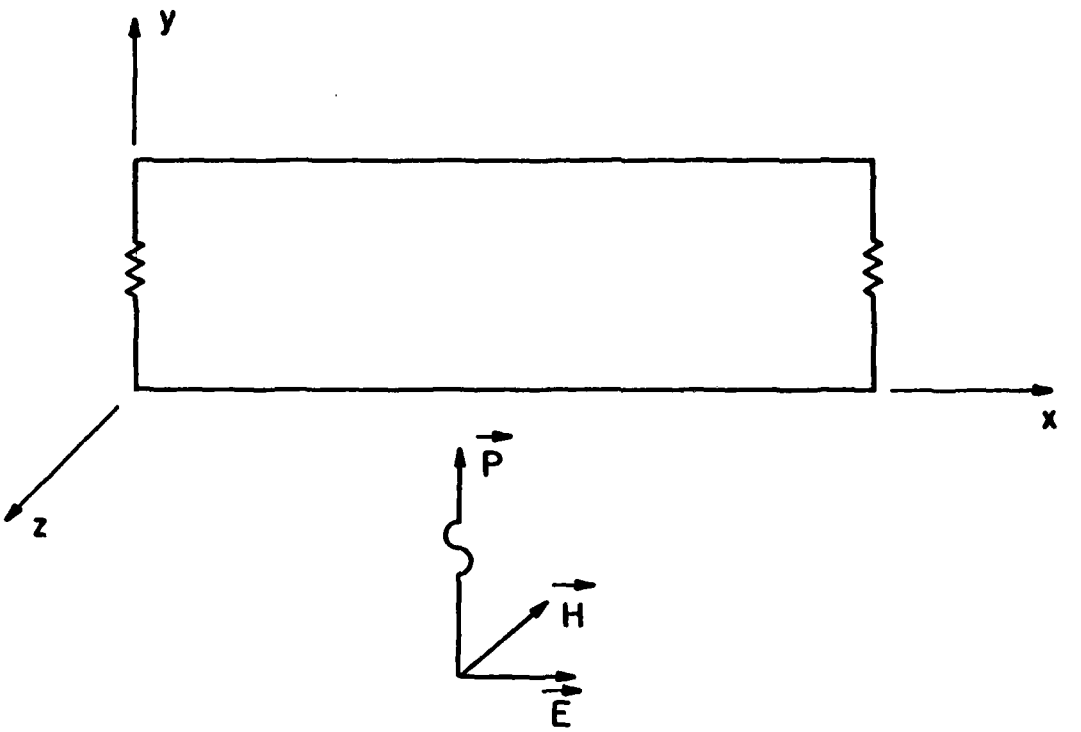

Sidefire

FIGURE 4-2

E field aligns the H field with the negative z axis, giving it maximum pickup by the structure. As with the ENDFIRE case, rotating the polarization 90 degrees either direction would cause no induced sources to be produced in the transmission line model and hence, no induced currents.

For the SIDEFIRE case E_y^i and H_z^i are as follows.

$$E_y^i = 0 \tag{4-19}$$

$$H_z^i = -\frac{E_m}{\eta} e^{-jky} \tag{4-20}$$

Substituting these values into equations (2-32) and (2-33),

$$V_s(x) = j\omega\mu \int_0^d -\frac{E_m}{\eta} e^{-jky} dy$$

$$= \frac{\omega\mu}{nk} E_m (e^{-jkd} - 1) \tag{4-21}$$

and

$$I_s(x) = 0 \tag{4-22}$$

Equation (4-21) can be simplified by noting that

$$\eta = \frac{\mu}{\varepsilon} \qquad \text{and} \qquad k = \omega\sqrt{\mu\varepsilon}$$

so that

$$\frac{\omega\mu}{\eta k} = \frac{\omega\mu}{\sqrt{\frac{\mu}{\varepsilon}}\,(\omega\sqrt{\mu\varepsilon})} = 1$$

Equation (4-21) now becomes

$$V_s = E_m(e^{-jkd} - 1) \tag{4-23}$$

With the substitution of equations (4-23) and (4-22), equation (2-42) becomes

$$V_s'(L) = \int_0^L \cos(k(L-\tau))E_m(e^{-jkd} - 1)d\tau$$

$$= \frac{E_m}{k}(e^{-jkd} - 1)\sin(kL) \tag{4-24}$$

Again substituting equations (4-23) and (4-22), equation (2-43) becomes

$$I_s'(L) = \int_0^L - jvc\,\sin(k(L-\tau))E_m(e^{-jkd} - 1)d\tau$$

$$= \frac{-jE_m}{k\,R_c}(e^{-jkd} - 1)(1 - \cos(kL)) \tag{4-25}$$

Equations (4-24) and (4-25) can now be substituted into equation (2-51) to yield the following relation.

$$I(0) = \frac{\frac{E_m}{k}(e^{-jkd}-1)\sin(kL) + j\frac{E_m R}{k R_c}(e^{-jkd}-1)(1-\cos(kL))}{2(R\cos(kL)) + j(R_c + \frac{R^2}{R_c})\sin(kL)}$$

$$= \frac{\frac{E_m}{k}(e^{-jkd}-1)[R_c \sin(kL) + jR(1-\cos(kL))]}{2 R R_c \cos(kL) + j(R_c^2 + R^2)\sin(kL)} \qquad (4\text{-}26)$$

Again, the denominator of equation (4-26) can never be zero, as was the case with equation (4-11). Nulls will occur when sin(kL) equals zero and cos(kL) equals one, causing the numerator to become zero. This condition corresponds to

$$kL = n(2\pi), \quad n=0,1,2,... \qquad (4\text{-}27)$$

or

$$f = n(300\ \text{MHz}) \qquad (4\text{-}28)$$

which indicates that nulls occur at frequencies which are multiples of 300 megahertz, or when the line length is a multiple of one wavelength. The value of the current halfway between each null is not constant, as it had been with the ENDFIRE case. These current values

occur when

$$kL = n(2\pi) + \pi \tag{4-29}$$

or

$$f = n(300\ \text{MHz}) + 150\ \text{MHz} \tag{4-30}$$

At these frequencies, cos(kL) equals minus one and sin(kL) equals zero, yielding the following from equation (4-26).

$$I(0) = - j \frac{E_m(e^{-jkd} - 1)}{k R_c} \tag{4-31}$$

This equation yields the current halfway between any two nulls and varies with frequency as $\frac{e^{-jkd} - 1}{k}$.

At low frequencies, the imaginary term will become insignificant compared to the real term in the denominator of equation (4-26). In the numerator, cos(kL) will approach one, sin(kL) will become kL, and e^{-jkd} will become 1 - jsin(kd) or 1 - jkd. Therefore equation (4-26) will become

$$I(0) = \frac{- j E_m kdL}{2R} \tag{4-32}$$

which suggests that current will become approximately a linear function of frequency at low frequencies, as it did in the ENDFIRE case.

The plots of data for the SIDEFIRE case follow the same format as the plots for the ENDFIRE case. Three loading conditions were again examined for two different ranges of frequency. The plots are identified in TABLE 4-1(b). Each plot number has two corresponding plots, (a) and (b), showing magnitude and phase, respectively.

The matched case shows very good correlation between the method of moments and the transmission line model results. Reradiation is again observed in the low impedance case causing some discrepancies at higher frequencies. The current peaks observed for the high impedance case are not infinite in magnitude. These currents adhere to the values predicted by equation (4-31). The low frequency results again illustrate the numerical breakdown of the method of moments. That is, numerical noise and round-off error in the computer begin to affect the solution significantly.

The third case to be considered has the plane wave arriving at all parts of the transmission line simultaneously. The wave is propagating in the negative z direction. The phase front of the wave strikes the structure broadside; hence, this will be referred to as the BROADSIDE case. (See FIGURE 4-3.) Again the polarization is such

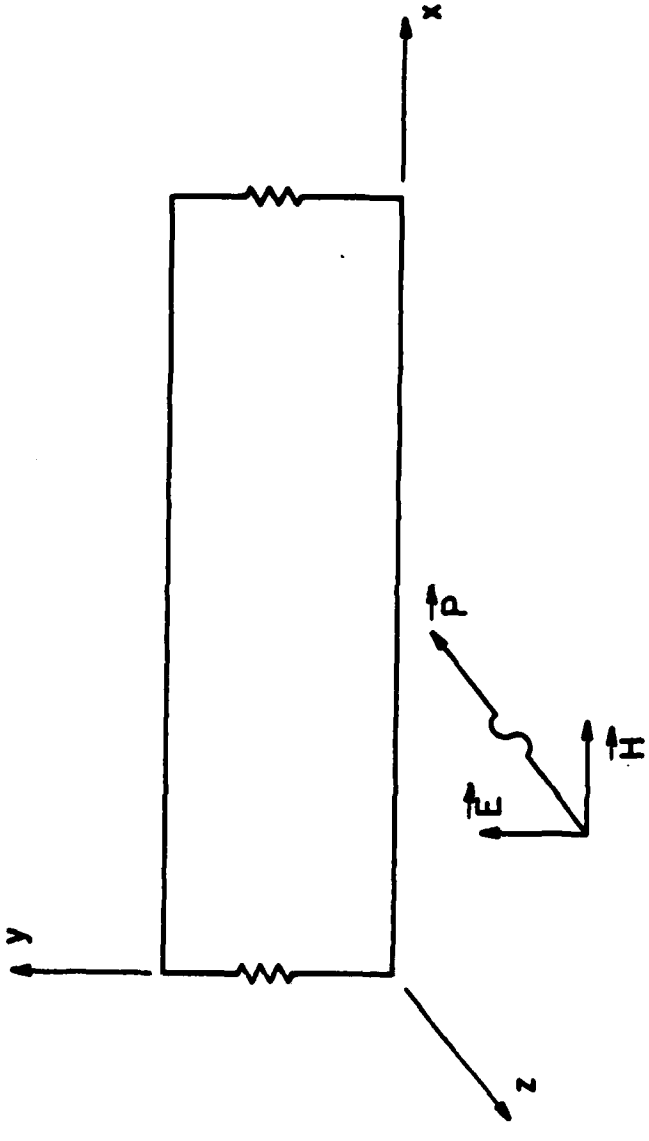

Broadside

FIGURE 4-3

that the E field is oriented for maximum pickup by the structure. Choosing a y-directed E field leaves an x-directed H field. However, the H field contributes no induced sources since it cannot have a z component. This configuration yields the following.

$$E_y = E_m e^{jkz} = E_m \tag{4-33}$$

$$H_z = 0 \tag{4-34}$$

In equation (4-33), e^{jkz} is always equal to one because the structure is located at z=0.

Substituting these values into equations (2-32) and (2-33) yields

$$V_s(x) = 0 \tag{4-35}$$

$$I_s(L) = I_s = - j\omega c \int_0^d E_m dy = - j\omega c\, E_m d \tag{4-36}$$

With the substitution of equations (4-35) and (4-36) into (2-42) we obtain the following

$$V_s'(L) = - v\ell c\omega\, E_m d \int_0^L \sin(k(L-\tau))d\tau$$

$$= - E_m d\,(1 - \cos(kL)) \qquad (4\text{-}37)$$

where the relation $v\ell c\omega = k$ was used, as illustrated in Appendix IV. Substituting equation (4-35) and (4-36) into equation (2-43) yields

$$I_s'(L) = - j\omega c\, E_m d \int_0^L \cos(k(L-\tau))d\tau$$

$$= - j \frac{E_m d}{R_c} \sin(kL) \qquad (4\text{-}38)$$

where the relation $\frac{k}{\omega c} = R_c$ was used as was illustrated in Appendix IV.

Equations (4-37) and (4-38) can now be substituted into equation (2-51) to obtain the following equation for I(0).

$$I(0) = \frac{- E_m d(1-\cos(kL)) + j\, E_m d \frac{R}{R_c} \sin(kL)}{2\,(R\cos(kL)) + j(R_c + \frac{R^2}{R_c}) \sin(kL)}$$

$$= \frac{E_m d[j\, R \sin(kL) - R_c(1 - \cos(kL))]}{2\, R\, R_c \cos(kL) + j(R_c^2 + R^2) \sin(kL)} \qquad (4\text{-}39)$$

As with both of the previous cases, the denominator of equation (4-39) can never be zero so the equation will never be singular. I(0) will however be zero whenever

$$kL = n2\pi, \qquad n = 0,1,2,... \tag{4-40}$$

or

$$f = n(300\ \text{MHz}) \tag{4-41}$$

At frequencies that are multiples of 300 megahertz the line length is a multiple of one wavelength. Current values at intervals half way between nulls occur when

$$kL = n2\pi + \pi \tag{4-42}$$

or

$$f = n(300\ \text{MHz}) + 150\ \text{MHz} \tag{4-43}$$

At each of these frequencies the current will have the constant value given by the following equation, which was obtained by evaluating equation (4-39) at the frequencies given by equation (4-43).

$$I(0) = \frac{E_m d}{R} \tag{4-44}$$

The linear behavior observed for the ENDFIRE and SIDEFIRE cases at low frequencies occurs here for the BROADSIDE case also. At low

frequencies equation (4-39) becomes

$$I(0) = \frac{jE_m dkL}{2R_c} \qquad (4\text{-}45)$$

This equation was obtained by the same method used to obtain equation (4-32). It shows that the linear relationship between I(0) and frequency occurs here in the BROADSIDE case as it did in the two previous cases.

Plots of the data for the BROADSIDE case with the three loading conditions and two ranges of frequency are identified in TABLE 4-1(c). The matched case again shows excellent correlation between the method of moments and the transmission line model solutions. The effects of reradiation are not as noticeable as they were in the previous cases for low impedance loading. This is probably related to the fact that the excitation over the entire structure is at the same phase. The peaks observed for the low impedance case are similar to those observed for the high impedance loading in the SIDEFIRE case. However, here each peak has the same value, given by equation (4-44). The results for high impedance loading for the BROADSIDE case are very good. However, at low frequencies and for all loading conditions, the Method of Moments predictions appear to be inaccurate.

In Chapter 5, the structure used in this chapter is modified to illustrate several important points. All of the plots in this chapter compare only differential mode currents. In Chapter 6, the common mode currents and their relation to the prediction of total currents is discussed.

CHAPTER 5

SPECIAL CONSIDERATIONS FOR MODIFIED STRUCTURES

The transmission line model predictions for the structure considered in Chapter 4 showed a slight deviation from the method of moments solution, when the line was terminated with low impedance loads. Reradiation from the terminal wires was discussed as a possible cause for the differences between the two solutions. If reradiation is causing this discrepancy, its effects should become more noticeable as the wire separation is increased. The longer the terminal wire, the greater the coupling between this wire and the incident field; hence, the induced current is larger, causing greater reradiation.

To illustrate this point, consider the SIDEFIRE case of Chapter 4, with low impedance loading. The solution of this case for a wire separation of 0.01 meter is shown by PLOT 4-9. Here the effects of reradiation near the nulls are noticed. These effects are greatly magnified when the wire separation is increased to 0.05 meter, as shown by PLOT 5-1. Here the predictions by the transmission line model and the method of moments differ significantly.

Although most of the noticeable differences between the two solutions of PLOT 5-1 are probably caused by reradiation, increased separa-

PLOT 5-1

EXCITATION: SIDEFIRE
LOADING: LOW IMPEDANCE

LINE DIMENSIONS (METERS)

LENGTH	=	1.0
SEPARATION	=	0.05
RADIUS	=	0.0001

TRANSMISSION LINE MODEL — OSMOM ⊙

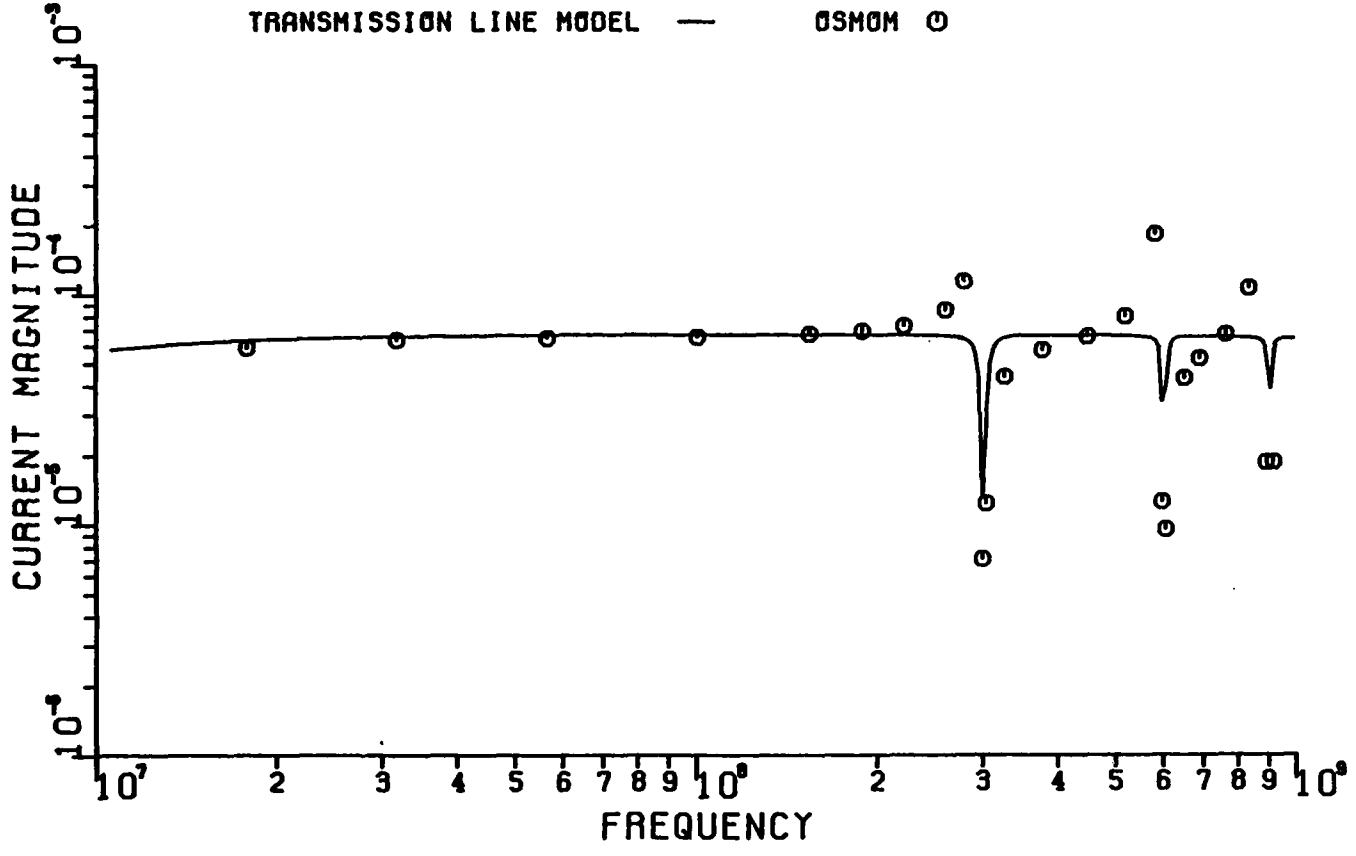

tion creates other problems. As the transmission line wires are moved further apart, gradually the transmission line assumptions (in particular the TEM assumption) begin to break down. To examine these problems, however, the effects of reradiation must be removed. To accomplish this, the load is replaced by an open circuit. This entirely eliminates terminal wire reradiation by eliminating the terminal wire. The structure is now modeled by the method of moments as two parallel wires. Obviously, the terminal currents can no longer be compared because they will be zero. Therefore, the differential mode currents at equally spaced points along the transmission line will be compared. Again using 24 subsections on each wire, the method of moments solution (OSMOM) provides the value of the current at 23 points, interior to the terminals, on each wire (25 points, including the zero current value obtained at the end of each wire). The differential mode current can be extracted from the total current solution, as was done in Chapter 4. The transmission line model predictions can be obtained at these points by the use of the chain parameter matrix. The derivation of the transmission line model solution of I(x) for the SIDEFIRE case with open circuit terminations follows. The SIDEFIRE case was selected because the ENDFIRE and BROADSIDE cases produce zero differential mode currents for all x. This is shown in Appendix V.

From equation (2-41), with x=L, we obtain

$$I(L) = - jvc \sin(\beta L)V(0) + \cos(\beta L)I(0) + I_s'(L) \quad (5\text{-}1)$$

Because the termination is an open circuit,

$$I(0) = I(L) = 0 \quad (5\text{-}2)$$

Therefore, equation (5-1) becomes

$$0 = - jvc \sin(\beta L)V(0) + I_s'(L) \quad (5\text{-}3)$$

or

$$V(0) = \frac{I_s'(L)}{jvc \sin(\beta L)} \quad (5\text{-}4)$$

Equation (2-41), for a general value of x, gives

$$I(x) = - jvc \sin(\beta x)V(0) + I_s'(x) \quad (5\text{-}5)$$

Substituting equation (5-4) into (5-5) and simplifying yields

$$I(x) = - \frac{\sin(\beta x)}{\sin(\beta L)} I_s'(L) + I_s'(x) \quad (5\text{-}6)$$

The values for $I_s'(L)$ and $I_s'(x)$ can be obtained from equation (4-25).

$$I_s'(L) = \frac{-j\ E_m}{k\ R_c} (e^{-jkd} - 1)(1 - \cos(kL)) \qquad (5\text{-}7)$$

$$I_s'(x) = \frac{-j\ E_m}{k\ R_c} (e^{-jkd} - 1)(1 - \cos(kx)) \qquad (5\text{-}8)$$

Equation (5-6) gives the value of the differential mode current at any value of x along the line.

The transmission line model and the method of moments provide solutions for currents on the open circuit structure at wire separations of 0.01, 0.05, and 0.10 meter. Current magnitudes versus position on the line for the three separations are shown by PLOTS 5-2, 5-3, and 5-4. TABLE 5-1 lists the percent error in the transmission line model solution for each point where the method of moments provides a current value. The error is very small for the closest separation (this is the same structure considered in Chapter 4, except with an infinite impedance load) but gets progressively worse as separation increases. This clearly indicates that reradiation is not the only problem brought on by wide separations between the wires. The conditions necessary for the TEM assumption to be valid are apparently not being satisfied, for these wider separations.

Up to this point, the method of moments solution has been supplied solely by the computer program OSMOM. In Chapter 3 the restrictions of the pulse expansion and point matching technique used in

PLOT 5-2

EXCITATION: SIDEFIRE
FREQUENCY= 525 MHZ

LINE DIMENSIONS (METERS)

LENGTH	=	1.0
SEPARATION	=	0.01
RADIUS	=	0.0001

TRANSMISSION LINE MODEL — OSMOM ⊙

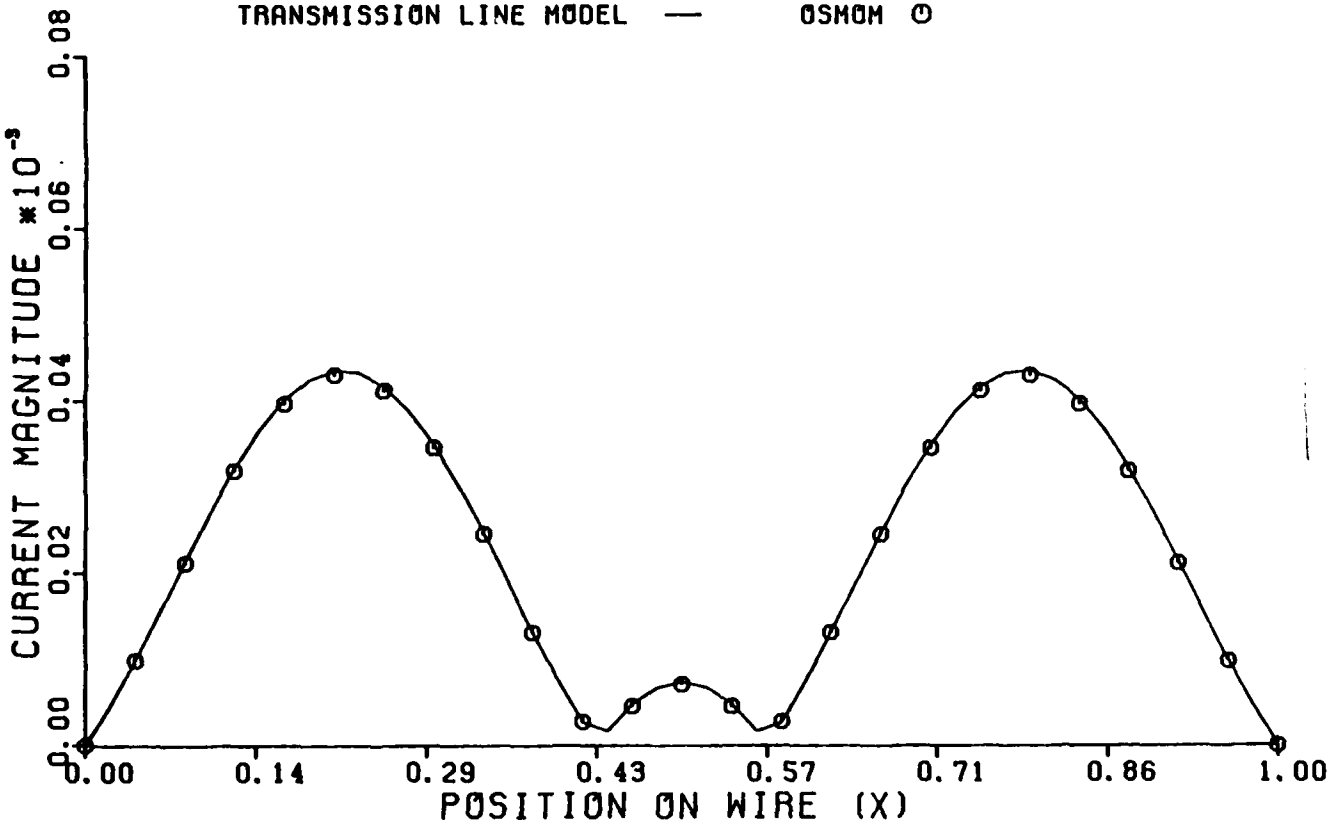

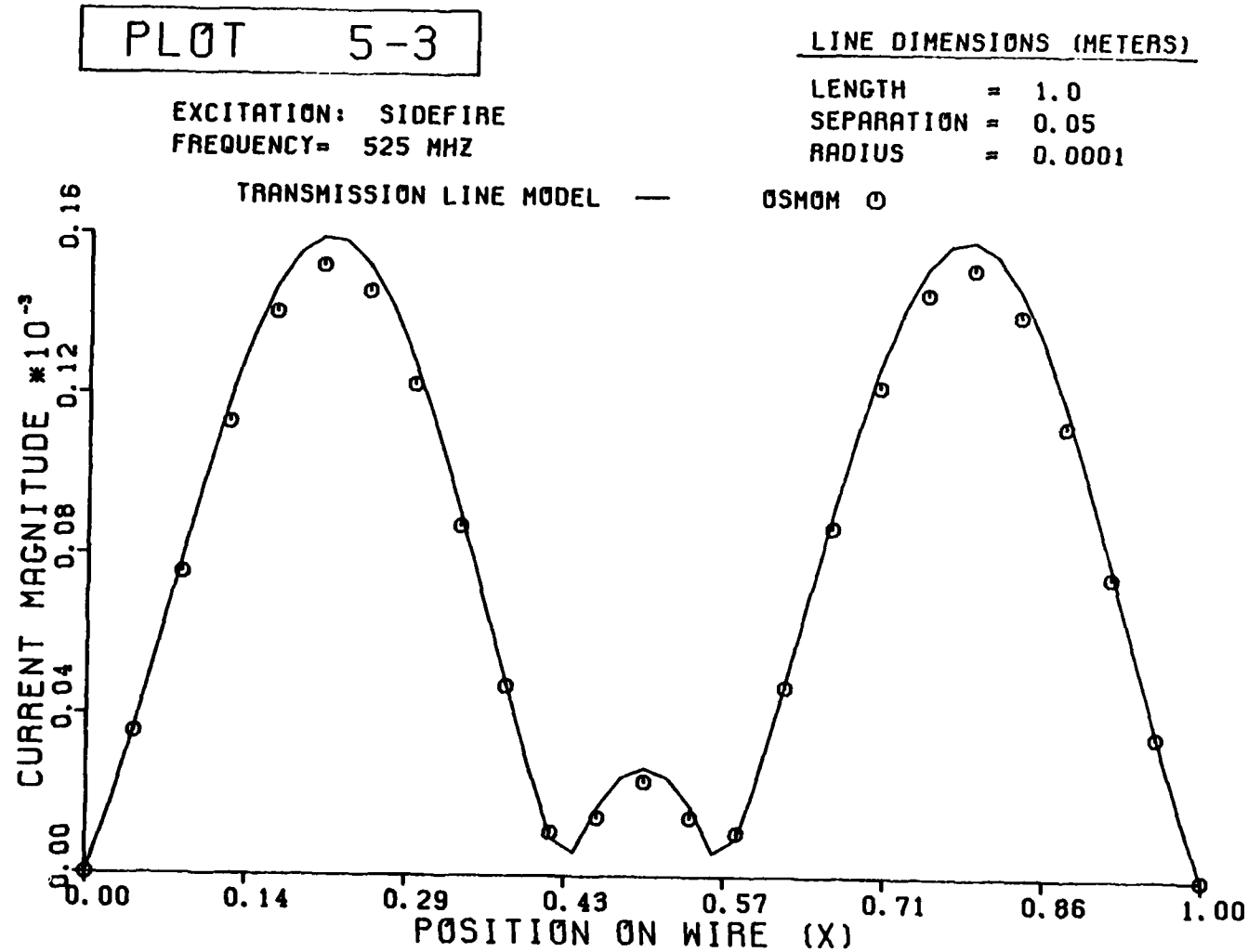
PLOT 5-3
EXCITATION: SIDEFIRE
FREQUENCY= 525 MHZ
LINE DIMENSIONS (METERS)
LENGTH = 1.0
SEPARATION = 0.05
RADIUS = 0.0001
TRANSMISSION LINE MODEL — OSMOM ⊙
CURRENT MAGNITUDE *10⁻³
0.00
0.04
0.08
0.12
0.16
0.00
0.14
0.29
0.43
0.57
0.71
0.86
1.00
POSITION ON WIRE (X)

PLOT 5-4

EXCITATION: SIDEFIRE
FREQUENCY= 525 MHZ

LINE DIMENSIONS (METERS)

LENGTH	=	1.0
SEPARATION	=	0.10
RADIUS	=	0.0001

TRANSMISSION LINE MODEL — OSMOM ⊙

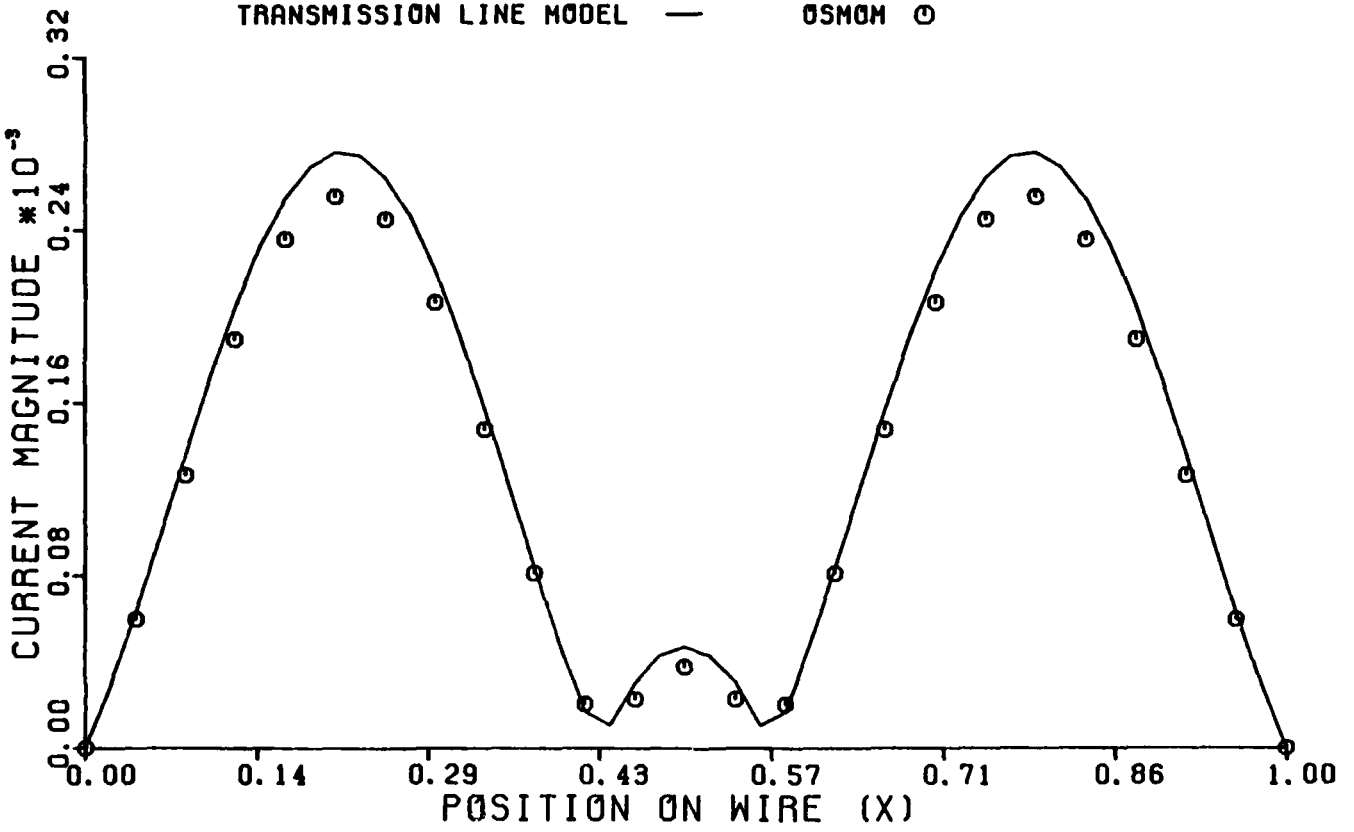

	PERCENT ERROR		
x	d=0.01	d=0.05	d=0.1
0.00000	0.00	0.00	0.00
0.04167	-0.05	1.45	4.54
0.08333	0.82	3.69	7.08
0.12500	1.06	4.34	7.83
0.16667	1.15	4.58	8.09
0.20833	1.18	4.64	8.10
0.25000	1.16	4.56	7.90
0.29167	1.09	4.28	7.40
0.33333	0.90	3.61	6.25
0.37500	0.34	1.68	3.06
0.41667	-4.27	-12.48	-18.26
0.45833	5.03	19.49	35.31
0.50000	3.75	14.25	25.10
0.54167	5.01	19.48	35.30
0.58333	-4.21	-12.47	-18.25
0.62500	0.35	1.68	3.06
0.66667	0.91	3.61	6.25
0.70833	1.10	4.28	7.40
0.75000	1.17	4.55	7.90
0.79167	1.18	4.64	8.10

TABLE 5-1

	PERCENT ERROR		
x	d=0.01	d=0.05	d=0.1
0.83333	1.15	4.58	8.08
0.87500	1.05	4.33	7.82
0.91667	1.81	3.68	7.07
0.95833	-0.05	1.44	4.53
1.00000	0.00	0.00	0.00

TABLE 5-1 (con't.)

WRSMOM, consistant zone size in particular, were discussed. The structure used in Chapter 4 involved a separation between wires that would have required a total of at least 202 subsections if all zones were of equal length. This creates a very large matrix system as mentioned earlier. However, with the introduction of a structure involving wider wire separation, solution by WRSMOM is feasible.

For reference sake, the three cases of excitation (ENDFIRE, SIDEFIRE, and BROADSIDE) are solved for matched loads by WRSMOM, for the same structure used in Chapter 4. This structure had a separation of 0.01 meter and the method of moments model used 24 zones on each line and 1 zone for each terminal wire. It must be pointed out that the requirements necessary for a valid solution by the point matching, pulse expansion technique (used in WRSMOM) have not been met. These predictions serve only as reference for results yet to be discussed. The current magnitudes predicted by WRSMOM have been added to PLOTS 4-1, 4-7, and 4-13 and are shown in PLOTS 5-5, 5-6, and 5-7, respectively. The solution by WRSMOM is inaccurate as expected, for the reasons discussed at the end of Chapter 3.

The structure is now changed by increasing the wire separation to 0.05 meter. Dividing each transmission line wire into 20 segments and modeling each terminal wire as one segment characterizes the structure with 42 equal length zones for solution by the method of

PLØT 5-5

EXCITATION: ENDFIRE
LOADING: MATCHED

LINE DIMENSIONS (METERS)

LENGTH	=	1.0
SEPARATION	=	0.01
RADIUS	=	0.0001

TRANSMISSION LINE MODEL — OSMOM ⊙ WRSMOM +

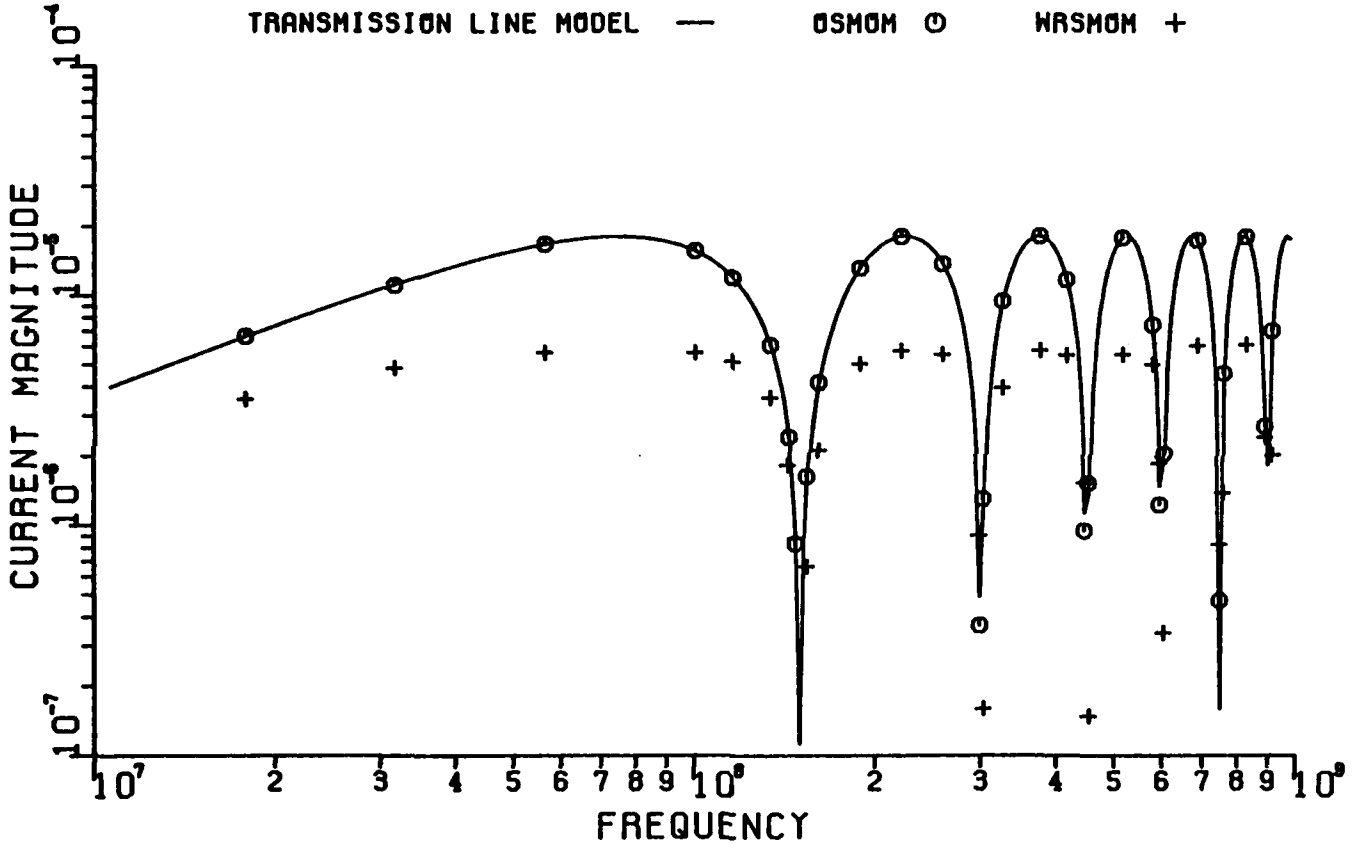

PLOT 5-6

EXCITATION: SIDEFIRE
LOADING: MATCHED

LINE DIMENSIONS (METERS)

LENGTH = 1.0
SEPARATION = 0.01
RADIUS = 0.0001

TRANSMISSION LINE MODEL — OSMOM ⊙ WRSMOM +

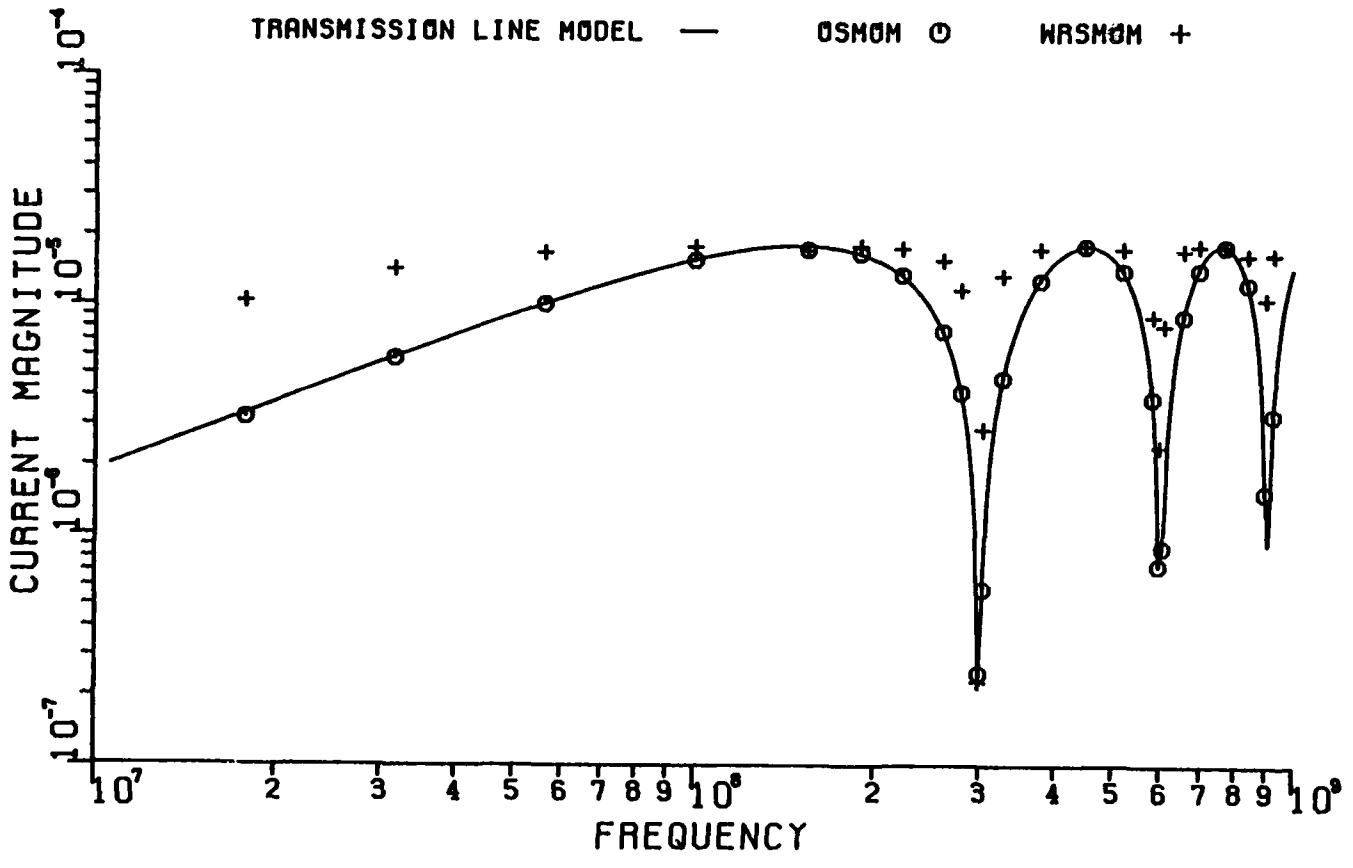

PLOT 5-7

EXCITATION: BROADSIDE
LOADING: MATCHED

LINE DIMENSIONS (METERS)

LENGTH	=	1.0
SEPARATION	=	0.01
RADIUS	=	0.0001

TRANSMISSION LINE MODEL — OSMOM ⊙ WASMOM +

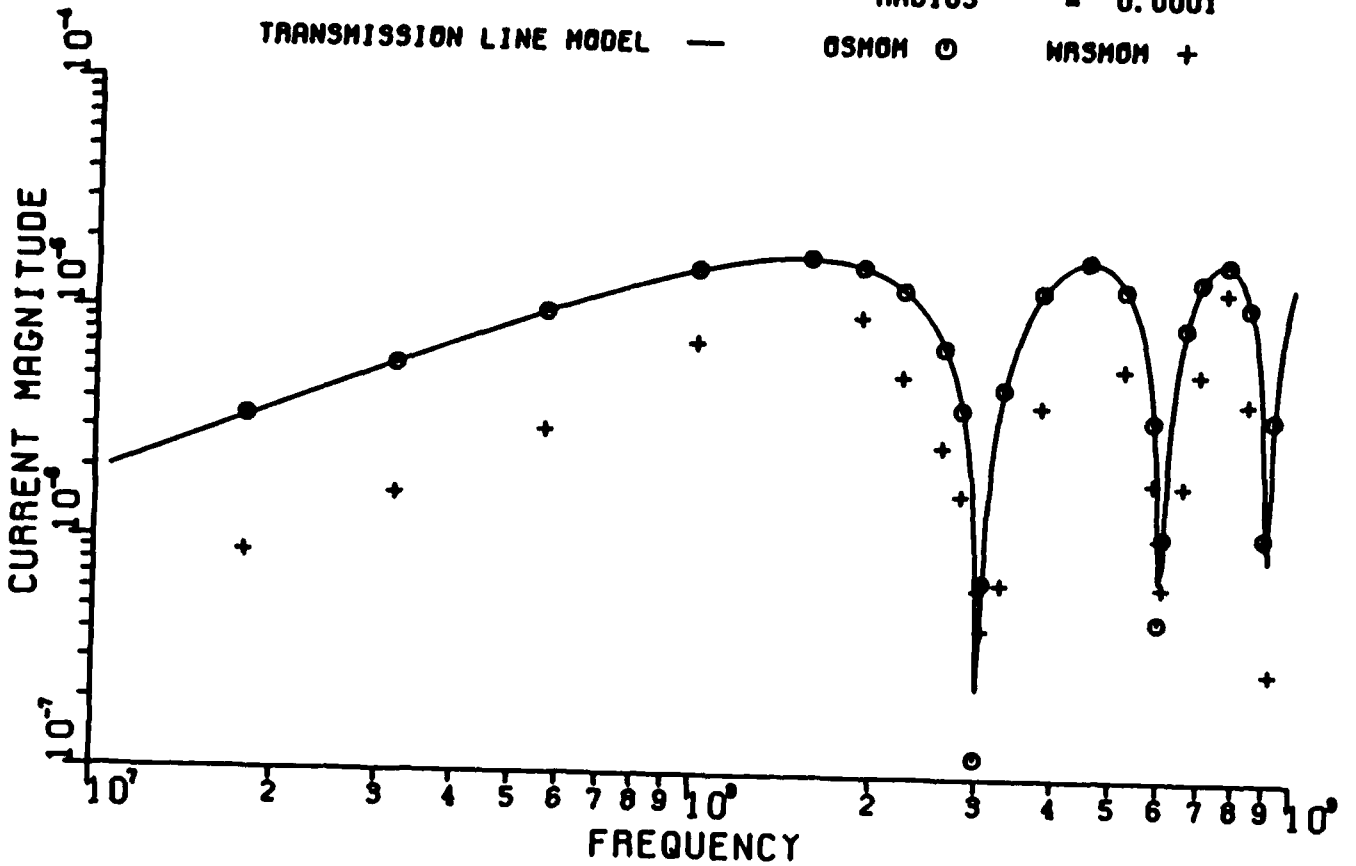

moments. Removing the abrupt change in subsection length found in the previous structure improves the WRSMOM results considerably. These results, for the ENDFIRE, SIDEFIRE, and BROADSIDE cases, are shown by PLOTS 5-8, 5-9, and 5-10 respectively. The two method of moments solutions compare quite favorably, even though the E field is only being "matched" at one point in the load with the WRSMOM solution. The OSMOM solution should be more accurate for an additional reason. In OSMOM, the elements in the impedance matrix are calculated using the rigorous closed-form impedance expressions in terms of exponential integrals. This method of calculation provides a much more accurate (but expensive) solution than the numerical integration techniques (such as Simpson's integration rule) which are normally used to generate the entries in the matrix. Both method of moments solutions are sensitive at frequencies near the current nulls, because of the rapidly changing currents. It is not surprising that predictions differ here. In general, the predictions from all three solution techniques compare well for all three cases of excitation.

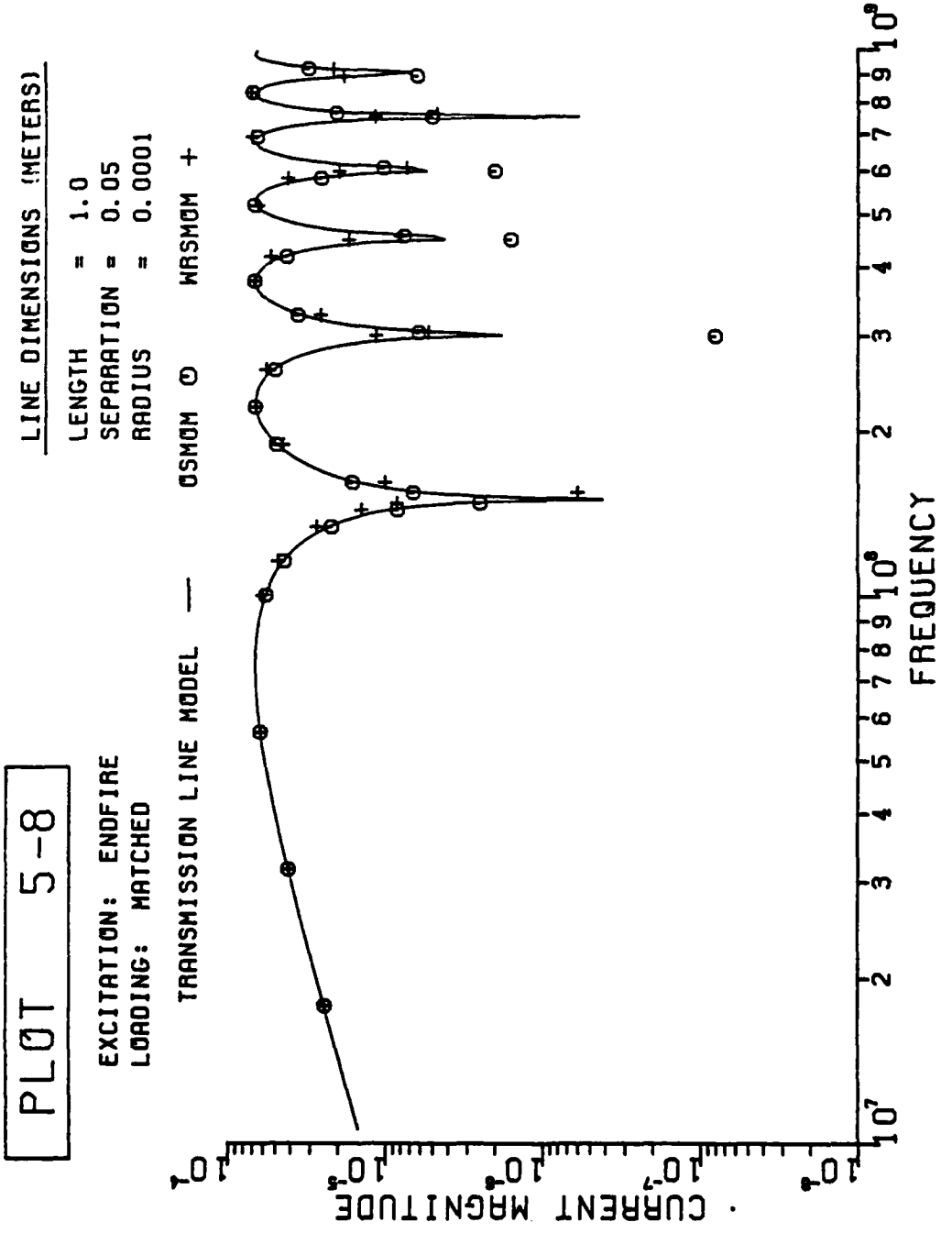
PLOT 5-8
EXCITATION: ENDFIRE
LOADING: MATCHED
TRANSMISSION LINE MODEL — OSMOM ⊙ WRSMOM +
LINE DIMENSIONS (METERS)
LENGTH = 1.0
SEPARATION = 0.05
RADIUS = 0.0001
CURRENT MAGNITUDE
FREQUENCY

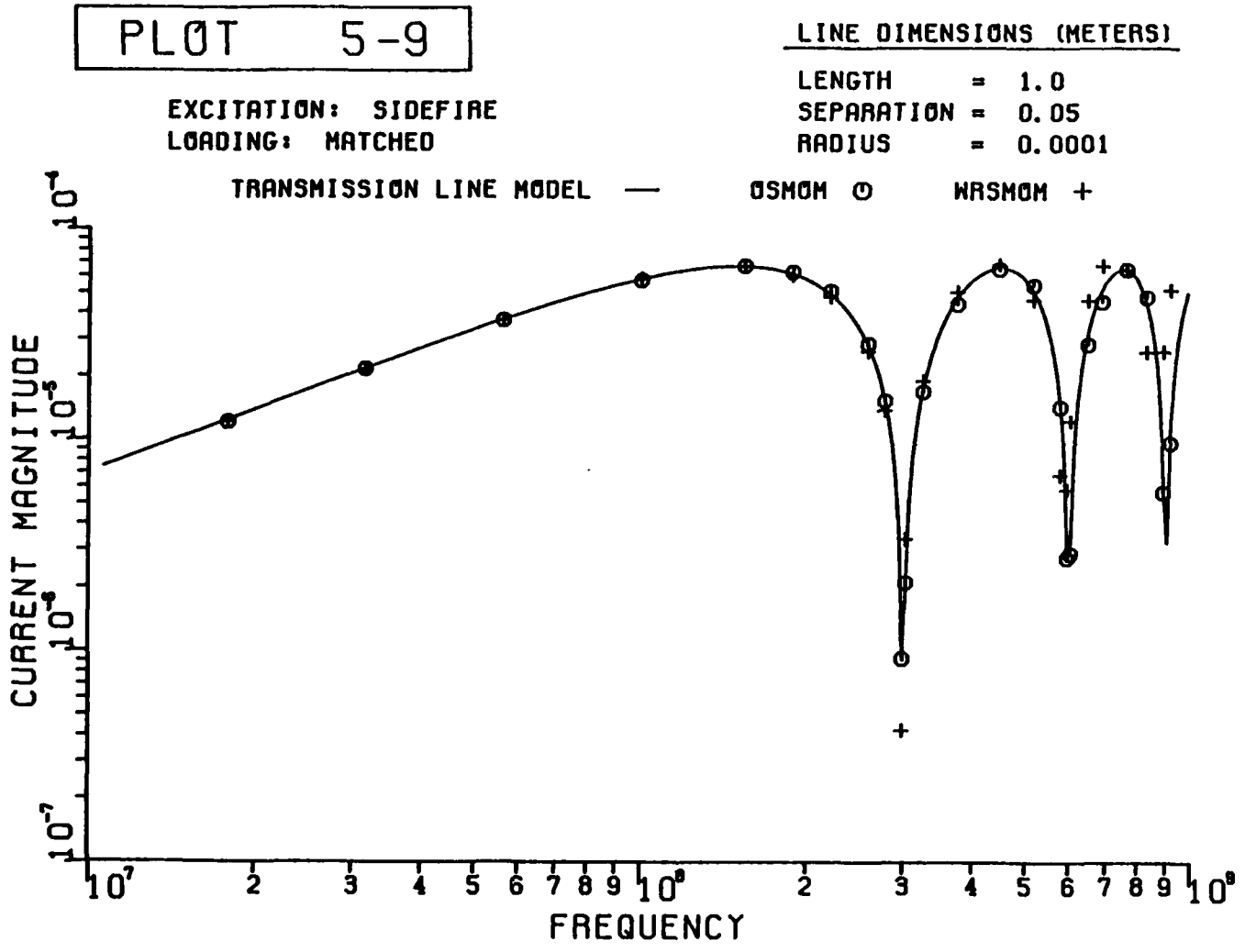
PLOT 5-9
EXCITATION: SIDEFIRE
LOADING: MATCHED
LINE DIMENSIONS (METERS)
LENGTH = 1.0
SEPARATION = 0.05
RADIUS = 0.0001
TRANSMISSION LINE MODEL — OSMOM ⊙ WRSMOM +
CURRENT MAGNITUDE
FREQUENCY

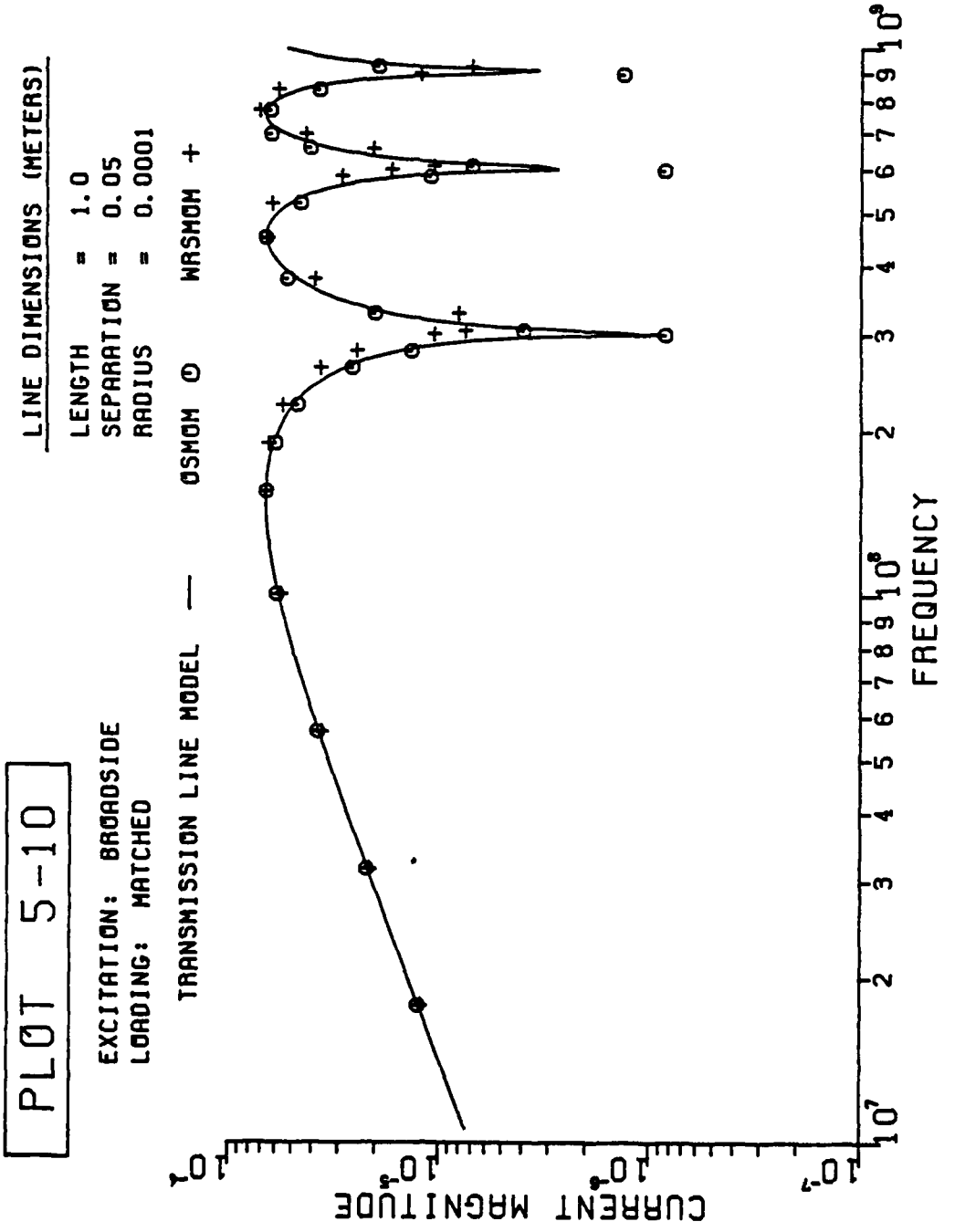
PLOT 5-10
EXCITATION: BROADSIDE
LOADING: MATCHED
TRANSMISSION LINE MODEL — OSMOM ⊙ WRSMOM +
LINE DIMENSIONS (METERS)
LENGTH = 1.0
SEPARATION = 0.05
RADIUS = 0.0001
CURRENT MAGNITUDE
FREQUENCY

CHAPTER 6

DIFFERENTIAL MODE AND COMMON MODE CURRENT COMPARISONS

The terms "common mode" and "differential mode" were defined in Chapter 2, and have been used repeatedly since then when discussing currents flowing on the structure. The sum or difference of these currents gives the total current flowing on the top or bottom wire at a specified value of x, as defined by the two equations:

$$I_T = I_C + I_D \tag{6-1}$$

$$I_B = I_C - I_D \tag{6-2}$$

These currents are illustrated in FIGURE 2-2. The common and differential mode currents, in terms of the top and bottom currents, are given by equation (4-1).

The transmission line model, by its assumption of TEM propagation, solves for the differential mode currents only. This was discussed in detail, in Chapter 2. The method of moments formulation assumes only that the currents are axially directed, so it gives a total current solution. This solution is decomposed into common and differential mode currents for comparison to the transmission line model solution, as described in Chapter 4. In this chapter, the rel-

evance of the differential mode current prediction is discussed.

First it might be helpful to gain some insight into the common mode. The common mode current, sometimes referred to as the antenna mode current, can be though of as the "net" current passing through a plane transverse to the transmission line. This is why there are no common mode currents in the transmission line model; the sum of the currents passing through any transverse plan is zero (or, zero net current). We should expect the common mode currents to be larger for the SIDEFIRE case, than for the BROADSIDE or ENDFIRE case, due to the orientation of the E field. In the SIDEFIRE case the E field is aligned (parallel) with the transmission line wires, allowing for maximum pickup. In the other two cases the E field is perpendicular to the transmission line wires. (It should be pointed out that this orientation is exactly opposite from the E field orientation needed to induce sources in the transmission line model. There, maximum E field pickup was achieved with the E field orientated transverse to the wires, as in the ENDFIRE and BROADSIDE cases.) The results from all of the cases discussed in Chapters 4 and 5 confirm this expectation. Common mode currents for the ENDFIRE and BROADSIDE cases were several orders of magnitude smaller than the differential mode currents in solutions by the method of moments codes. They, for the most part, are probably a result of numerical "noise" generated during the matrix computations. However, for the SIDEFIRE case, the

common mode currents were the same order of magnitude as the differential mode currents. In [16] it is pointed out that the relationship between common and differential modes currents depends upon the terminations and may be a function of frequency. From the results just discussed, it would seem that the incident field excitation is also very important.

This raises a very important issue. If the common mode currents are as large as the differential mode currents, of what value are the transmission line model predictions? For an arbitrary value of x along the line, the transmission line model solves only for the differential mode current, as stated several times. The total current on the line is therefore not necessarily represented. However, transmission line theory views the terminal loads as lumped parameters. So, at the terminations, the common mode currents on the top and bottom wires cancel. Therefore, the net terminal current passing through each load is the differential mode current.

This says that the transmission line model should give an accurate solution for the total load current. This last statement should be qualified with two restrictions which have been pointed out in previous chapters. At high frequencies, it is no longer valid to assume that the load will behave as a lumped parameter. Wide separations between the wires will also cause this assumption to be questionable.

Both of these restrictions can be summed up by saying that the load and terminal network must remain electrically small.

To illustrate the correlation between total load current and differential mode terminal current, WRSMOM is used. Consider the transmission line structure used for current predictions in PLOTS 5-8, 5-9 and 5-10. These plots compare the differential mode terminal currents supplied by WRSMOM, OSMOM, and the transmission line model. Using the same structure, the transmission line model results can be compared to the total load current, supplied by WRSMOM. For this structure, WRSMOM models the load as one segment with a match-point at the center. PLOTS 6-1, 6-2 and 6-3 show the transmission line model prediction for differential mode terminal current and the WRSMOM prediction of total load current for the ENDFIRE, SIDEFIRE and BROADSIDE cases respectively.

There are several characteristics to note about these plots. For all three cases, the greatest deviation occurs at higher frequencies. This is due to the fact that the load is not behaving as a lumped parameter. (Results should be considerably better for the wire separation considered in Chapter 4, but valid WRSMOM results are not available for those cases.) Unfortunately, a great deal of the deviation noticed here is not related to the present issue, but to the pulse expansion, point matching technique. As was discussed in Chap-

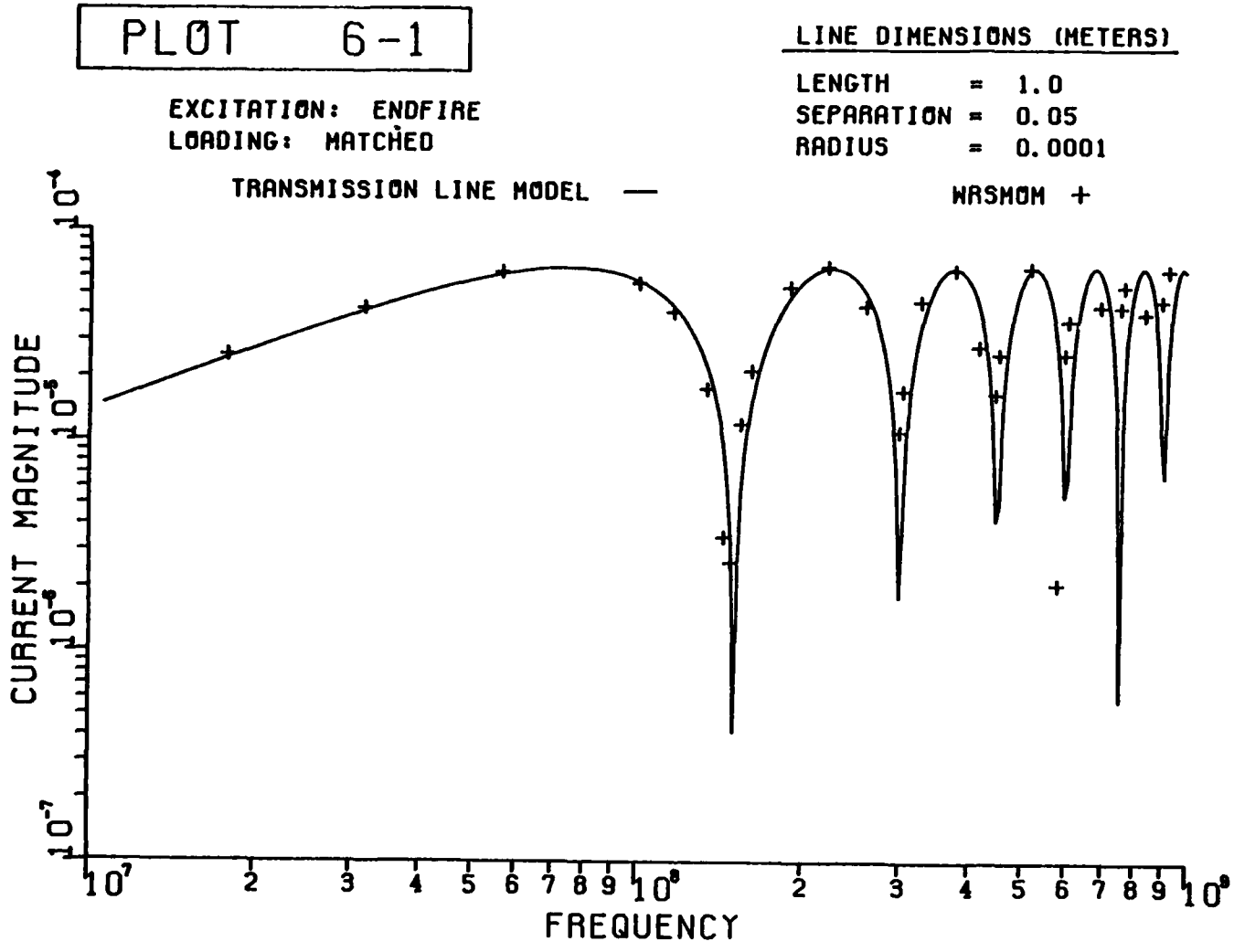
PLOT 6-1
EXCITATION: ENDFIRE
LOADING: MATCHED
LINE DIMENSIONS (METERS)
LENGTH = 1.0
SEPARATION = 0.05
RADIUS = 0.0001
TRANSMISSION LINE MODEL —
WRSMOM +
CURRENT MAGNITUDE
FREQUENCY

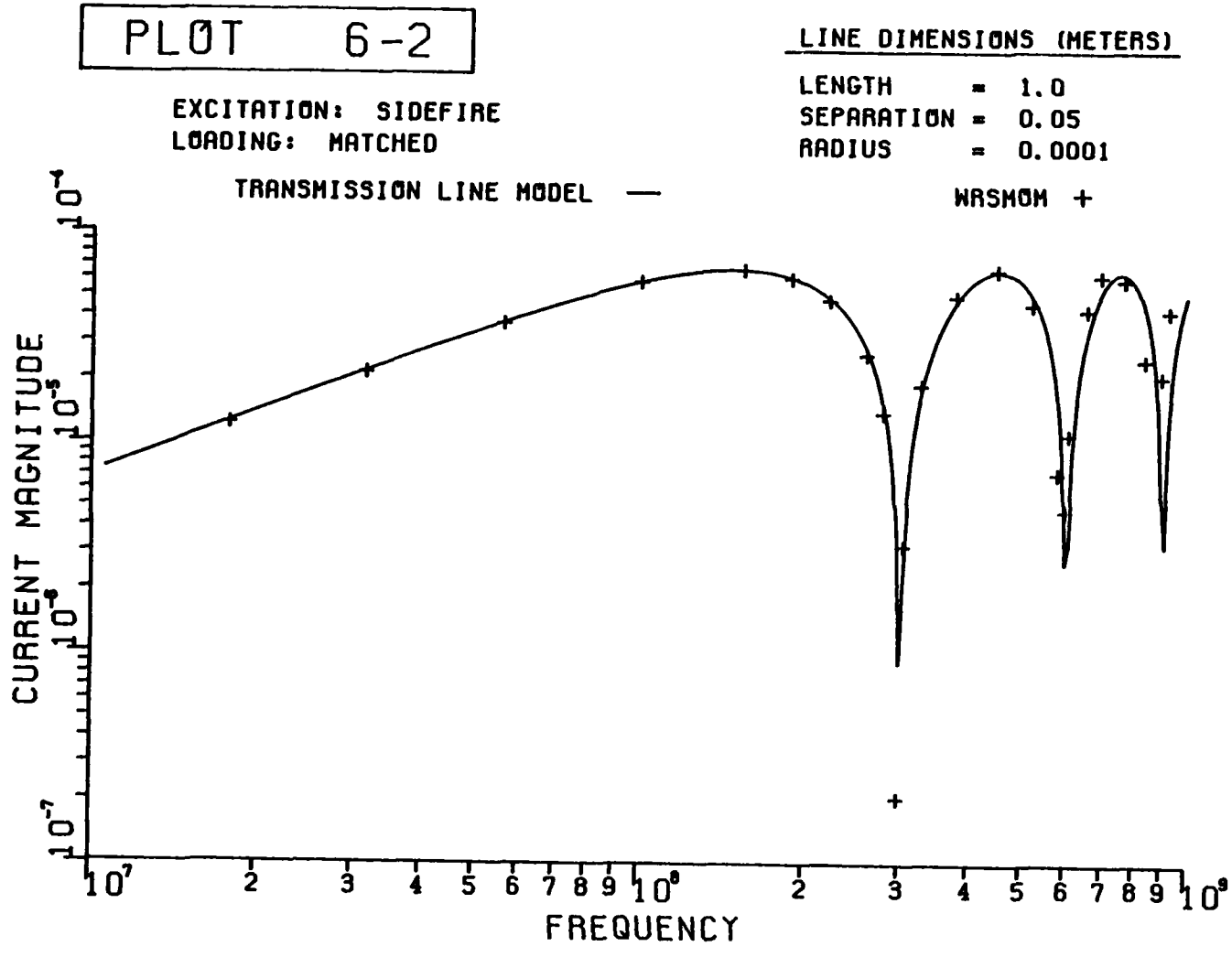
PLOT 6-2
EXCITATION: SIDEFIRE
LOADING: MATCHED
LINE DIMENSIONS (METERS)
LENGTH = 1.0
SEPARATION = 0.05
RADIUS = 0.0001
TRANSMISSION LINE MODEL —
WRSMOM +
CURRENT MAGNITUDE
FREQUENCY
10⁻⁴
10⁻⁵
10⁻⁶
10⁻⁷
10⁷ 2 3 4 5 6 7 8 9 10⁸ 2 3 4 5 6 7 8 9 10⁹

PLOT 6-3

EXCITATION: BROADSIDE
LOADING: MATCHED

LINE DIMENSIONS (METERS)

LENGTH = 1.0
SEPARATION = 0.05
RADIUS = 0.0001

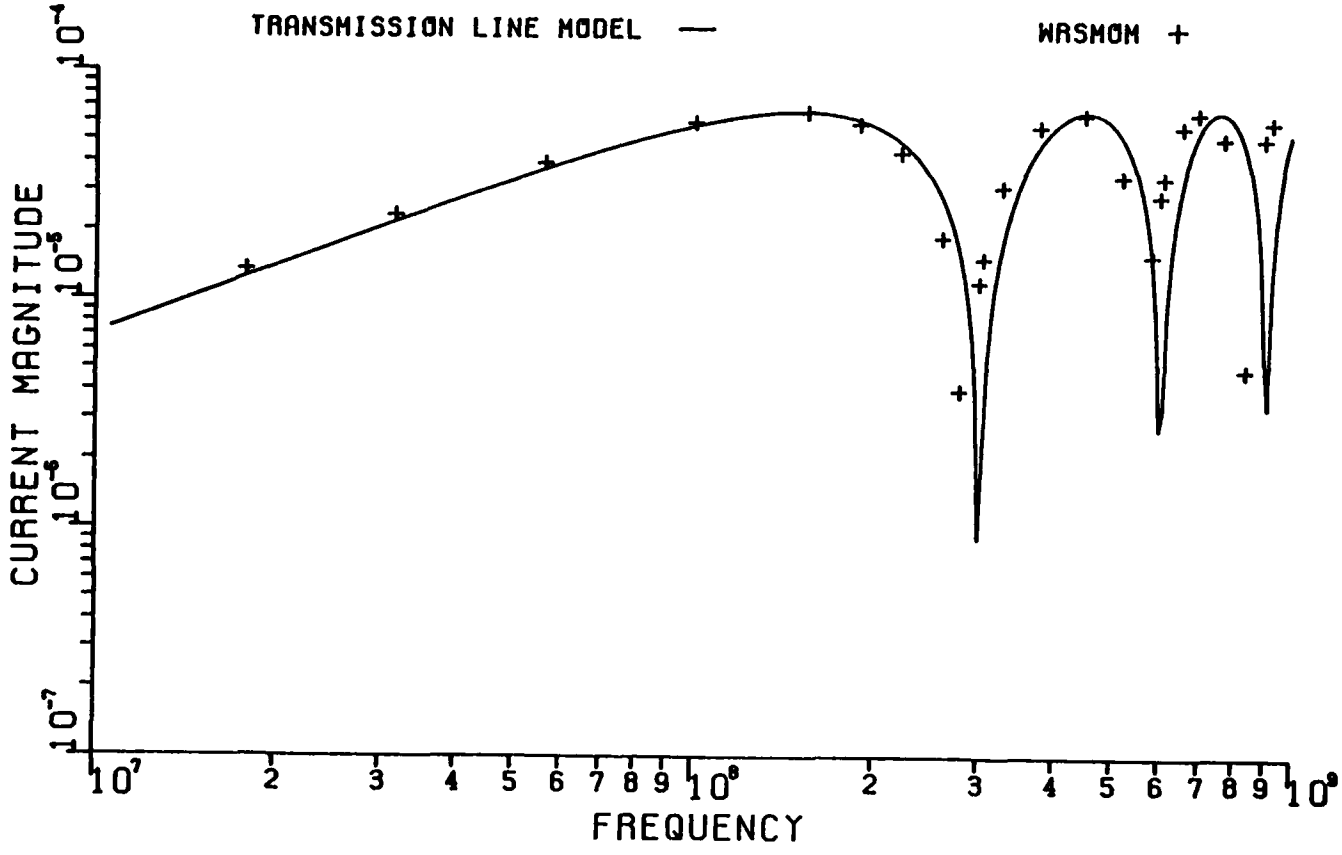

ter 3, this technique does not allow adequate sampling of the E field in the termination. More zones are needed to provide for more matchpoints. Unfortunately, adding more zones creates problems with consistency of subsection length and creates an overly large system of equations. The inadequate representation of the E field is particularly important for the ENDFIRE case, where the method of moments incorporates the incident field by adding sources only to the load segments.

Nevertheless, the plots do illustrate that for this structure and at least for frequencies up through 300 megahertz, the common mode currents do cancel in the load. On this basis, the results of all three cases are good. This holds true even for the SIDEFIRE case, where the common mode current along the line is large.

CHAPTER 7

SUMMARY AND CONCLUSIONS

In any situation where electronic devices communicate with one another via transmission lines, we are faced with the possibility of unwanted electromagnetic coupling. No matter what the source may be, the presence of an incident electromagnetic field can interfere with this communication process. Given that we must contend with this problem, a reliable, accurate and efficient method is needed to predict the effects of this incident field. Transmission line theory is an obvious choice.

The transmission line model offers several advantages when compared with other methods. First, it probably provides the most efficient solution technique known. This is important when considering several cases, such as several different values of loading, or solving over a range of frequencies. Several thousand dollars in computer time have been invested in the work presented here; transmission line model solutions made up less than two percent of that cost. A second advantage to the transmission line model is that the mathematical equations involved are not totally disassociated from physical intuition. Specific forms, allowing insight into the solution, can be derived, as was illustrated several times in Chapter 4. Transmission

line theory acquires these characteristics by making several key assumptions. These assumptions set forth certain requirements which must be met by the problem at hand. It is the lack of specific values for these restrictions that prevent the establishment of limits of validity for transmission line theory. It is certainly impossible to validate the transmission line model on a case by case basis. The results presented in this work are not intended as an attempt to validate transmission line theory for all possible cases. Rather, these results should be used to indicate some of the circumstances where and why this theory may become invalid. At the same time, it is shown that the transmission line model provides valid and accurate solutions for several important cases within its domain, when compared to the solution provided by the much more rigorous method of moments.

The series of plots in Chapter 4 covers three important loading conditions (low impedance, high impedance and matched impedance) which are somewhat representative of the wide variety of possible loads. Each of these loading conditions is examined for the three most significant (from a transmission line theory standpoint) cases of incident field excitation, over a wide range of frequencies. The electrical separation between the transmission line wires is small, never becoming larger than 1/30 of a wavelength for all frequencies considered. In each plot, results produced by the transmission line model solution for the terminal currents are compared with the method of

moments solution for the differential mode terminal currents provided by OSMOM (method of moments computer program described in Chapter 3).

Excellent correspondence is observed between the two solutions for the matched and high impedance load cases. The transmission line solution remains accurate through at least 900 megahertz for these two loading conditions. The method of moments solution begins to break down at frequencies just below 10 megahertz for all loads. This is expected and due to numerical instability encountered during matrix operations. Correspondence between the two solutions did not appear to be significantly effected by the angle of incidence or polarization of the plane wave used for excitation (at least for the three cases of excitation considered here). The parameter which seemed to have the most effect in the comparison between solutions was the loading, in particular the low impedance loads.

Although the matched and high impedance transmission line model solutions compared very well with the method of moments, the solutions for the low impedance case showed some slight discrepancies at frequencies above 300 megahertz. This difference in solution is most prominent at frequencies near those producing terminal current nulls. This effect is similar to that noticed in [16] for a transmission line with short circuit terminations. The fact that this occurrence is

brought on by low impedance loads might indicate that the problem lies in reradiation by the terminal wires. The transmission line model views the load as a lumped parameter, thereby having no electromagnetic properties. The method of moments, however, views the load as a short terminal wire containing a load. Therefore, significant current flowing on this terminal wire would cause it to radiate, as an antenna, an effect which is accounted for in the method of moments solution, but not in transmission line theory. Low impedance loading tends toward greater reradiation.

To investigate reradiation as a possible cause for the discrepancy, the structure is slightly modified in Chapter 5. If reradiation is the problem, lengthening the terminal wire should cause the correspondence between the two solutions to worsen. The wire separation is increased, and indeed the correspondence does deteriorate with low impedance loads.

Although reradiation is probably causing the greater part of the discrepancy, the transmission line model begins to break down for other reasons for wide wire separation. As the separation between the transmission line wires is increased, the TEM assumption, essential to transmission line theory, begins to break down and higher order modes become significant as they begin to propagate. To see the effects of this assumption losing its validity, reradiation must be

removed. To accomplish this, the low impedance loads are replaced by open circuits. Since this will obviously cause the terminal currents to become zero, the two methods of solution can be compared by looking at various points along the line. The transmission line model, via the chain parameter matrix, can generate the differential mode current at any point along the line. The method of moments, by the nature of the technique, produces current values at various points on the structure. This method of moments solution for total current can then be decomposed into common and differential mode currents, and the differential mode current can be compared to the transmission line model solution for these points along the line. Three separations are considered. Each time the separation is increased, the transmission line solution deviates further from the method of moments solution, as expected. For the widest separation, the ratio of line length to separation is 10:1, causing a questionable transmission line model solution.

Transmission line theory, by the TEM assumption, assumes that common mode currents are not present. That is, it solves only for differential mode currents. This raises a significant question. Of what value are the transmission line results if they only predict the differential mode component of the total current? Remembering that transmission line theory views the load as a lumped parameter, the common mode currents cancel in the load. Therefore, only the differential current flows through the load. This remains true as long

as the assumption that the load behaves as a lumped parameter remains valid; the load must remain electrically small. High frequency and wide separation will cause the use of the transmission line model solution as an accurate prediction for total load current to be questionable. In Chapter 6, the transmission line model solution is compared to the total load current prediction provided by WRSMOM (method of moments computer program discussed in Chapter 3). The results show that, for this separation the transmission line model solution provides an accurate prediction of total load current up through 300 megahertz, or when the separation is 1/20 of a wavelength.

At this point, a few comments should be made concerning the method of moments computer program used. OSMOM [13], [14], which uses Galerkin's method and piecewise sinusoidal expansion functions, was very effective in producing baseline data for comparison. It seems to handle the corners and terminations very well and appeared to give very reliable results for all cases considered. As was discussed in Chapter 5, some problems were encountered with the pulse expansion and point matching technique used in WRSMOM [12]. Although there appear to be no programming problems, the technique itself does not seem to be very well suited for transmission line analysis. It often becomes difficult to model a transmission line structure and maintain the consistency in subsection length necessary for a valid solution. Also, in many cases the E field cannot be adequately

sampled in the termination to provide a valid solution, using point matching. This is discussed in further detail in Chapters 3 and 5.

In general, the results of this investigation show that the transmission line model can be successfully applied to a certain class of problems. The efficiency, intuitive nature of the equations and accuracy in the lower frequency range make it particularly inviting as a solution technique. The user must be conscientious in the observance of restrictions placed on the method by the assumptions of transmission line theory. The transmission line model is obviously not designed to solve all types of coupling problems. However, it does appear to serve a class of problems commonly encountered in present wiring techniques. The next step in the process of establishing validity to the technique is to further define the restrictions on the electrical dimensions of the structure (restrictions required for a valid transmission line model solution), e.g.: wire separation defined in terms of wavelength. This step will probably be difficult because, as shown earlier, several factors intervene, e.g.: low impedance loading. Used correctly, the transmission line model can be a very effective and useful solution technique.

APPENDIX I

The use of an incident electromagnetic plane wave to excite a two wire transmission line is described in this appendix. The plane wave is assumed to be traveling in free space away from the origin of the coordinate system. Four parameters are necessary to describe the wave. Two angles are used to describe the direction of propagation. (See FIGURE I-1.) The angles, θ_p and ϕ_p, are very similar to the angles, θ and ϕ, encountered in a spherical coordinate system. θ_p is the angle between the y axis and the propagation path of the incoming wave. ϕ_p is measured from the z axis to the projection of the propagation vector in the x-z plane. A third angle, θ_E, is needed to describe the polarization of the plane wave (the direction of the E field). Assume a plane, containing the origin, and perpendicular to the propagation vector. Because of the TEM structure of the wave, the E field vector will lie in this plane. θ_E is measured clockwise (looking in the direction of propagation) from the projection of the y axis (onto the plane) to the E field vector. The last parameter needed to describe the wave is the magnitude of the E field. The H field magnitude can be related to the E field magnitude by the intrinsic impedance of free space, η.

$$H_m = \frac{E_m}{\eta} \qquad \text{(I-1)}$$

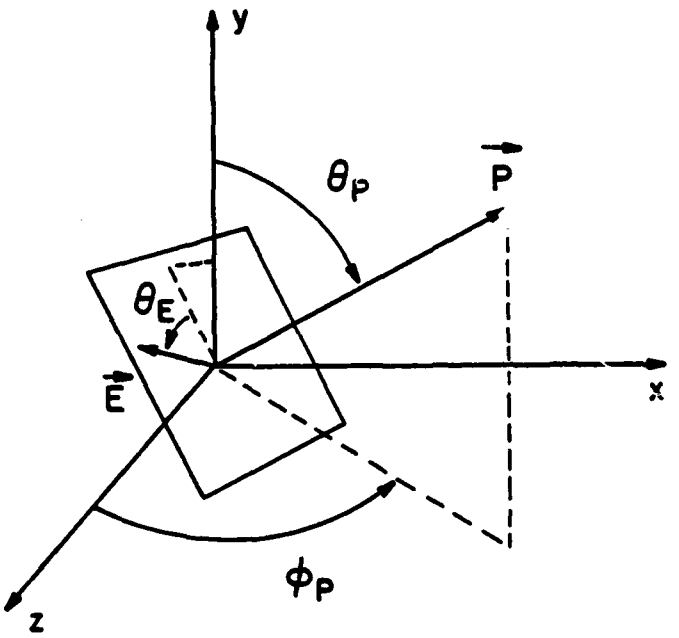

FIGURE I-1

where

$$\eta = \sqrt{\mu_0/\epsilon_0} \qquad \text{(I-2)}$$

and μ_0 is the permeability of free space and ϵ_0 is the permittivity of free space. The orientation of the H field can be obtained by equation (2-52).

The plane wave is propagating with a propagation constant of k. For free space $k=\beta$, described in Chapter 2. Having the plane wave so defined still leaves us with the problem of obtaining the components of k and E_m (E field magnitude) in x, y, and z for use in the transmission line equations. This becomes, for the most part, a coordinate transformation. The three components of k can be obtained by a transformation from spherical to rectangular coordinates, as described in [5]. Given the magnitude of k, the following equations yield values for the rectangular components of k.

$$k_x = k \sin\theta_p \sin\phi_p \qquad \text{(I-3)}$$

$$k_y = k \cos\theta_p \qquad \text{(I-4)}$$

$$k_z = k \sin\theta_p \cos\phi_p \qquad \text{(I-5)}$$

Obtaining the rectangular components of the E field is slightly more difficult. Given the value of E_m, the total E field magnitude, the values of the rectangular components are as follows:

$$E_{xm} = - E_m \cos\theta_E \cos\theta_P \sin\phi_P - E_m \sin\theta_E \cos\phi_P \quad \text{(I-6)}$$

$$E_{ym} = E_m \cos\theta_E \sin\theta_P \quad \text{(I-7)}$$

$$E_{zm} = - E \cos\theta_E \cos\theta_P + E \sin\theta_E \sin\phi_P \quad \text{(I-8)}$$

APPENDIX II

In Appendix III a listing is given for the computer program, written in FORTRAN, which was used to predict the terminal currents of the two wire structure, by transmission line theory techniques. The format of the input data is also given. This appendix describes that program and the required input data.

The first task of the program is to define the wire structure using the parameters discussed in Chapter 2. The data inputs necessary are wire radius, wire separation, wire length, the load at x=0, and the load at x=L. The program will calculate the transmission line solution for arbitrary loads; that is, there are no constraints on the loads. The loads at x=0 and x=L are independent (they can be different from each other) and can be complex. The next inputs describe the uniform plane wave used as the incident field excitation. The four parameters necessary to define the wave are E_m, θ_E, θ_P, and ϕ_P as described in Appendix I.

All calculations are done using double precision to assure accuracy. A special effort was made to do all calculations using a numerically stable form of the equations involved. For example, the calculation of

$$e^{j\alpha} - 1 \qquad \text{(II-1)}$$

where α is small, was done using the stable form

$$j\alpha\, e^{j\alpha/2} \left[\frac{\sin\left(\frac{\alpha}{2}\right)}{\left(\frac{\alpha}{2}\right)} \right] \qquad \text{(II-2)}$$

where sin(x)/(x) is employed.

First, calculations that do not involve frequency are performed. The rectangular coordinate components for the E field are obtained as described in Appendix I. Next, the per-unit-length capacitance is calculated using the wire radius and separation, as given in [6].

$$c = \frac{\pi\varepsilon_o}{\ell n \left[\frac{d}{2r} + \sqrt{\left(\frac{d}{2r}\right)^2 - 1} \right]} \qquad \text{(II-3)}$$

Once the value for c has been obtained, R_c, the characteristic resistance of the line is calculated as given by equation (2-50).

$$R_c = \frac{1}{vc} \qquad \text{(II-4)}$$

The next section performs operations involving frequency for each of the frequencies input as data. The calculations start with obtaining β and rectangular components of k. The calculation of I(0) and I(L) is done using slightly modified versions of the forms pre-

sented by [7]. These equations for the terminal currents are more convenient and concise than the forms derived in Chapter 2.

APPENDIX III

The following three pages contain a listing of the computer program which was used to generate all of the transmission line model results presented in Chapters 4, 5, and 6. A description of this program is presented in Appendix II. The format of the input data is shown on the page immediately following the program listing. Multiple runs, for different frequencies, can easily be executed by simply adding the desired frequencies to the end of the data string, using the format shown. The program will produce a solution for each frequency and stop execution when it runs out of data (when it runs out of frequency data entries).

Output produced by this program was compared to output produced by the program WIRE [17] for several representative test cases. The results from both programs were the same.

```
      IMPLICIT REAL*8(A,B,D-H,O-Z),COMPLEX*16(C)                        00000010
      REAL*8 LEN,L                                                      00000020
      CJ=DCMPLX(0.D0,1.D0)                                              00000030
      VELT=2.997925D8                                                   00000040
      PI=4.D0*DATAN(1.D0)                                               00000050
      RADEG=180.D0/PI                                                   00000060
      E0=1.0D0/(PI*4.0D-7*VELT**2)                                      00000070
C1----------------------------------------------------------------------00000080
      READ(5,10)RAD,SEP,LEN,CZ0,CZL                                     00000090
10    FORMAT(3(T30,E13.6,/),T30,E13.6,2X,E13.6,/,T30,E13.6,2X,E13.6)    00000100
      WRITE(6,50)RAD,SEP,LEN,CZ0,CZL                                    00000110
50    FORMAT('1','WIRE RADIUS',T46,1PE13.6,T63,'METERS',/,              00000120
     &   ' WIRE SEPARATION',T46,1PE13.6,T63,'METERS',/,                 00000130
     &   ' WIRE LENGTH',T46,1PE13.6,T63,'METERS',/,                     00000140
     &   ' IMPEDANCE AT X=0',T30,1PE13.6,T46,1PE13.6,T63,'OHMS',/,      00000150
     &   ' IMPEDANCE AT X=L',T30,1PE13.6,T46,1PE13.6,T63,'OHMS')        00000160
      READ(5,11)EM,THETAE,THETAP,PHIP                                   00000170
11    FORMAT(T30,E13.6,3(/,T30,F6.1))                                   00000180
      WRITE(6,51)EM,THETAE,THETAP,PHIP                                  00000190
51    FORMAT(/,' E-FIELD MAGNITUDE',T46,1PE13.6,T63,'VOLTS/METER',/,    00000200
     &   ' THETAE',T46,7X,0PF6.1,T63,'DEGREES',/,                       00000210
     &   ' THETAP',T46,7X,0PF6.1,T63,'DEGREES',/,                       00000220
     &   ' PHIP',T46,7X,0PF6.1,T63,'DEGREES')                           00000230
C2----------------------------------------------------------------------00000240
      Z=DREAL(CZ0)                                                      00000250
      L=LEN                                                             00000260
      THERAD=THETAE/RADEG                                               00000270
      THPRAD=THETAP/RADEG                                               00000280
      PHPRAD=PHIP/RADEG                                                 00000290
      EXM=-EM*DCOS(THERAD)*DCOS(THPRAD)*DSIN(PHPRAD)-EM*DSIN(THERAD)*   00000300
     &   DCOS(PHPRAD)                                                   00000310
      EYM=EM*DCOS(THERAD)*DSIN(THPRAD)                                  00000320
      WRITE(6,52)EXM,EYM                                                00000330
52    FORMAT(/,' EXM',T30,1PE13.6,/,' EYM',T30,1PE13.6)                 00000340
      PULC=PI*E0/DLOG(SEP/(RAD*2.0D0)+DSQRT((SEP/(RAD*2.0D0))**2        00000350
     &   -1.0D0))                                                       00000360
```

```
      RC=1.0D0/(VELT*PULC)                                                  00000370
      WRITE(6,53)PULC,RC                                                    00000380
53    FORMAT(/,' PULC=',T30,1PE13.6,/,' RC=',T30,1PE13.6)                   00000390
      IPHIP=IDINT(PHIP+0.5)                                                 00000400
C3----------------------------------------------------------------------- 00000410
1000  READ(5,12,END=9999)FREQ                                               00000420
12    FORMAT(T30,E9.1)                                                      00000430
      WRITE(6,54)FREQ                                                       00000440
54    FORMAT(///,' FREQUENCY= ',1PE13.6,3X,'HERTZ')                         00000450
      BETA=2.0D0*PI*FREQ/VELT                                               00000460
      B=BETA                                                                00000470
      BL=B*L                                                                00000480
      RK=B                                                                  00000490
      RKX=RK*DSIN(THPRAD)*DSIN(PHPRAD)                                      00000500
      RKY=RK*DCOS(THPRAD)                                                   00000510
      WRITE(6,55)B,RKX,RKY                                                  00000520
55    FORMAT(/,' BETA',T30,1PE13.6,/,' KX',T30,1PE13.6,/,                   00000530
     &    ' KY',T30,1PE13.6)                                               00000540
      CD=(RC*CZ0+CZL*RC)*DCOS(BL)+CJ*(RC**2+CZL*CZ0)*DSIN(BL)               00000550
C4----------------------------------------------------------------------- 00000560
      X1=(-RKX+B)*L/2.0D0                                                   00000570
      SXOX1=1.0D0                                                           00000580
      IF(DABS(X1).LT.1.0D-50)GO TO 1005                                     00000590
      SXOX1=DSIN(X1)/(X1)                                                   00000600
1005  X2=(-RKX-B)*L/2.0D0                                                   00000610
      SXOX2=1.0D0                                                           00000620
      IF(DABS(X2).LT.1.0D-50)GO TO 1010                                     00000630
      SXOX2=DSIN(X2)/(X2)                                                   00000640
1010  CE1=CDEXP(-CJ*BL)*CDEXP(CJ*X1)*SXOX1                                  00000650
      CE2=CDEXP(CJ*BL)*CDEXP(CJ*X2)*SXOX2                                   00000660
      X3=-RKY*SEP/2.0D0                                                     00000670
      CE3=CJ*EXM*L*CDEXP(CJ*X3)*DSIN(X3)                                    00000680
      CI01=RC*CE3*(CE1+CE2)                                                 00000690
      CI02=CZL*CE3*(CE1-CE2)                                                00000700
      SXOX3=1.0D0                                                           00000710
      IF(DABS(X3).LT.1.0D-50)GO TO 1015                                     00000720
```

```
      SXOX3=DSIN(X3)/(X3)                                                    00000730
1015  CE4=EYM*SEP*CDEXP(CJ*X3)*SXOX3                                         00000740
      CI03=RC*CDEXP(-CJ*RKX*L)*CE4                                           00000750
      CI04=(RC*DCOS(BL)+CJ*CZL*DSIN(BL))*CE4                                 00000760
      CI0=(CI01-CI02-CI03+CI04)/CD                                           00000770
      CE5=CDEXP(CJ*X1)*SXOX1                                                 00000780
      CE6=CDEXP(CJ*X2)*SXOX2                                                 00000790
      CE7=CJ*EXM*L*CDEXP(CJ*X3)*DSIN(X3)                                     00000800
      CIL1=RC*CE7*(CE5+CE6)                                                  00000810
      CIL2=CZ0*CE7*(CE5-CE6)                                                 00000820
      CE8=EYM*SEP*CDEXP(CJ*X3)*SXOX3                                         00000830
      CIL3=RC*CE8                                                            00000840
      CIL4=(RC*DCOS(BL)+CJ*CZ0*DSIN(BL))*CDEXP(-CJ*RKX*L)*CE8                00000850
      CIL=(CIL1+CIL2+CIL3-CIL4)/CD                                           00000860
      RI0MAG=CDABS(CI0)                                                      00000870
      RILMAG=CDABS(CIL)                                                      00000880
      RI0RE=DREAL(CI0)                                                       00000890
      RI0IM=DIMAG(CI0)                                                       00000900
      RILRE=DREAL(CIL)                                                       00000910
      RILIM=DIMAG(CIL)                                                       00000920
      IF(RI0IM.EQ.0.0D0.AND.RI0RE.EQ.0.0D0)RI0RE=1.0D0                       00000930
      IF(RILIM.EQ.0.0D0.AND.RILRE.EQ.0.0D0)RILRE=1.0D0                       00000940
      RI0ANG=DATAN2(RI0IM,RI0RE)*RADEG                                       00000950
      RILANG=DATAN2(RILIM,RILRE)*RADEG                                       00000960
C5----------------------------------------------------------------------    00000970
      WRITE(6,56)                                                            00000980
56    FORMAT(/,12X,'REAL',10X,'IMAGINARY',8X,'MAGNITUDE',7X,'PHASE')         00000990
      WRITE(6,57)CI0,RI0MAG,RI0ANG,CIL,RILMAG,RILANG                         00001000
57    FORMAT(' I(0)= ',3(1PE13.6,4X),0PF7.2,/,                               00001010
     &   ' I(L)= ',3(1PE13.6,4X),0PF7.2)                                     00001020
      GO TO 1000                                                             00001030
9999  WRITE(6,1)                                                             00001040
1     FORMAT('1')                                                            00001050
      STOP                                                                   00001060
      END                                                                    00001070
```

WIRE RADIUS	=	0.000100D+00	
WIRE SEPARATION	=	0.010000D+00	
WIRE LENGTH	=	1.000000D+00	
LOAD IMPEDANCE (X=0)	=	552.2262D+00	+0.000000D+00
LOAD IMPEDANCE (X=L)	=	552.2262D+00	+0.000000D+00
E-FIELD MAGNITUDE	=	1.000000D+00	
THETAE	=	000.0	
THETAP	=	000.0	
PHIP	=	270.0	
FREQUENCY=		x.xxxD+xx	

APPENDIX IV

In this appendix $V_s'(L)$ and $I_s'(L)$ are evaluated for the ENDFIRE case. Equations (4-4) and (4-5) give the following relations for $V_s(x)$ and $I_s(x)$ in the ENDFIRE case.

$$V_s(x) = j\omega\mu \frac{E_m}{\eta} d\, e^{-jkx} \tag{IV-1}$$

$$I_s(x) = - j\omega c E_m d\, e^{-jkx} \tag{IV-2}$$

Substituting equations (IV-1) and (IV-2) into equation (2-42) gives equation (IV-3). The steps of evaluation leading to a simplified form for $V_s'(L)$ follow.

$$V_s'(L) = \int_0^L [\cos(k(L-\tau))V_s(\tau) - jv\ell \sin(k(L-\tau))I_s(\tau)]d\tau$$

$$= \int_0^L [\cos(k(L-\tau)\, j\omega\mu \frac{E_m}{\eta} d\, e^{-jk\tau} \tag{IV-3}$$

$$+ jv\ell \sin(k(L-\tau))j\omega c E_m d\, e^{-jk\tau}]d\tau$$

$$= E_m d \int_0^L [j \frac{\omega\mu}{\eta} \cos(k(L-\tau) - v\ell\omega c \sin(k(L-\tau))]e^{-jk\tau}d\tau$$

Note that $$\frac{\omega\mu}{\eta} = \frac{\omega\mu}{\sqrt{\mu\varepsilon}} = \omega\sqrt{\mu\varepsilon} = \frac{\omega}{v} = k$$

also $$\omega v \ell c = \omega v(\sqrt{\ell c})^2 = \omega v(\frac{1}{v}) = \frac{\omega}{v} = k$$

Making these substitutions,

$$V_s'(L) = jkE_m d \int_0^L [\cos(k(L-\tau)) + j \sin(k(L-\tau))]\, e^{-jk\tau} d\tau$$

$$= jkE_m d \int_0^L e^{jk(L-\tau)}\, e^{-jk\tau} d\tau$$

$$= jkE_m d \int_0^L e^{jkL}\, e^{-j2k\tau} d\tau$$

$$= jkE_m d\, e^{jkL} \left[\frac{e^{-j2k\tau}}{-j2k}\right]_0^L$$

$$= -\frac{E_m}{2} d\, e^{jkL}\, (e^{-j2kL} - 1)$$

$$= -E_m d \left(\frac{e^{-jkL} - e^{jkL}}{2}\right)$$

$$V_s'(L) = jE_m d \sin(kL) \qquad \text{(IV-4)}$$

Substituting equation (IV-1) and (IV-2) into equation (2-43) gives equation (IV-5). The steps of evaluation leading to a simplified form for $I_s'(L)$ follow.

$$I_s'(L) = \int_0^L [- jvc \sin(k(L-\tau))V_s(\tau)$$

$$+ \cos(k(L-\tau))I_s(\tau)]d\tau$$

$$= \int_0^L - jvc \sin(k(L-\tau))\ j\omega\mu \frac{E_m}{\eta} d\ e^{-jk\tau} \qquad \text{(IV-5)}$$

$$- \cos(k(L-\tau))\ j\omega c E_m d\ e^{-jk\tau}]d\tau$$

$$= E_m d \int_0^L \frac{vc\omega\mu}{\eta} \sin(k(L-\tau)) - j\omega c \cos(k(L-\tau))\ e^{-jk\tau} d\tau$$

Note that $$\frac{\mu v}{\eta} = \frac{\mu}{\eta}\frac{1}{\sqrt{\mu\varepsilon}} = \frac{\mu}{\sqrt{\mu/\varepsilon}}\frac{1}{\sqrt{\mu\varepsilon}} = 1$$

$$I_s'(L) = - j\omega c E_m d \int_0^L [\cos(k(L-\tau)) + j \sin(k(L-\tau))]e^{-jk\tau} d\tau$$

$$= - j\omega c E_m d \int_0^L e^{jk(L-\tau)}\ e^{-jk\tau} d\tau$$

$$= - j\omega c E_m d \int_0^L e^{jkL}\ e^{-j2k\tau} d\tau$$

$$= - j\omega c E_m d\ e^{jkL} \left[\frac{e^{-j2k\tau}}{-j2k}\right]_0^L$$

$$= \frac{\omega c}{2k} E_m d\ e^{jkL}\ (e^{-j2kL} - 1)$$

$$= \frac{\omega c E_m d}{k}\left(\frac{e^{-jkL} - e^{jkL}}{2}\right)$$

$$= - j \frac{\omega c E_m d}{k} \sin(kL)$$

Note that

$$\frac{\omega c}{k} = vc = \frac{1}{R_c}$$

$$I_s'(L) = - j \frac{E_m d}{R_c} \sin(kL) \qquad \text{(IV-6)}$$

APPENDIX V

The purpose of this appendix is to show that for ENDFIRE and BROADSIDE excitation, with open circuit loading, the transmission line solution of Chapter 2 gives zero currents for all values of x along the line.

Equation (5-6) has been specialized to open circuit loading but is still valid for all three cases of excitation. It is given here, as equation (V-1).

$$I(x) = - \frac{\sin(\beta x)}{\sin(\beta L)} I_s'(L) + I_s'(x) \qquad \text{(V-1)}$$

First consider the ENDFIRE case. The value of $I_s'(L)$ is given by equation (4-9).

$$I_s'(L) = - j \frac{E_m d}{R_c} \sin(\beta L) \qquad \text{(V-2)}$$

Variable substitution yields

$$I_s'(x) = - j \frac{E_m d}{R_c} \sin(\beta x) \qquad \text{(V-3)}$$

Substituting (V-2) and (V-3) into (V-1), we obtain

$$I(x) = j\frac{\sin(\beta x)}{\sin(\beta L)}\frac{E_m d}{R_c}\sin(\beta L) - j\frac{E_m d}{R_c}\sin(\beta x) \qquad \text{(V-4)}$$

Simplification yields the following.

$$I(x) = j\frac{E_m d}{R_c}\sin(\beta x) - j\frac{E_m d}{R_c}\sin(\beta x) = 0 \qquad \text{(V-5)}$$

the BROADSIDE case is very similar. The value of $I_s'(L)$ (specialized to the BROADSIDE case), as given by equation (4-38):

$$I_s'(L) = -j\frac{E_m d}{R_c}\sin(\beta L)$$

This relation is identical to equation (V-2). Therefore the result will be exactly the same as that given by equation (V-5).

REFERENCES

[1] C. R. Paul, "Frequency Response of Multiconductor Transmission Lines Illuminated by an Electromagnetic Field", IEEE Trans. on Electromagnetic Compatibility, Vol. EMC-18, No. 4, November 1976.

[2] C. D. Taylor, R. S. Satterwhite and C. W. Harrison, Jr., "The Response of a Terminated Two-Wire Transmission Line Excited by a Nonuniform Electromagnetic Field", IEEE Trans. on Antennas and Propagation, pp. 987-989, November 1965.

[3] K. S. H. Lee, "Two Parallel Terminated Conductors in External Fields", IEEE Trans. on Electromagnetic Compatibility, Vol. EMC-20, No. 2, May 1978.

[4] C. T. Chen, Introduction to Linear System Theory. New York: Holt, Rinehart and Winston, Inc., 1970.

[5] D. T. Paris and F. K. Hurd, Basic Electromagnetic Theory. New York: McGraw-Hill, Inc., 1969, pp. 7-9.

[6] C. T. A. Johnk, Engineering Electromagnetic Fields and Waves. New York: John Wiley and Sons, 1975, p. 232.

[7] A. A. Smith, "A More Convenient Form of the Equations for the Response of a Transmission Line Excited by Nonuniform Fields", IEEE Trans. on Electromagnetic Compatibility, Vol. EMC-15, pp. 151-152, August 1973.

[8] C. R. Paul, "Applications of Multiconductor Transmission Line Theory to the Prediction of Cable Coupling, Vol. 1, Multiconductor Transmission Line Theory", Technical Report, RADC-TR-76-101, Vol. I, Rome Air Development Center, Griffiss AFB, New York, April 1976.

[9] R. B. Adler, L. J. Chu and R. M. Fano, Electromagnetic Energy Transmission and Radiation. New York: John Wiley and Sons, Inc. 1960, pp. 499-505.

[10] B. Strait, "Computer Programs for EMC Based on the Method of Moments", Technical Report, RADC-TR-80-93, Rome Air Development Center, Griffiss AFB, New York, April 1980.

[11] R. F. Harrington, Field Computation by Moment Methods. New York: Macmillan Co., 1968.

[12] D. E. Warren, "A User Manual for Program WRSMOM", Dept. of Elec. and Comp. Engr., Syracuse University, Syracuse, New York.

[13] J. H. Richmond, "Radiation and Scattering by Thin-Wire Structures in the Complex Frequency Domain", Interaction Notes, Note 202, Air Force Weapons Laboratory, Albuquerque, N.M., May 1974.

[14] J. H. Richmond, "Computer Program for Thin-Wire Structures in a Homogeneous Conducting Medium", Technical Report, NASA CR-2399, National Aeronautics and Space Administration, Washington, D.C., June 1974.

[15] L. W. Pearson and C. M. Butler, "Inadequacies of Collocation Solutions to Pocklinton-Type Models of Thin-Wire Structures",

[15] (continued)

IEEE Trans. on Antennas and Propagation, pp. 295-298, March 1975.

[16] C. D. Taylor and J. P. Castillo, "On Electromagnetic-Field Excitation of Unshielded Multiconductor Cables", IEEE Trans. on Electromagnetic Compatibility, Vol. EMC-20, No. 4, pp. 495-500.

[17] C. R. Paul, "Applications of Multiconductor Transmission Line Theory to the Prediction of Cable Coupling, A Digital Computer Program for Determining Terminal Currents Induced in a Multiconductor Transmission Line by an Incident Electromagnetic Field", Technical Report, RADC-TR-76-101, Vol. VI, Rome Air Development Center, Griffiss AFB, New York, February 1978.

MISSION
of
Rome Air Development Center

RADC plans and executes research, development, test and selected acquisition programs in support of Command, Control Communications and Intelligence (C^3I) activities. Technical and engineering support within areas of technical competence is provided to ESD Program Offices (POs) and other ESD elements. The principal technical mission areas are communications, electromagnetic guidance and control, surveillance of ground and aerospace objects, intelligence data collection and handling, information system technology, ionospheric propagation, solid state sciences, microwave physics and electronic reliability, maintainability and compatibility.

END

DATE
FILMED

3-83

DTIC